Efficiency Loss Due To Defects In AlGaAs/GaAs Hetero-junction Solar Cell

A Dissertation Submitted in Partial Fulfillment of Requirement for the Degree of Bachelor of Science in Electrical and Electronic Engineering

Submitted by

Khandaker Md. Sydur Rahman (102436)
MD. Tasnim Hossain (102442)
Sadi M Jawad Ahsan (102480)
Odai Waheed Amin Hasoneh (092479)

Under The Supervision of

PROF. DR. MD. ASHRAFUL HOQUE
PROFESSOR
DEPARTMENT OF ELECTRICAL AND ELECTRONIC ENGINEERING (EEE)

Co-Supervision of

K. A. S. M. EHTESHAMUL HAQUE
LECTURER
DEPARTMENT OF ELECTRICAL AND ELECTRONIC ENGINEERING (EEE)

ISLAMIC UNIVERSITY OF TECHNOLOGY (IUT)
THE ORGANIZATION OF THE ISLAMIC COOPERATION (OIC)
GAZIPUR-1704, DHAKA, BANGLADESH.

Efficiency Loss Due To Defects In AlGaAs/GaAs Hetero-junction Solar Cell

A Thesis Presented to

The Academic Faculty

By

Khandaker Md. Sydur Rahman (102436)
MD. Tasnim Hossain (102442)
Sadi M Jawad Ahsan (102480)
Odai Waheed Amin Hasoneh (092479)

In Partial Fulfillment of Requirement for the Degree of Bachelor of Science in Electrical and Electronic Engineering

Approved By

PROF. DR. MD. ASHRAFUL HOQUE

DEPARTMENT OF ELECTRICAL AND ELECTRONIC ENGINEERING (EEE)

ISLAMIC UNIVERSITY OF TECHNOLOGY (IUT)

November, 2014

Efficiency Loss Due To Defects In AlGaAs/GaAs Hetero-junction Solar Cell

Khandaker Md. Sydur Rahman
Student ID : 102436
(Author)

MD. Tasnim Hossain
Student ID : 102442
(Author)

Sadi M Jawad Ahsan
Student ID : 102480
(Author)

Odai Waheed Amin Hasoneh
Student ID : 102442
(Author)

Prof. Dr. Md. Ashraful Hoque
Professor
Dept. of EEE, IUT
Supervisor

Prof. Dr. Md. Shahid Ullah
Professor
Head of the Department
EEE, IUT

Table of Contents

Chapter 1- Introduction

	Pg. No
1.1 Solar Cells	13
1.1.1 History	13
1.1.2 Principle of Operation	13
1.1.3 Hetero-junction Solar Cells	15
1.1.4 Comparison among Hetero-junctions, Silicon Alloys and III-V Materials?	15
1.1.5 Characteristics of III-V Compounds as Photovoltaic Materials	16
1.1.6 Drawback of III-V Solar Cells	17
1.1.7 Defects in Hetero-junction Materials	17-20
1.1.8 Research Outlines	20
1.1.9 Novelty in the Work	20

Chapter 2- The Software Simulation

2.1 About The Software	21
2.1.1 Adept	21
2.2 Simulation Parameters	21
2.2.1 Bandgap (E_g)	21
2.2.2 Dielectric Constant (K_s)	23
2.2.3 Refractive Index (n_{dx})	23
2.2.4 Density of States (n_c & n_v)	24
2.2.5 Electron Mobility (μ_n)	24
2.2.6 Hole Mobility (μ_p)	25
2.3 Values of Simulation Parameters For Different Mole Fraction	25
Remarks	31

Chapter 3 - Simulation Result **Pg. No**
3.1 Simulation Coding 32
3.2 Simulation Output 33
3.3.1 Short-Circuit Current Density (J_{SC}) 59
3.3.2 Open-Circuit Voltage (V_{OC}) 59
3.3.3 Fill Factor (FF) 59
3.3.4 Efficiency (η)
3.4 J_{SC}, V_{OC}, FF and Efficiency For Different Values of Mole Fraction(x) 61
3.5 Mole Fraction Vs. Efficenency Graph(Simulation Based) 65
Remarks 65

Chapter 4 - Solar Radiation Measurements

4.1 Solar Radiation Components at the Ground Level 66
4.2 Energy of Photon 69
4.3 Photon Flux 70
4.4 Absorption Coefficient, α 72
Remarks 74

Chapter 5 - Efficiency Calculation and Theoretical Modelling

5.1 Generation Rate 75
5.2 Calculation Of G_L 76
5.3 Calculation of short circuit Current Density J_{sc} and open circuit Voltage V_{OC} 77
5.4 Fill Factor 77
5.5 Efficiency 79
5.6 Efficiency Loss 83
5.6.1 Losses in Hetero-junction 84
5.7 Comparison Between Theoretical, Simulation Based and Efficiency Loss graphs 85
Remarks 85

Chapter 6 – Summary

6.1 Overview of the Work 86
6.2 Future Work 87

References 88

List of Figures

Pg. No

Fig 1.1 Structure of solar cell 14
Fig 2.1 (a) the straddled alignment, (b) staggered lineup alignment (c) broken gap alignment 21
Fig. 3.1 Light J-V curve for x=0 33
Fig. 3.2 Light J-V curve for x=0.01 33
Fig. 3.3 Light J-V curve for x=0.02 34
Fig. 3.4 Light J-V curve for x=0.03 34
Fig. 3.5 Light J-V curve for x=0.04 34
Fig. 3.6 Light J-V curve for x=0.05 34
Fig. 3.7 Light J-V curve for x=0.06 35
Fig. 3.8 Light J-V curve for x=0.07 35
Fig. 3.9 Light J-V curve for x=0.08 35
Fig. 3.10 Light J-V curve for x=0.09 35
Fig. 3.11 Light J-V curve for x=0.10 36
Fig. 3.12 Light J-V curve for x=0.11 36
Fig. 3.13 Light J-V curve for x=0.12 36
Fig. 3.14 Light J-V curve for x =0.13 36
Fig. 3.15 Light J-V curve for x=0.14 37
Fig. 3.16 Light J-V curve for x=0.15 37
Fig. 3.17 Light J-V curve for x=0.16 37
Fig. 3.18 Light J-V curve for x=0.17 37
Fig. 3.19 Light J-V curve for x=0.18 38
Fig. 3.20 Light J-V curve for x=0.19 38
Fig. 3.21 Light J-V curve for x=0.20 38
Fig. 3.22 Light J-V curve for x=0.21 38
Fig. 3.23 Light J-V curve for x=0.22 39
Fig. 3.24 Light J-V curve for x=0.23 39
Fig. 3.25 Light J-V curve for x=0.24 39
Fig. 3.26 Light J-V curve for x=0.25 39
Fig. 3.27 Light J-V curve for x=0.26 40
Fig. 3.28 Light J-V curve for x=0.27 40
Fig. 3.29 Light J-V curve for x=0.28 40
Fig. 3.30 Light J-V curve for x=0.29 40
Fig. 3.31 Light J-V curve for x=0.30 41
Fig. 3.32 Light J-V curve for x=0.31 41
Fig. 3.33 Light J-V curve for x=0.32 41
Fig. 3.34 Light J-V curve for x=0.33 41
Fig. 3.35 Light J-V curve for x=0.34 42

Fig. 3.36 Light J-V curve for x=0.35 42
Fig. 3.37 Light J-V curve for x=0.36 42
Fig. 3.38 Light J-V curve for x=0.37 42
Fig. 3.39 Light J-V curve for x=0.38 43
Fig. 3.40 Light J-V curve for x=0.39 43
Fig. 3.41 Light J-V curve for x=0.40 43
Fig. 3.42 Light J-V curve for x=0.41 43
Fig. 3.43 Light J-V curve for x=0.42 44
Fig. 3.44 Light J-V curve for x=0.43 44
Fig. 3.45 Light J-V curve for x=0.44 44
Fig. 3.46 Light J-V curve for x=0.45 44
Fig. 3.47 Light J-V curve for x=0.46 45
Fig. 3.48 Light J-V curve for x=0.47 45
Fig. 3.49 Light J-V curve for x=0.48 45
Fig. 3.50 Light J-V curve for x=0.49 45
Fig. 3.51 Light J-V curve for x=0.50 46
Fig. 3.52 Light J-V curve for x=0.51 46
Fig. 3.53 Light J-V curve for x=0.52 46
Fig. 3.54 Light J-V curve for x=0.53 46
Fig. 3.55 Light J-V curve for x=0.54 47
Fig. 3.56 Light J-V curve for x=0.55 47
Fig. 3.57 Light J-V curve for x=0.56 47
Fig. 3.58 Light J-V curve for x=0.57 47
Fig. 3.59 Light J-V curve for x=0.58 48
Fig. 3.60 Light J-V curve for x=0.59 48
Fig. 3.61 Light J-V curve for x=0.60 48
Fig. 3.62 Light J-V curve for x=0.61 48
Fig. 3.63 Light J-V curve for x=0.62 49
Fig. 3.64 Light J-V curve for x=0.63 49
Fig. 3.65 Light J-V curve for x=0.64 49
Fig. 3.66 Light J-V curve for x=0.65 49
Fig. 3.67 Light J-V curve for x=0.66 50
Fig. 3.68 Light J-V curve for x=0.67 50
Fig. 3.69 Light J-V curve for x=0.68 50
Fig. 3.70 Light J-V curve for x=0.69 50
Fig. 3.71 Light J-V curve for x=0.70 51
Fig. 3.72 Light J-V curve for x=0.71 51
Fig. 3.73 Light J-V curve for x=0.72 51
Fig. 3.74 Light J-V curve for x=0.73 51
Fig. 3.75 Light J-V curve for x=0.74 52
Fig. 3.76 Light J-V curve for x=0.75 52
Fig. 3.77 Light J-V curve for x=0.76 52
Fig. 3.78 Light J-V curve for x=0.77 52

Fig. 3.79 Light J-V curve for x=0.78 53
Fig. 3.80 Light J-V curve for x=0.79 53
Fig. 3.81 Light J-V curve for x=0.80 53
Fig. 3.82 Light J-V curve for x=0.81 53
Fig. 3.83 Light J-V curve for x=0.82 54
Fig. 3.84 Light J-V curve for x=0.83 54
Fig. 3.85 Light J-V curve for x=0.84 54
Fig. 3.86 Light J-V curve for x=0.85 54
Fig. 3.87 Light J-V curve for x=0.86 55
Fig. 3.88 Light J-V curve for x=0.87 55
Fig. 3.89 Light J-V curve for x=0.88 55
Fig. 3.90 Light J-V curve for x=0.89 55
Fig. 3.91 Light J-V curve for x=0.90 56
Fig. 3.92 Light J-V curve for x=0.91 56
Fig. 3.93 Light J-V curve for x=0.92 56
Fig. 3.94 Light J-V curve for x=0.93 56
Fig. 3.95 Light J-V curve for x=0.94 57
Fig. 3.96 Light J-V curve for x=0.95 57
Fig. 3.97 Light J-V curve for x=0.96 57
Fig. 3.98 Light J-V curve for x=0.97 57
Fig. 3.99 Light J-V curve for x=0.98 58
Fig. 3.100 Light J-V curve for x=0.99 58
Fig. 3.101 Light J-V curve for x=1.00 58
Fig 3.102: Simulation Based Efficiency vs mole fraction plot using MATLAB 65

Fig. 4.1 Extraterrestrial solar spectrum (ETS) and terrestrial standard solar spectrum AM1.5G. 67
Fig. 4.2 Angles describing the position of the sun: θz—zenith angle; h—elevation angle, μ_s—azimuth angle. Angles describing the position of the surface: β—slope angle, μ—surface azimuth angle. The incidence angle θ is the angle between the sun direction and the surface's normal n. 68
Fig 4.3 The absorption coefficient, α, in a variety of semiconductor materials at 300K as a function of the vacuum wavelength of light. 72
Fig 4.4 Absorption Co-efficient vs Photon Energy graph 73

Fig 5.1 Normalized Generation rate (m-3) vs cell depth (μm) curve 76
Fig 5.2 Graph of cell output current (red line) and power (blue line) as function of voltage. 78
Fig 5.3 Theoretical Efficiency vs mole fraction plot using MATLAB 83
Fig 5.4 Efficiency Loss vs mole fraction MATLAB plot 84
Fig 5.5 Theoretical and simulation based efficiency plots vs mole fraction and their difference as Efficiency Loss vs mole fraction 85

List of Tables

Pg. No

Table 2.1 Values of Simulation Parameters From Mole Fraction 0.00 to 1.00 25-31

Table 3.1 Values J_{SC}, V_{OC}, FF and Efficiency from Mole Fraction 0.00 to 1.00 61-64

Table 4.1 Percentage Of Solar Radiation and Photon Chart according to different Wavelengths (nm) 71

Table 5.1 Theoretical Data Table 79-82

Efficiency Loss Due To Defects In AlGaAs/GaAs Hetero-junction Solar Cell

Abstract

The principle of Energy conservation is -Energy can neither be created nor be destroyed, it can only be converted from one form to another. So energy conversion efficiency is a major issue for photovoltaic cells. Researchers are continuously trying to improve the efficiency level of photovoltaic devices by introducing new materials and advanced concepts. The target is to reach a high efficiency level within affordable cost, which will lead to a mass generation of electricity using photovoltaic devices.

In this work, a III-V hetero-junction solar cell has been introduced and characterized, which uses an $Al_xGa_{1-x}As$/GaAs hetero-junction as the working p-n junction. ADEPT, 1D simulation software was used throughout the whole work for the simulation of light J-V characteristics for different designs. Energy conversion efficiency for each design was calculated from its corresponding light J-V characteristics curve. An illumination level of 1000 W/m^2 (AM1.5G standard) and a concentration level of 1 sun was considered for all the simulations in the work. The photovoltaic cell has an n-on-p structure, where the n-type $Al_xGa_{1-x}As$ layer acts as an base, and the p-type GaAs layer serves as the emitter. The base thickness was kept at 2 μm. Germanium (Ge) substrate (p-doped) was used for the structure.

We used ADAPT software for simulating J-V curve. From the curves, we got Open circuit voltage V_{oc} and short circuit current I_{sc} . Then, from these, Fill Factor and efficiency was calculated for each mole fraction of 0 to 1 with a gap of 0.01. And, then generation on electron hole pair was calculated. Then parameters including absorption coefficient $\alpha(\lambda)$, number of photons φ_0 were calculated for a mole fraction of 0 to 1 with a gap of 0.01 . Short circuit current and open circuit voltage were calculated and from that, fill factor and efficiency was calculated for each mole fraction from 0 to 1 with a gap of 0.01. Then, simulated efficiency and theoretical efficiency were plotted against mole fraction from 0 to 1. And then, efficiency loss vs. mole fraction was plotted.

Acknowledgements

We are grateful to our thesis supervisor, Prof. Dr. Md. Ashraful Hoque, for his continuous guidance and motivation in completing our thesis. His constant demand for making the work more elaborate finally resulted in satisfactory and successful outcomes. We would like to thank our co-supervisor K. A. S. M. Ehteshamul Haque, lecturer of the Department of Electrical and Electronics Engineering, Islamic University of Technology, for providing us with necessary information about hetero-junction solar cells and for offering us a helpful introduction to ADEPT.

Symbols & Abbreviations

I	Current (A)
I_L	Photocurrent (A)
I_F	Forward Current (A)
I_S	Saturation current (A)
k	Boltzmann constant (JK^{-1})
q	Charge of an electron (C)
I_{sc}	Short-circuit current (A)
V_{oc}	Open-circuit voltage (V)
V_t	Thermal voltage (V)
P_m	Maximum output power (W)
V_m	Voltage at maximum power point (V)
I_m	Current at maximum power point (A)
FF	Fill Factor
η	Energy conversion efficiency (%)
E	Solar irradiance (W/cm^2)
A	Area of the solar cell (cm^2)
J_{sc}	Short-circuit current density (A/cm^2)
r	Fraction of photons that are to be reflected.
x	Mole fraction
α	Absorption Coefficient (cm^{-1})
Φ_0	Number of photons

Chapter 1- Introduction

1.1 Solar Cells

1.1.1 History

Solar cells are semiconductor devices which convert incident light into electricity by the absorption of photons and subsequent generation of electron-hole pairs. This effect of electricity generation from light absorption, which is known as the photovoltaic effect, was first observed by the French physicist A. E. Becquerel in 1839 [1]. In 1883 The first solid-state photovoltaic cell was built many years later, by Charles Fritts, He coated Selenium (Se) with an extremely thin layer of gold to form the junction. The photovoltaic device was less than 1% efficient [2]. Then in 1954 the first practical photovoltaic cell was developed in at Bell Laboratories [3] by the three scientists- Daryl Chapin, Calvin Souther Fuller and Gerald Pearson. They used a diffused Silicon p-n junction that achieved 6% efficiency. At present, solar cells are built with many different technologies, and the efficiency level that these devices can achieve is pretty good. In today's world, we have bulk Si solar cells, we have thin film solar cells fabricated from Si or CdTe, we have dye-sensitized solar cells, and so on. There are even more advanced concept solar cells like Quantum Dot (QD) solar cells, hot carrier solar cells etc. Today, solar cells are used for mass generation of electricity. The added advantage of solar power plants is that they require minimum maintenance, and the input energy is clean and free.

1.1.2 Principle of Operation

Figure 1.1 presents a simplified diagram [4] of a solar cell that utilizes a single p-n junction. With no voltage applied to this junction, an electric field exists in the depletion region of the p-n junction. For simplicity, we consider that a resistive load is connected with the device. Now, photons incident on the device can create electron-hole pairs in the space-charge region, which are forcibly swept out of the depletion region by the built-in electric field, as the depletion region must be depleted of free charges. This swept out carriers produce a photocurrent I_L, in the reverse-bias direction for the p-n junction. Now, the photocurrent I_L produces a voltage drop across the

resistive load, which forward biases the p-n junction. This forward bias produces a forward current I_F in the forward-bias direction for the p-n junction. The net current, I, in the reverse bias direction for the p-n junction, is given by equation (1).

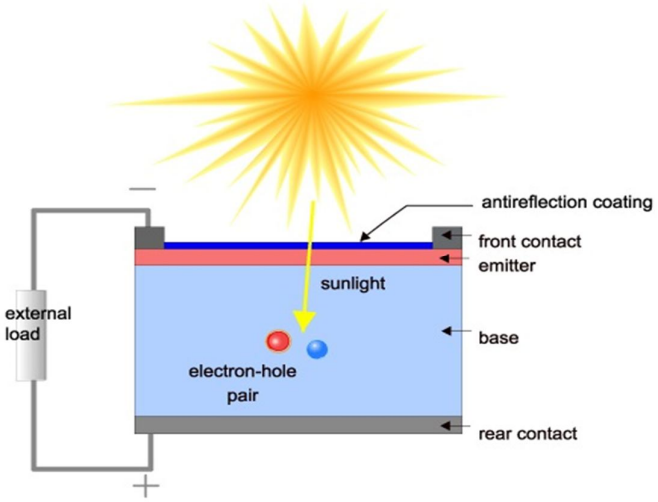

Fig: 1.1 Structure of solar cell (Image courtesy : pveducation.org)

$$I = I_L - I_F = I_L - I_S [\exp (qV / nkT) - 1] \qquad (1)$$

Where,

n = Ideality factor (taken as 1)

k = Boltzmann constant

T = Temperature in K

q = charge of an electron

I_S = saturation current

1.1.3 Hetero-junction Solar Cells

A hetero-junction is a p -n junction formed between two different semiconducting materials. Hetero-junctions have got numerous applications in optoelectronic devices [17]. Hetero-junction solar cells generally employ a p-n or p-i-n structure. In the simplified p-n structure, one material essentially works as an absorber, while the other can be a window layer, or another absorber [18]. The functioning layer for optical absorption and generation of electron-hole pairs is the absorber. The window layer is usually 16 a high bandgap material which is highly transparent to light, so that it can allow almost all the incident photons to reach the absorber.

Hetero-junction devices have an inherent advantage over homo-junction devices, which require materials that can be doped both p-type and n-type. Many semiconducting materials can be doped either p-type or n-type, but not the both. Hetero-junctions do not suffer from this limitation. So, many promising materials with good optical absorption capabilities can be investigated to produce optimal cells.[19]

Again, a high bandgap window layer reduces the cell's series resistance, and improves the output voltage [19]. It also helps to reduce recombination of minority carriers at the metal-semiconductor interface around the contacts [20].

For solar cells and other optoelectronic components, it is not sufficient to choose materials with suitable bandgap values and bring them to form a junction. It is also important to make sure that the chosen materials form a junction such that the interface is as much free of energy states in the forbidden band as possible, in order to prevent additional recombination of carriers and carrier trapping [20]. Material combinations satisfying such conditions are not very common. However, many combinations of III-V compounds, especially the ternary compounds based on GaAs, satisfy these criteria to large extents [20]

1.1.4 Comparison among Hetero-junctions, Silicon Alloys and III-V Materials

Hetero-junction solar cells involving Si and Si alloys have been thoroughly investigated [23]. But Si is not a very good choice because its bandgap is lower than the optimum bandgap required for achieving the highest level of efficiency. For terrestrial applications, the optimum bandgap of the absorber should be around 1.4 eV [24], while Si has an indirect bandgap of 1.12 eV. Besides this, Si has low optical absorption coefficient, compared to the high optical absorption compounds[25]

Recently, III-V compounds have gained considerable interest as constituents of both single-junction and multi-junction solar cells. The special advantage that these materials offer is their wide range of variation in bandgaps [26]. Besides this, they have got high optical absorption properties, along with high electron mobility and high minority carrier lifetime. They also provide numerous options for proper lattice matching between the hetero-junction materials. So, photovoltaic cells fabricated from III-V compounds typically provide high output current and high efficiency. III-V ternary and quaternary alloys can offer yet 17 more flexibility, as their bandgaps and other properties can be finely tuned by changing the alloy composition.

1.1.5 Characteristics of III-V Compounds as Photovoltaic Materials

Except for the Nitrides, III-V semiconductors typically have the Zinc blende crystal structure, with a lattice constant varying in the range of 5.4 to 6.2 Å, depending on the material [16]. Along with the binary compounds, there are also ternary and quaternary compounds available. Among all the III-V compounds, the most widely used one for solar cells and many other applications is GaAs, due to its optimum direct bandgap (1.42 eV). Besides this, GaAs has got high electron mobility (8500 cm^2/ V-s), which makes it attractive for all types of solid-state devices. Single-junction solar cells fabricated from GaAs have achieved efficiency values as high as 28% [33]. Other compounds like AlxGa1-xAs, GaxIn1-xAs, GaxIn1-xP and AlxGa1-x AsyP1-y have been frequently used in multijunction solar cells. High bandgap

materials like GaP (Eg=2.26 eV) and AlAs (Eg=2.16 eV) have been utilized as the window layer of hetero-junction solar cells [27].
The III-V Nitrides typically have Wurtzite lattice structure (except for BN), and they can provide a very wide range of bandgap variation. Application of ternary III-V Nitrides, such as $Al_xGa_{1-x}N$, has been investigated for multijunction cells in recent years [34].

1.1.6 Drawback of III-V Solar Cells

The problem of III-V solar cells is that these cells are very expensive, compared to the commonly used terrestrial solar cell technologies [36]. This is mainly due to the high fabrication cost of III-V materials and unavailability of necessary fabrication technology in few cases. So, the use of III-V solar cells is still limited to space applications, where the efficiency is prioritized over the cost [38,6]. Utilization of such solar cells for terrestrial applications requires reduction of materials processing and fabrication costs. Another way to address this problem is to use concentrators with solar cells. Concentrated solar cells can give up to 2000 times the power output of a solar cell working under 1 sun, depending on the concentration level. Though concentrators are very expensive, they can offer a good trade-off between the PV system cost and the achievable high efficiency [6].

1.1.7 Defects in Heterojuction Materials

Spectral mismatch:

There are two principal losses that strongly reduce the energy conversion efficiency solar cells.[39] An important part of a solar cell is the absorber layer, in which the photons of the incident radiation are efficiently absorbed resulting in a creation of electron-hole pairs. The absorber layer of the solar cells is in most cases formed by a semiconductor material, which has its distinct optical properties characterized by the band gap energy and the complex refractive index, ñ = n - ik. In principle, only photons with energy higher than the band gap energy of the absorber generate electron-hole pairs. Since the electrons and holes tend to occupy energy levels at the bottom of the conduction band and the

top of the valence band, respectively, the extra energy that the electron-hole pairs receive from the photons is released as heat into the semiconductor lattice in the Thermalization process. Photons with energy lower than the band gap energy of the semiconductor absorber are in principle not absorbed and cannot generate electron-hole pairs. Therefore these photons are not involved in the energy conversion process. The Non-absorption of photons carrying less energy than the semiconductor band gap and the excess energy of photons, larger than the band gap, are the two main losses in the energy conversion process using solar cells. Both of these losses are thus related to the spectral mismatch of the energy distribution of photons in the solar spectrum and the band gap of a

semiconductor material.

Solar cell optical properties:

There are also other optical parameters than Eg that have influence on the conversion efficiency of a solar cell.[39] These are optical constants of the individual layers. In general, when light arrives on an interface between two media, a part of the light is reflected from and the other part is transmitted through the interface. The interface is therefore characterized by the wavelength dependent reflectance, R(λ), and transmittance, T(λ). Reflectance is the ratio of the energy reflected from the surface of the interface to the total incident energy. There is a reflection of light at the interface between the first layer of a solar cell and the incident medium, usually air, and there is also reflection at the interfaces between the individual layers within the solar cell. All these processes result in a total reflectance between the solar cell and air. This means that a part of the incident energy that can be converted into a usable energy by the solar cell is lost by reflection. In general, light is absorbed in all layers that form the solar cell. However, the solar cell is optimally designed when most of the incident light is absorbed in the absorber layer. Due to the limited thickness of the absorber layer, not all the light entering the absorber layer is absorbed. Incomplete absorption in the absorber due to its limited thickness is an additional loss that lowers the efficiency of the energy conversion. Since there is a chance that a high energetic photon can generate more than one electron-hole pair, we define the quantum efficiency for

carrier generation, ηg, which represents the number of electron-hole pairs generated by one absorbed photon. Usually ηg is assumed to be unity.

Soler cell collection losses

Not all charge carries that are generated in a solar cell are collected at the electrodes.[39] The photo-generated carriers are the excess carriers with respect to the thermal equilibrium and are subjected to the recombination. The carriers recombine in the bulk, at the interfaces, and/or at the surfaces of the junction. The recombination is determined by the electronic properties of materials that form the junction, such as density of states introduced into the band gap by the R-G centers. The concentration of R-G centers strongly influences the minority-carrier lifetimes. The contributions of both the electronic and optical properties of the solar cell materials to the photovoltaic performance are taken into account in the absolute external quantum efficiency. The absolute external quantum efficiency is defined as the number of charge carriers collected (from all layers of the device) per incident photon at each wavelength λ.

Additional Defects

The open circuit voltage Voc of a solar cell depends on the saturation current and the photo-generated current of the solar cell.[39] The saturation current density depends on the recombination in the solar cell that cannot be avoided and is referred to as the fundamental recombination. This fundamental recombination depends on the doping of the different regions (n-type and p-type regions) of a junction and the electronic quality of materials forming the junction. The doping levels and the recombination determine the voltage factor, qVoc/EG, that is the ratio of the maximum voltage developed by the solar cell (Voc) to the voltage related to the band-gap of the absorber (EG/q). The maximum power generated by a solar cell is dependent on the fill factor, FF. In case of a solar cell that behaves as an ideal diode only direct recombination occurs and the maximal FF is a function of Voc. In a practical solar cell the FF is lower than the ideal value due to following reasons:

- The voltage drop due to the series resistance Rs of a solar cell. The series resistance is introduced by the resistance of the main current path through which the photo-generated carriers arrive to the external circuit.
- The contributions to the series resistance come from the bulk ressistance of the junction, the contact resistance between the junction andelectrodes, the resistance of the electrodes.
- The voltage drop due to the leakage current and characterized by the shunt resistance Rp of a solar cell. The leakage current is caused by the current through local defects in the junction or due to the shunts at the edges of solar cells. The recombination in a non-ideal solar cell results in a decrease of the FF.

1.1.8 Research Outlines

In our work, we have introduced, characterized and optimized a novel III-V hetero-junction solar cell using ADEPT simulator that incorporates an $Al_xGa_{1-x}As$/GaAs hetero-junction. Here, the GaAs layer functions as the emitter layer of the cell. A highly doped bottom layer of Ge was also introduced in the design, which works as substrate. We calculated the efficiency and plotted in the graph, then, using theoretical formulas, we calculated efficiency for each mole fraction of 0 to 1 with a gap of 0.01. Then we calculated the loss of efficiency due to heterojuction defects and plotted it in the graph.

1.1.9 Novelty in the Work

We studied the efficiency loss due to defects in GaAs/AlGaAs hetero-junction solar cell for Al mole fraction between 0 and 1, in steps of 0.01. We also plotted the efficiency loss against Al mole fraction. This work gives an idea of which particular composition of AlGaAs minimizes the effect of defects in GaAs/AlGaAS soler cell. It also presents a picture of trade-off between efficiency and lifetime, as lifetime is directly related with the amount of defects. The larger is the amount of defects, the less is the lifetime.

Chapter 2- The Software Simulation

2.1 About The Software

2.1.1 Adept

ADEPT solves Poisson's equation coupled with the hole and electron continuity equations in one spatial dimension in compositionally nonuniform semiconductors. It was originally written to model solar cells fabricated from a wide variety of materials, including amorphous silicon, copper indium diselenide, and cadmium telluride. However, since material parameters (band gap, mobility, etc.) can be input by the user, devices fabricated from any material for which these parameters are known can be modeled. Dark I-V, light I-V, and spectral response of solar cells (or any two terminal devices) can be computed. Plots of many internal parameters, such as carrier density, recombination, electric field, etc., can be plotted at any operating point.

Homostructures and heterostructures, both abrupt and graded, can be modeled. Solar cell material systems modeled include ZnO/CdS/CIS, ZnO/CdS/CIGS, CdS/CdTe, a-Si, Si, AlGaAs/GaAs, GaSb, InP, and several others.

ADEPT/F simulator was written by Jeffrey L. Gray. User interface for launching simulations and analyzing results created by Michael McLennan.

2.2 Simulation Parameters

2.2.1 Bandgap (E_g)

In solid-state physics, a band gap, also called an energy gap or bandgap, is an energy range in a solid where no electron states can exist. In graphs of the electronic band structure of solids, the band gap generally refers to the energy difference (in electron volts) between the top of the valence band and the bottom of the conduction band in insulators and semiconductors.[15]

In a semiconductor heterostructure, two different semiconductors are brought into physical contact. In practice, different semiconductors are “brought into contact” by epitaxially growing one semiconductor on top of another semiconductor. We classify heterostructures according to the

alignment of the bands of the two semiconductors. Three different alignments of the conduction and valence bands and of the forbidden gap.Shows the most common alignment which will be referred to as the straddled alignment or "Type I" alignment. GaAs / $Al_xGa_{1-x}As$ heterostructure, exhibits this straddled band alignment [10] . In staggered lineup the steps in the valence and conduction band go in the same direction. The staggered band alignment occurs for a wide composition range in the $Ga_xIn_{1-x}As$ / $GaAs_ySb_{1-y}$ material system [11]. The most extreme band alignment is the broken gap alignment .This alignment occurs in the InAs / GaSb material system [12]. Both the staggered lineup and the broken-gap alignment are called "Type II" energy band alignments.

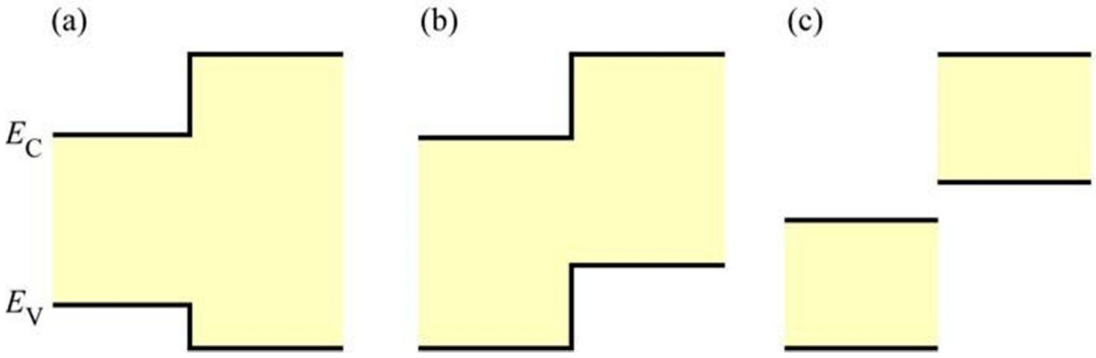

Fig.2.1: (a) the straddled alignment, (b) staggered lineup alignment (c) broken gap alignment

$Al_xGa_{1-x}As$, has an energy gap of 1.424 eV to 2.168 [13], a dielectric constant of 12.9 to 10.6 [13]. This material has been extensively used to fabricate hetero-junction and tandem solar cells [6].Theoretically, the energy which is greater than or equal 1.424 eV to 2.168 is absorbed in this layer, but it transmits all the photons having less energy than its bandgap [5].

$x<0.45$ for $1.424+1.247x$ eV [13]

$x>0.45$ for $1.9+0.125x+0.143x^2$ eV [13]

Gallium arsenide (GaAs) is a compound of the elements gallium and arsenic. It is a III-V direct bandgap semiconductor with a zinc blende crystal structure. It has a bandgap of 1.424ev and dielectric constant 12.9.

Germanium is a widely-used substrate for both hetero-junction and multi junction solar cells. We choice Ge as the substrate material. Germanium has

almost the same lattice constant (5.658 Å) [13] as GaAs (5.65325 Å) [13]. Germanium is chosen because of it's low cost and mechanical strength although it has same thermal expansion coefficient.

2.2.2 Dielectric Constant (K_s)

The dielectric constant is the ratio of the permittivity of a substance to the permittivity of free space. It is an expression of the extent to which a material concentrates electric flux, and is the electrical equivalent of relative magnetic permeability.[14]

As the dielectric constant increases, the electric flux density increases, if all other factors remain unchanged. This enables objects of a given size, such as sets of metal plates, to hold their electric charge for long periods of time, and/or to hold large quantities of charge. Materials with high dielectric constants are useful in the manufacture of high-value capacitors.[14]

The dielectric constant of GaAs and Ge is 12.9[7] and 16.2[8] respectively.

For $Al_xGa_{1-x}As$, this equation is used:

$$12.90-2.84x \qquad [9]$$

2.2.3 Refractive Index (n_{dx})

In optics the refractive index or index of refraction n of an optical medium is a dimensionless number that describes how light, or any other radiation, propagates through that medium[16]. It is defined as,

$$n = \frac{c}{v}$$

where c is the speed of light in vacuum and v is the speed of light in the substance. For example, the refractive index of water is 1.33, meaning that light travels 1.33 times faster in a vacuum than it does in water.

Refractive index of GaAs and Ge is 3.00[7] and 4.00[8] respectively.

For $Al_xGa_{1-x}As$, the equation is

$$n=3.3-0.53x+0.09x^2 \quad [22]$$

2.2.4 Density of States (n_c & n_v)

In solid-state and condensed matter physics, the density of states (DOS) of a system describes the number of states per interval of energy at each energy level that are available to be occupied by electrons. Unlikeisolated systems, like atoms or molecules in gas phase, the density distributions are not discrete like a spectral density but continuous. A high DOS at a specific energy level means that there are many states available for occupation. A DOS of zero means that no states can be occupied at that energy level. In general a DOS is an average over the space and time domains occupied by the system. Local variations, most often due to distortions of the original system, are often called local density of states (LDOS). If the DOS of an undisturbed system is zero, the LDOS can locally be non-zero due to the presence of a local potential.[21]

There is two kinds of effective density of states conduction band effective density of states (n_c) and valence band effective of density (n_v). The conduction band effective density of states (n_c) and valence band effective of density (n_v) is fixed value for Ge and GaAs. For Ge $n_c=1x10^{-19}$ $cm^{-}3$[8] and $nv=5x10^{-18}cm^{-3}$[8].For GaAs $n_c=4.7x10^{-17}$ $cm^{-}3$[7]and $nv=9.0x10^{-18}cm^{-3}$[7].

For $Al_xGa_{1-x}As$, the equation is

n_c: $x<0.41$ for $2.5\cdot10^{19}\cdot(0.063+0.083x)^{3/2}$ cm^{-3} [8]

$x>0.45$ for $2.5\cdot10^{19}\cdot(0.85-0.14x)^{3/2}$ cm^{-3} [8]

n_v: $2.5\cdot10^{19}\cdot(0.51+0.25x)^{3/2}$ cm^{-3}

2.2.5 Electron Mobility (μ_n)

In solid-state physics, the electron mobility characterizes how quickly an electron can move through a metal or semiconductor, when pulled by an electric field[27].The term carrier mobility refers in general to both electron and hole mobility in semiconductors.

When an electric field E is applied across a piece of material, the electrons respond by moving with an average velocity called the drift velocity,v_d. Then the electron mobility μ is defined as

$$V_d=\mu E$$

Electron mobility is almost always specified in units of $cm^2/(V\cdot s)$.

Electron mobility for GaAs and Ge is <=8500 $cm^2v^{-1}s^{-1}$ and <=3500 $cm^2v^{-1}s^{-1}$.

For $Al_xGa_{1-x}As$, the electron mobility is calculated by,

$0<x<0.45$ for $8\cdot10^3-2.2\cdot10^4x+10^4\cdot x^2$ $cm^2\ V^{-1}\ s^{-1}$ [29]

$0.45<x<1$ for $-255+1160x-720x^2$ $cm^2\ V^{-1}\ s^{-1}$ [29]

2.2.6 Hole Mobility (μ_p)

Hole Mobility is the parameter which is a measure of hole scattering in a semiconductor; proportionality factor between hole drift velocity and electric field as well as conductivity and hole concentration in semiconductor; due to its higher effective mass, hole mobility is typically significantly lower than electron mobility[30].

Hole mobility for GaAs and Ge is <=1900 $cm^2v^{-1}s^{-1}$ and <=400 $cm^2v^{-1}s^{-1}$. For For $Al_xGa_{1-x}As$, the hole mobility can be calculated by,

$370-970x+740x^2$ $cm^2\ V^{-1}\ s^{-1}$ [29]

2.3 Values of Simulation Parameters For Different Mole Fraction

Table 2.1 values of Simulation Parameters From Mole Fraction 0.00 to 1.00

Mole Fraction	E_g	K_s	n_{dx}	n_c ($*10^{17}$)	n_v	μ_n	μ_p
0	1.424	12.9	3.3	3.95	0.9105	8000	370
0.01	1.4365	12.8716	3.2947	4.03	0.9172	7781	360.374
0.02	1.4489	12.8432	3.2894	4.11	0.924	7564	350.896
0.03	1.4614	12.8148	3.2842	4.19	0.9307	7349	341.566
0.04	1.4739	12.7864	3.2789	4.27	0.9374	7136	332.384

Mole Fraction	E_g	K_s	n_{dx}	n_c ($*10^{17}$)	n_v	μ_n	μ_p
0.05	1.4863	12.758	3.2787	4.5	0.9442	6925	323.35
0.06	1.4988	12.7296	3.2685	4.43	0.951	3716	314.464
0.07	1.5113	12.7012	3.2633	4.51	0.9578	6509	305.726
0.08	1.5238	12.6128	3.2582	4.59	0.9646	6304	297.136
0.09	1.5238	12.6444	3.253	4.68	0.9714	6101	288.694
0.1	1.5487	12.616	3.2479	4.76	0.9783	5900	280.4
0.11	1.5612	12.5876	3.2428	4.84	0.9852	5701	272.254
0.12	1.5736	12.5592	3.2377	4.93	0.992	5504	264.256
0.13	1.5861	12.5308	3.2326	5.01	0.9989	5309	256.406
0.14	1.5986	12.2024	3.2276	5.10	1.0059	5116	248.704
0.15	1.611	12.474	3.2225	5.18	1.0128	4925	241.15
0.16	1.62385	12.4456	3.2175	5.27	1.0197	4736	233.744
0.17	1.636	12.4172	3.2125	5.35	1.0267	4549	226.486
0.18	1.6485	12.3888	3.2075	5.44	1.0337	4364	219.376
0.19	1.6609	12.3604	3.2025	5.53	1.0407	4181	212.414
0.20	1.6734	12.332	3.1976	5.61	1.0477	4000	205.6
0.21	1.6859	12.3036	3.1927	5.7	1.0547	3821	198.934
0.22	1.6983	12.2752	3.1878	5.79	1.0617	3644	192.416
0.23	1.7103	12.2468	3.1829	5.88	1.0688	3469	186.046

Mole Fraction	E_g	K_s	n_{dx}	n_c ($*10^{17}$)	n_v	μ_n	μ_p
0.24	1.7233	12.2184	3.178	5.97	1.0759	3296	179.824
0.25	1.7357	12.19	3.1731	6.06	1.0829	3125	173.75
0.26	1.7482	12.1616	3.1683	6.15	1.09	2956	167.824
0.27	1.7607	12.1332	3.1635	6.24	1.0972	2789	162.046
0.28	1.7732	12.1048	3.1587	6.33	1.1043	2620	156.416
0.29	1.7856	12.0764	3.1443	6.42	1.1114	2461	150.934
0.30	1.7981	12.048	3.1396	6.52	1.1186	2300	145.6
0.31	1.8106	12.0196	3.1349	6.61	1.1258	2142	140.414
0.32	1.823	11.9912	3.1302	6.70	1.133	1984	135.376
0.33	1.8355	11.9628	3.1255	6.79	1.1402	1829	130.486
0.34	1.848	11.9344	3.1209	6.89	1.1474	1680	125.744
0.35	1.8604	11.906	3.1162	6.98	1.1546	1530	121.15
0.36	1.8729	11.8776	3.1116	7.08	1.1619	1376	116.704
0.37	1.8854	11.8492	3.107	7.17	1.1692	1229	112.406
0.38	1.8979	11.8208	3.1024	7.27	1.1764	1084	108.256
0.39	1.9103	11.7924	3.0978	7.36	1.1837	941	104.254
0.40	1.9228	11.764	3.0933	7.46	1.1911	800	100.4
0.41	1.9353	11.7356	3.0978	$1.76*10^{19}$	1.1984	661	96.694

Mole Fraction	E_g	K_s	n_{dx}	n_c ($*10^{19}$)	n_v	μ_n	μ_p
0.42	1.9477	11.7072	3.0933	1.76	1.2057	524	93.136
0.43	1.9602	11.6788	3.0887	1.75	1.2131	389	89.726
0.44	1.9727	11.6204	3.0842	1.75	1.2205	256	86.464
0.45	1.9852	11.622	3.0797	1.75	1.2279	121.2	83.35
0.46	1.9878	11.5936	3.0752	1.74	1.2353	126.248	80.384
0.47	1.9903	11.5652	3.0708	1.74	1.2427	131.152	77.566
0.48	1.9929	11.5368	3.0663	1.73	1.2501	135.912	74.896
0.49	1.9956	11.5084	3.0619	1.73	1.2576	140.528	72.374
0.50	1.9952	11.48	3.0575	1.72	1.265	145	70
0.51	2.0009	11.4516	3.0531	1.72	1.2725	149.328	67.774
0.52	2.0037	11.4232	3.0487	1.71	1.28	153.512	65.696
0.53	2.0064	11.3948	3.0444	1.71	1.2875	157.552	63.766
0.54	2.0092	11.3664	3.04	1.70	1.295	161.448	61.984
0.55	2.012	11.338	3.0357	1.70	1.3026	165.2	60.35
0.56	2.0148	11.3096	3.0314	1.69	1.3101	168.808	61.984
0.57	2.0177	11.2812	3.0271	1.69	1.3177	172.272	57.526
0.58	2.0206	11.2528	3.0229	1.69	1.3253	175.592	56.336
0.59	2.0235	11.2244	3.0186	1.68	1.3329	178.768	55.294
0.60	2.0265	11.196	3.0144	1.68	1.3405	181.8	54.4

Mole Fraction	E_g	K_s	n_{dx}	n_c ($*10^{19}$)	n_v	μ_n	μ_p
0.61	2.0295	11.1676	3.0102	1.67	1.3481	184.688	53.654
0.62	2.0325	11.1392	3.006	1.67	1.3557	187.432	53.056
0.63	2.0355	11.1108	3.0018	1.66	1.3634	190.032	52.606
0.64	2.0386	11.0824	2.9977	1.66	1.371	192.488	52.304
0.65	2.0417	11.054	2.9935	1.65	1.3787	194.8	52.15
0.66	2.0448	11.0256	2.9894	1.65	1.3864	196.968	52.144
0.67	2.0479	10.9972	2.9853	1.64	1.3941	198.992	52.286
0.68	2.0511	10.9688	2.9812	1.64	1.4019	200.872	52.576
0.69	2.0543	10.9404	2.9771	1.63	1.4096	202.608	53.014
0.70	2.0576	10.912	2.9731	1.63	1.4173	204.2	53.6
0.71	2.0608	10.8836	2.9691	1.63	1.4251	205.648	54.334
0.72	2.0641	10.8552	2.9651	1.62	1.4359	206.952	55.216
0.73	2.0675	10.8268	2.9611	1.62	1.4407	208.112	56.246
0.74	2.0708	10.7984	2.9571	1.61	1.4485	209.125	57.424
0.75	2.0742	10.77	2.9531	1.61	1.4563	210	58.75
0.76	2.0776	10.7416	2.9492	1.60	1.4642	210.728	60.224
0.77	2.081	10.7132	2.9453	1.60	1.472	211.312	61.846
0.78	2.0845	10.6848	2.9414	1.59	1.4799	211.725	63.616
0.79	2.088	10.6564	2.9375	1.59	1.4877	212.048	65.534

Mole Fraction	E_g	K_s	n_{dx}	n_c ($*10^{19}$)	n_v	μ_n	μ_p
0.80	2.0915	10.628	2.9336	1.59	1.4956	212.2	67.6
0.81	2.0921	10.5996	2.9297	1.58	1.5035	212.208	69.814
0.82	2.0987	10.5712	2.9259	1.58	1.5115	212.072	72.176
0.83	2.1023	10.5428	2.9221	1.57	1.5194	211.792	74.686
0.84	2.1059	10.5144	2.9183	1.57	1.5274	211.368	77.344
0.85	2.1096	10.486	2.9145	1.56	1.5353	210.8	80.15
0.86	2.1133	10.4576	2.9108	1.56	1.5433	210.088	83.101
0.87	2.117	10.4262	2.907	1.55	1.5513	209.232	86.206
0.88	2.1207	10.4008	2.9033	1.55	1.5593	208.232	89.456
0.89	2.1245	10.3721	2.8996	1.54	1.5673	207.088	92.854
0.90	2.1283	10.344	2.8959	1.54	1.5753	205.8	96.4
0.91	2.1322	10.3156	2.8922	1.54	1.5834	204.368	100.094
0.92	2.136	10.2872	2.8886	1.53	1.5914	202.792	103.936
0.93	2.1399	10.2588	2.8849	1.53	1.5995	201.072	107.926
0.94	2.1439	10.2304	2.8813	1.52	1.6076	199.208	112.064
0.95	2.1478	10.202	2.8777	1.52	1.6157	197.2	116.35
0.96	2.1518	10.1736	2.8741	1.51	1.6238	195.048	120.784
0.97	2.1558	10.1452	2.8706	1.51	1.6319	192.752	125.366
0.98	2.1598	10.1168	2.867	1.50	1.6401	190.312	130.096

Mole Fraction	E_g	K_s	n_{dx}	n_c ($*10^{19}$)	n_v	μ_n	μ_p
0.99	2.1639	10.0884	2.8635	1.50	1.6482	187.728	134.974
1.00	2.168	10.06	2.86	1.50	1.6564	185	140

Remarks:

In this chapter, it is discussed about the different parameters that are for the simulation and the their values for different mole fraction.

Chapter 3 - Simulation Result

3.1 Simulation Coding

The coding was done using the ADEPT software. Because it is easy and it has tutorial. So the coding can be done easily.. The sample of the simulation coding is given below

```
*title AlGaAs cell
mesh  nx=250 xres=1. wt=1/1/2/1
*layer GaAs layer
layer  tm=0.1 eg=1.424 ks=12.9 ndx=3.3 nc=4.7e17 nv=9.0e18 b0.opt=1.e5
+ nd =1.0e18 ead=-1. up=400. un=8500.
+ taup.shr=1e-9 taun.shr=1e-7
*layer AlGaAs layer
layer  tm=2 eg=1.6859 ks=12.3036 ndx=3.1927 nc=5.70e17 nv=1.0547e19
+ na=1.e16 eaa=-1. up=198.934 un=3821
+ taup.shr=1e-7 taun.shr=1e-9
+ eg.opt=1.6859 b0.opt=18.364e3 b1.opt=45.698e3  b2.opt=-17.598e3
+ b3.opt=117.176e3 b4.opt=-5.09e3
*layer Ge layer
layer  tm=100 eg=0.661 ks=16.2 ndx=4.00 nc=1.0e19 nv=5e18
+ na=1.0e17 eaa=-1. up=40. un=200.
+ taup.shr=1e-7 taun.shr=1e-9
+ eg.opt=0.661 b0.opt=0.9182e4 b1.opt=2.2849e4  b2.opt=-0.8799e4
+ b3.opt=5.8588e4 b4.opt=-0.2545e4
genrec gen=am1p5g shadow=0.05
solcell
solve  itmax=100 delmax=1.e-5
output info=5 copies=1
```

3.2 Simulation Output

The following figures are the J-V curve of the simulation output.

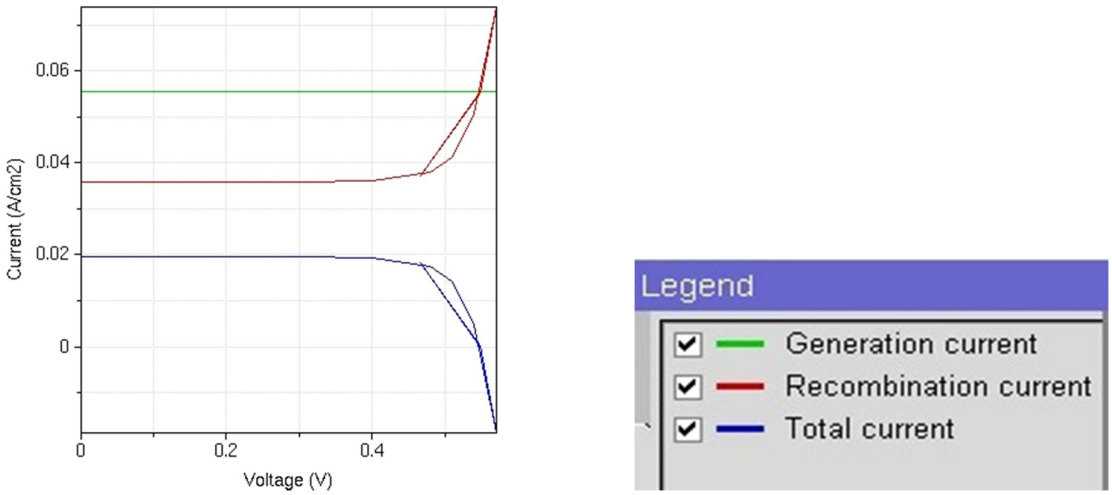

Fig. 3.1 Light J-V curve for x=0.0

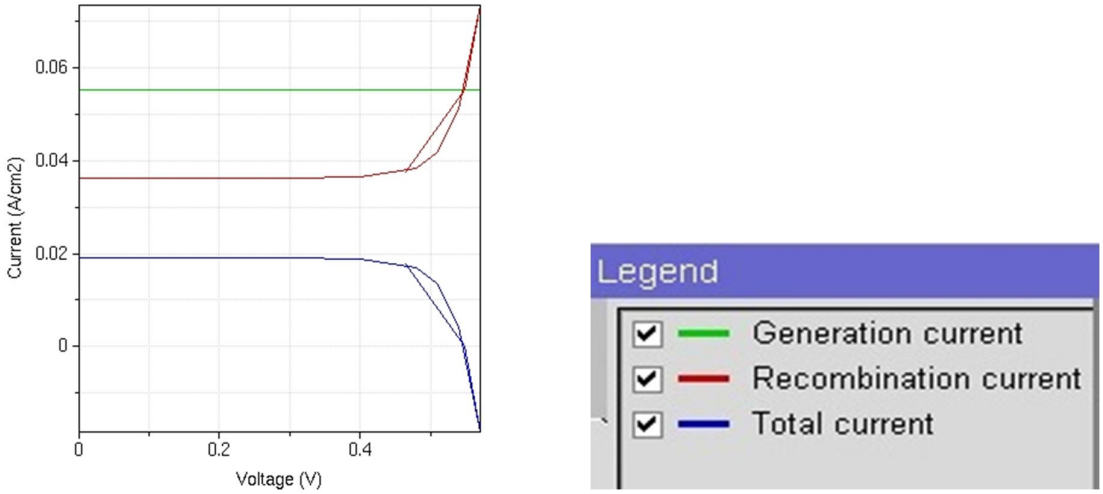

Fig. 3.2 Light J-V curve for x=0.01

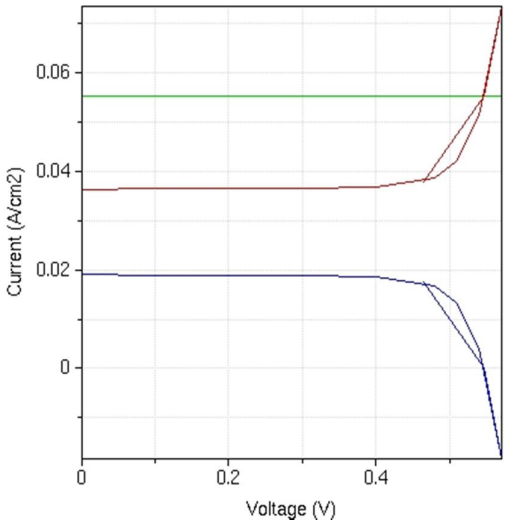

Fig. 3.3 Light J-V curve for x=0.02

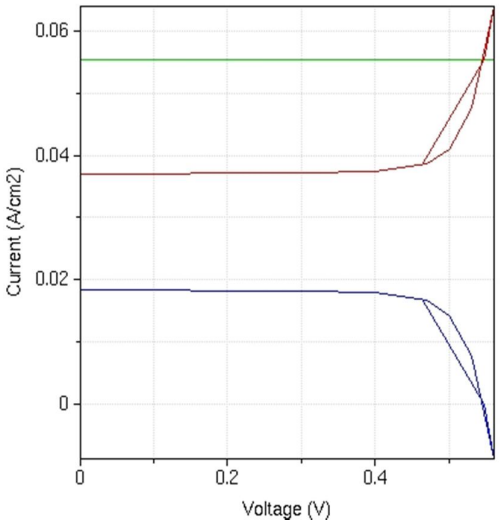

Fig. 3.4 Light J-V curve for x=0.03

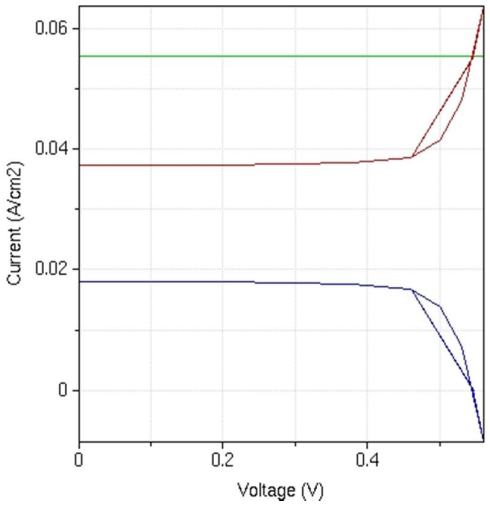

Fig. 3.5 Light J-V curve for x=0.04

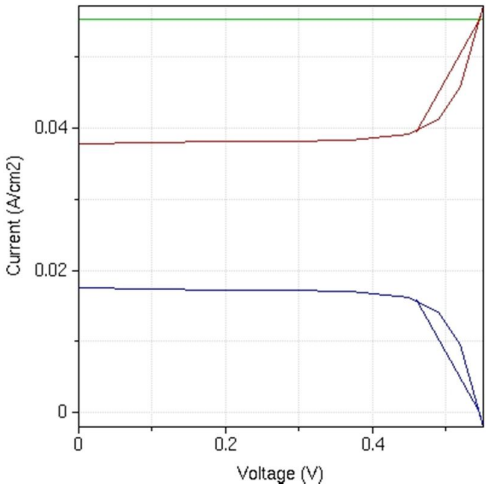

Fig. 3.6 Light J-V curve for x=0.05

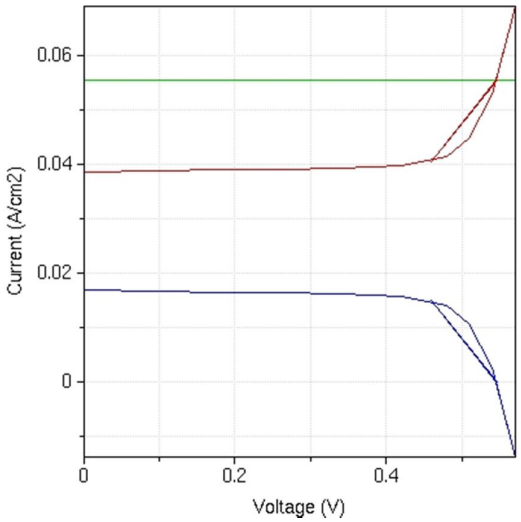

Fig. 3.7 Light J-V curve for x=0.06

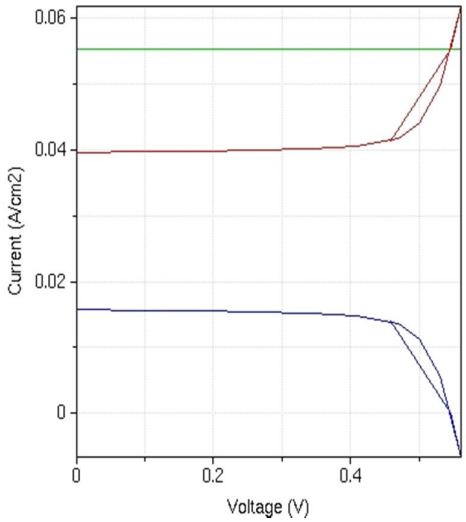

Fig. 3.8 Light J-V curve for x=0.07

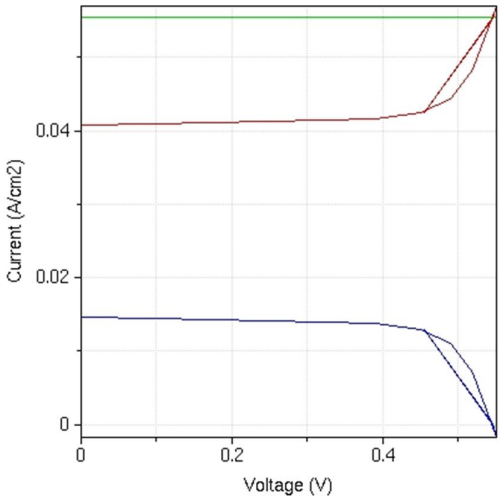

Fig. 3.9 Light J-V curve for x=0.08

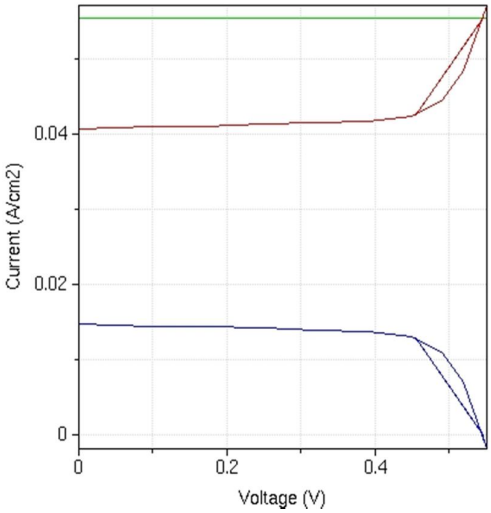

Fig. 3.10 Light J-V curve for x=0.09

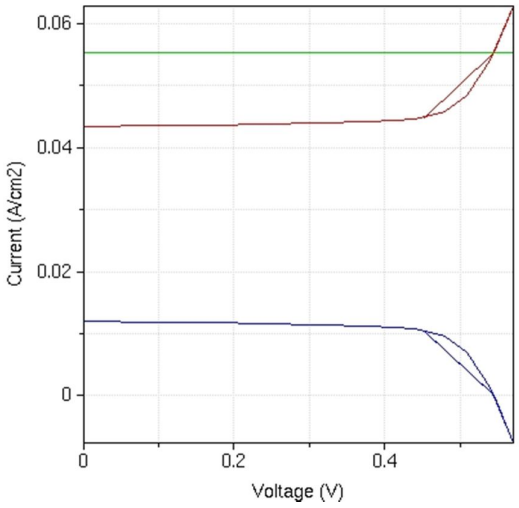

Fig. 3.11 Light J-V curve for x=0.10

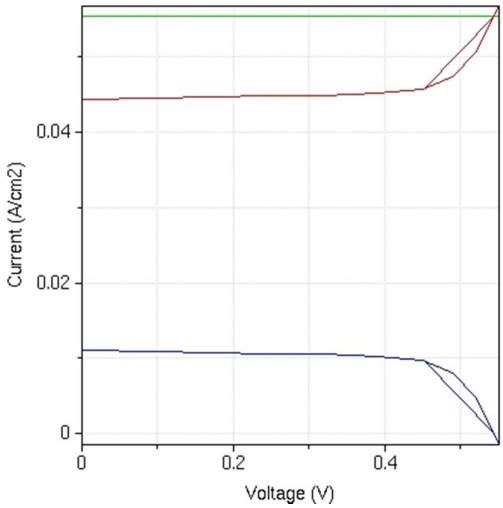

Fig. 3.12 Light J-V curve for x=0.11

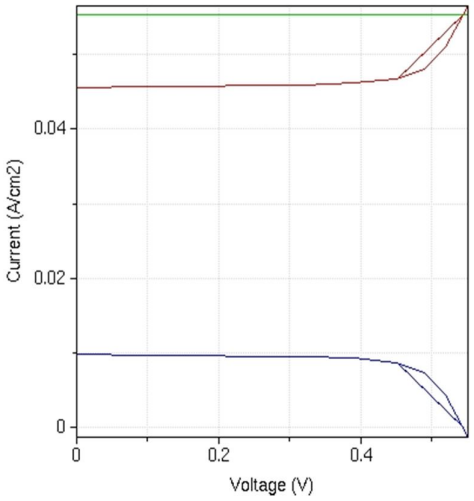

Fig. 3.13 Light J-V curve for x=0.12

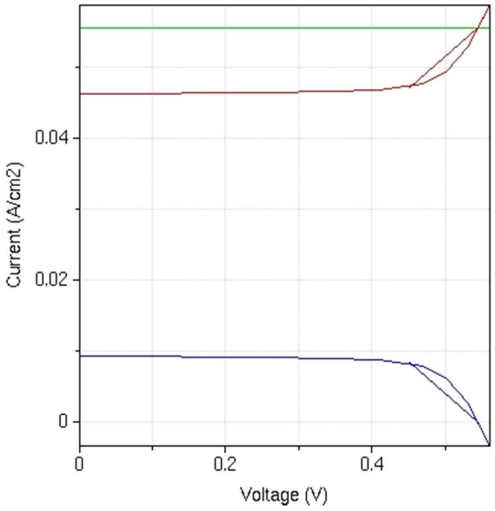

Fig. 3.14 Light J-V curve for x=0.13

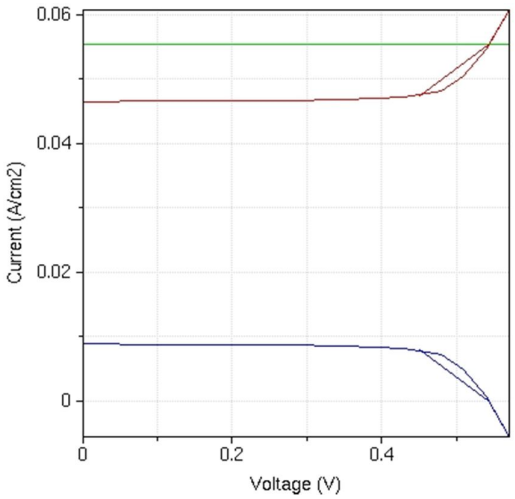

Fig. 3.15 Light J-V curve for x=0.14

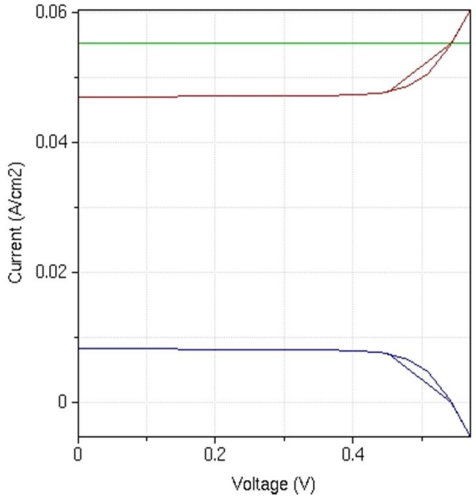

Fig. 3.16 Light J-V curve for x=0.15

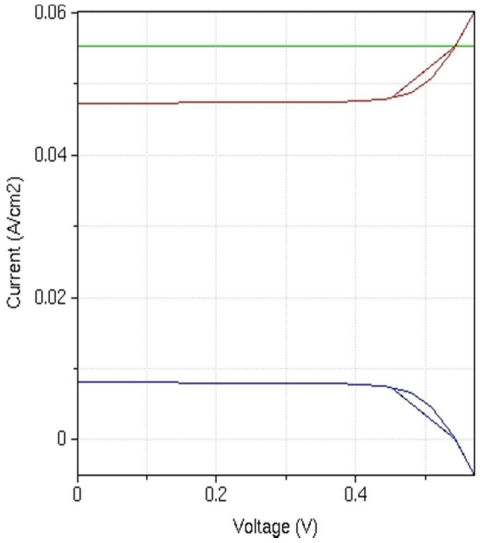

Fig. 3.17 Light J-V curve for x=0.16

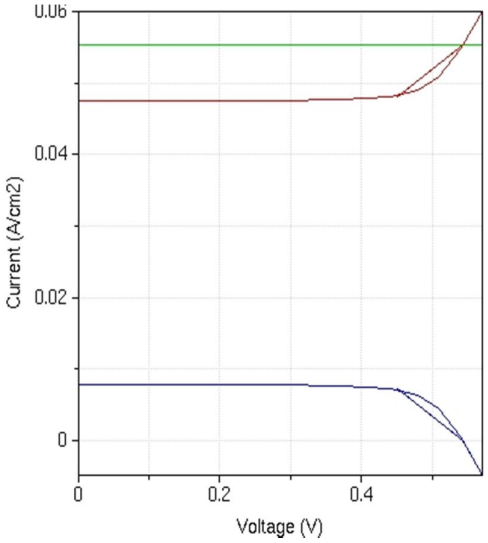

Fig. 3.18 Light J-V curve for x=0.17

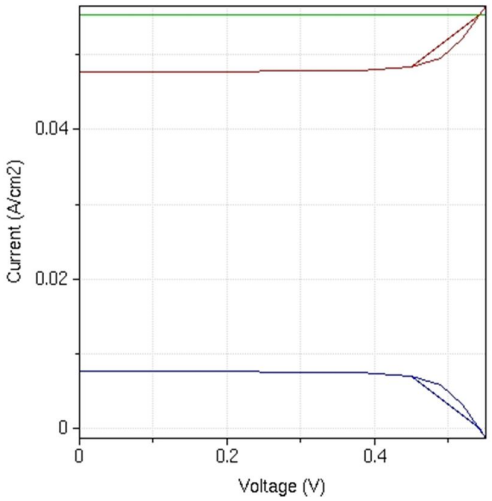

Fig. 3.19 Light J-V curve for x=0.18

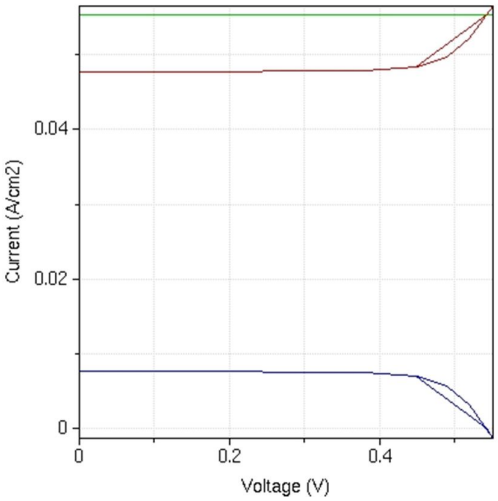

Fig. 3.20 Light J-V curve for x=0.19

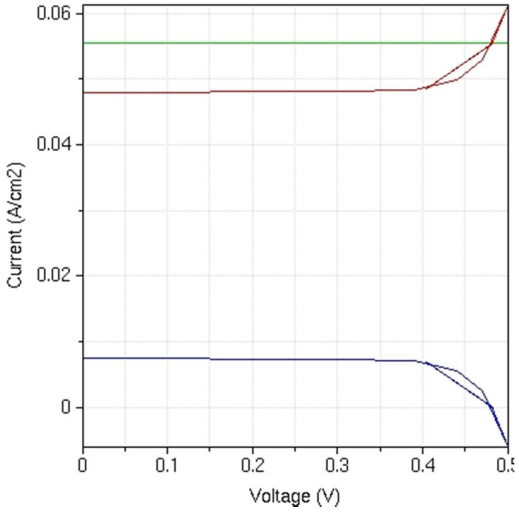

Fig. 3.21 Light J-V curve for x=0.20

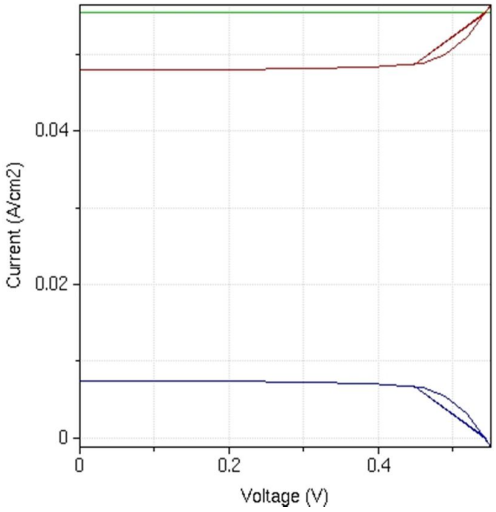

Fig. 3.22 Light J-V curve for x=0.21

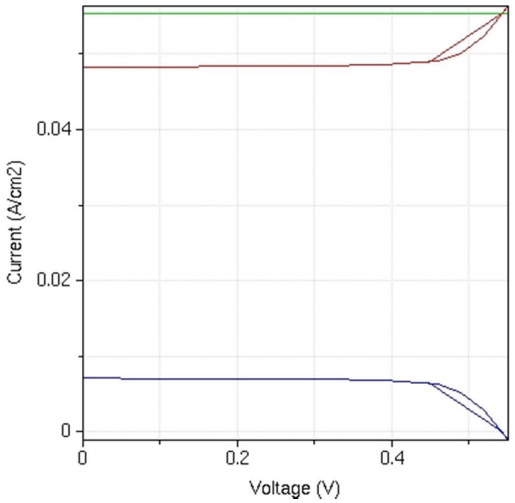

Fig. 3.23 Light J-V curve for x=0.22

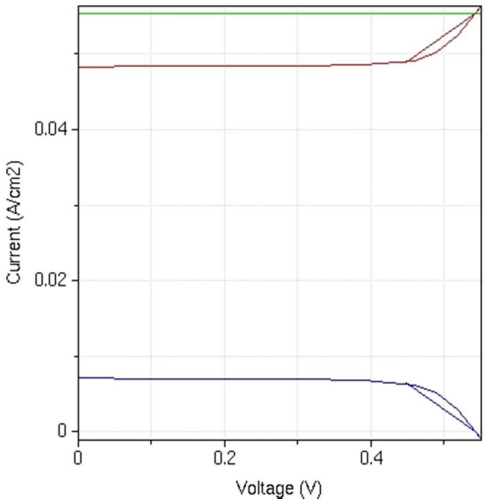

Fig. 3.24 Light J-V curve for x=0.23

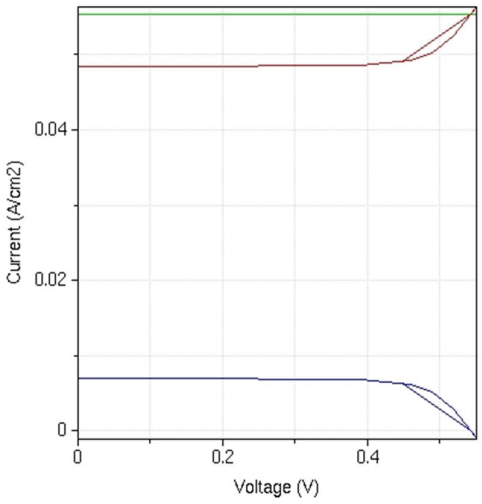

Fig. 3.25 Light J-V curve for x=0.24

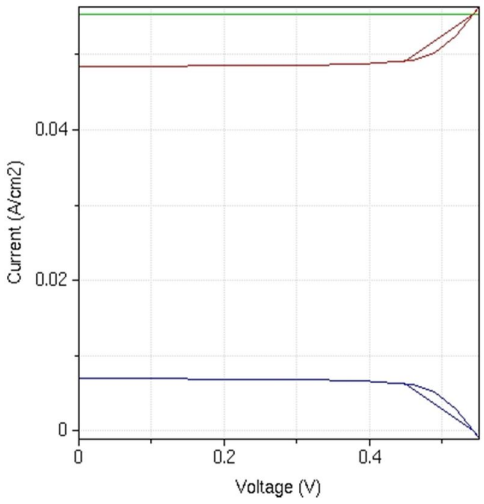

Fig. 3.26 Light J-V curve for x=0.25

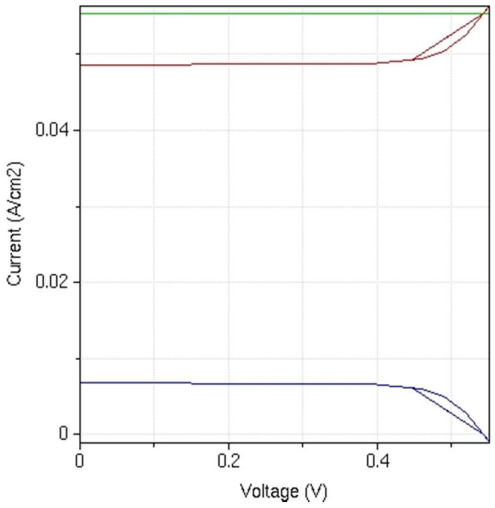

Fig. 3.27 Light J-V curve for x=0.26

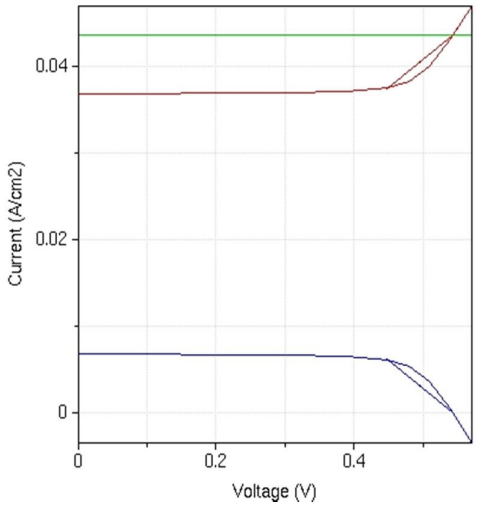

Fig. 3.28 Light J-V curve for x=0.27

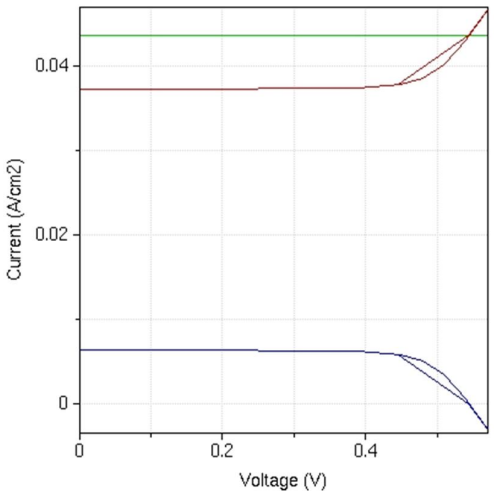

Fig. 3.29 Light J-V curve for x=0.28

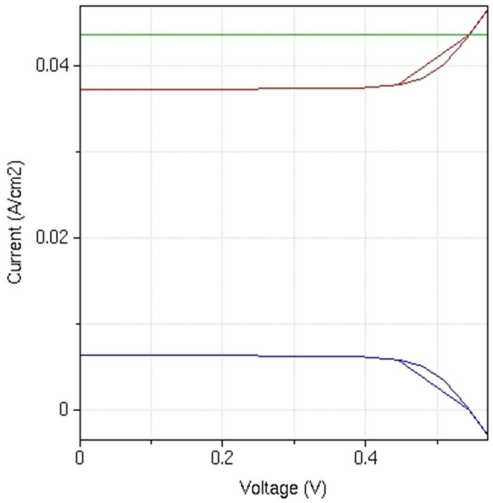

Fig. 3.30 Light J-V curve for x=0.29

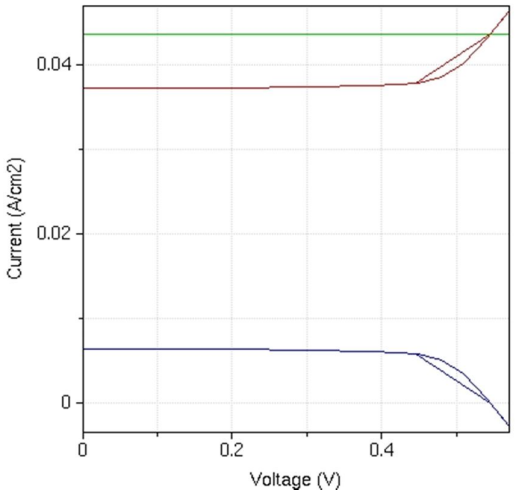

Fig. 3.31 Light J-V curve for x=0.30

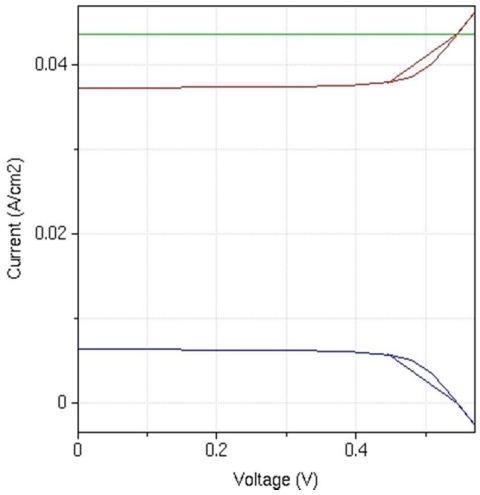

Fig. 3.32 Light J-V curve for x=0.31

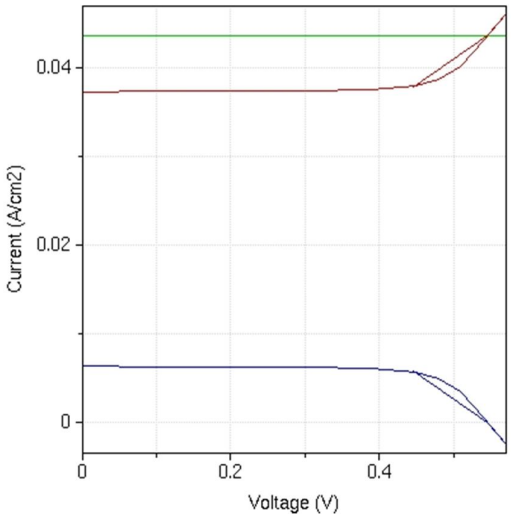

Fig. 3.33 Light J-V curve for x=0.32

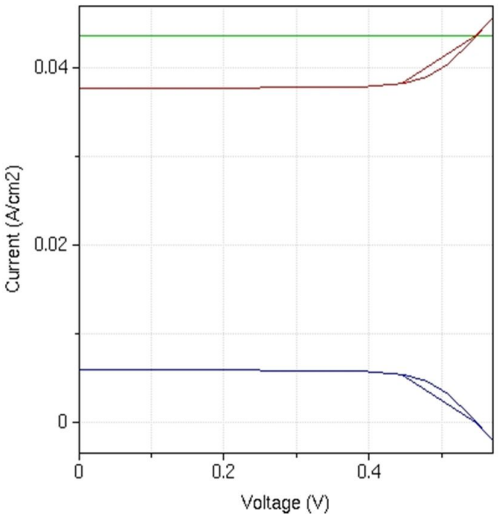

Fig. 3.34 Light J-V curve for x=0.33

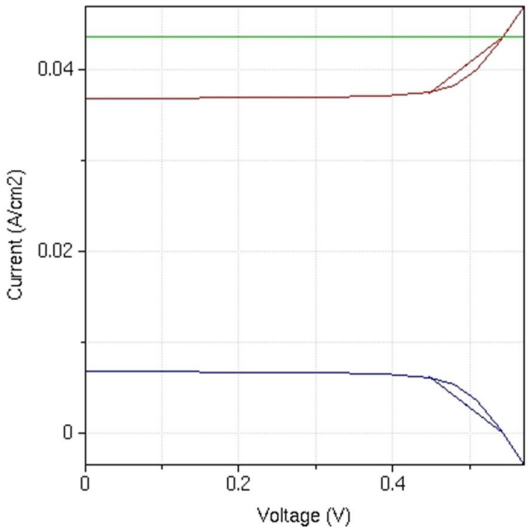

Fig. 3.35 Light J-V curve for x=0.34

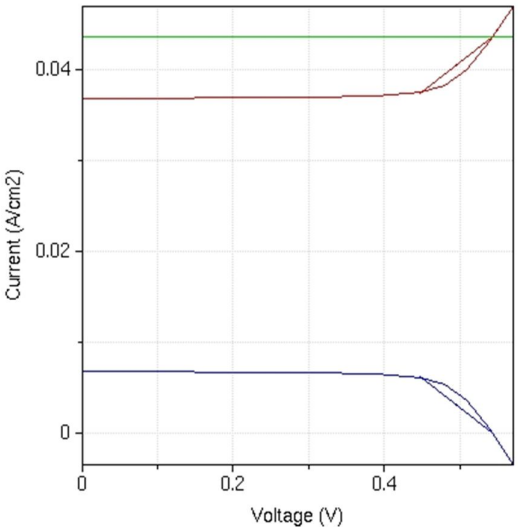

Fig. 3.36 Light J-V curve for x=0.35

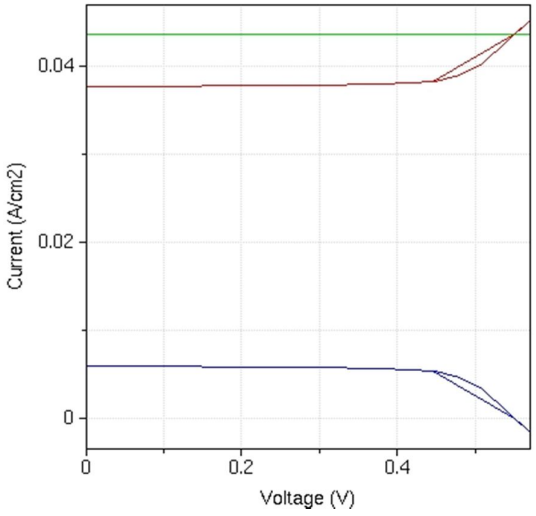

Fig. 3.37 Light J-V curve for x=0.36

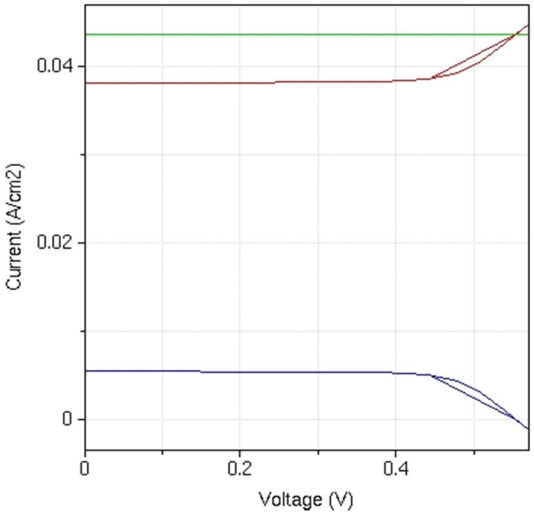

Fig. 3.38 Light J-V curve for x=0.37

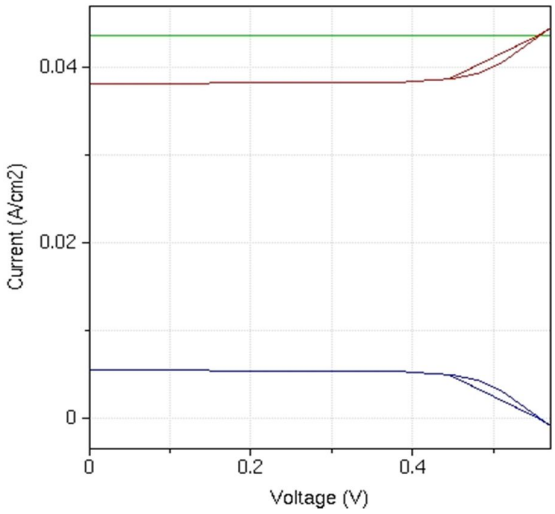

Fig. 3.39 Light J-V curve for x=0.38

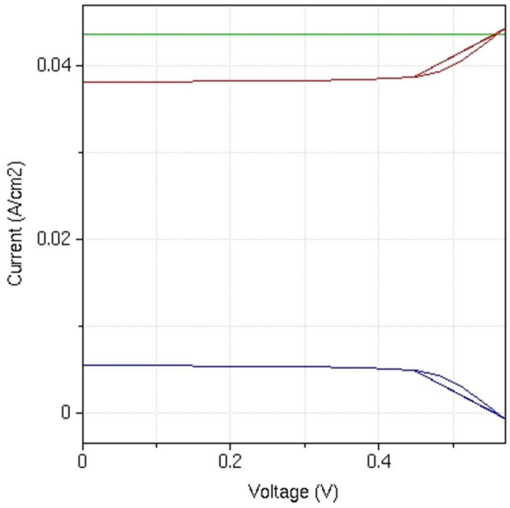

Fig. 3.40 Light J-V curve for x=0.39

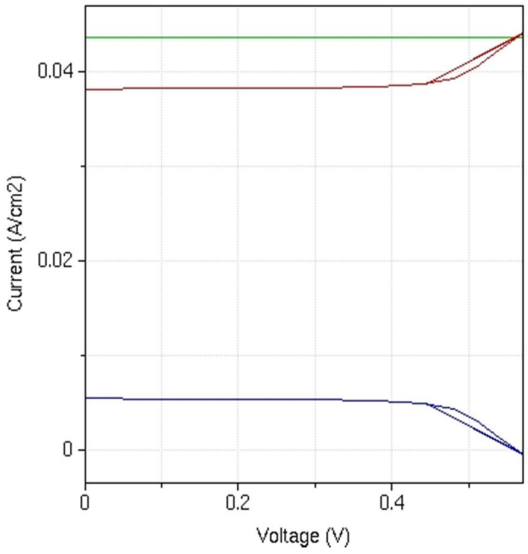

Fig. 3.41 Light J-V curve for x=0.40

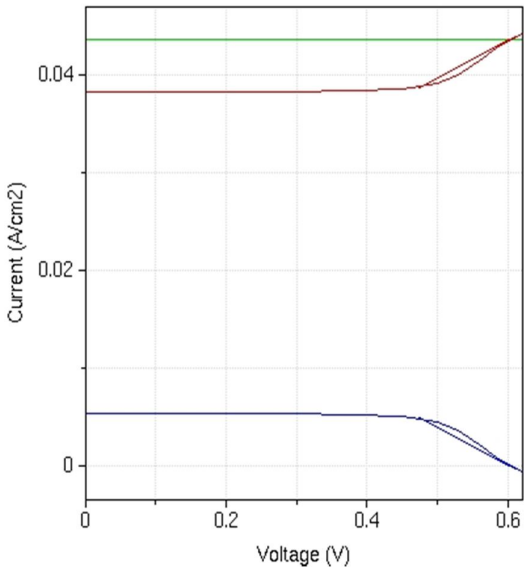

Fig. 3.42 Light J-V curve for x=0.41

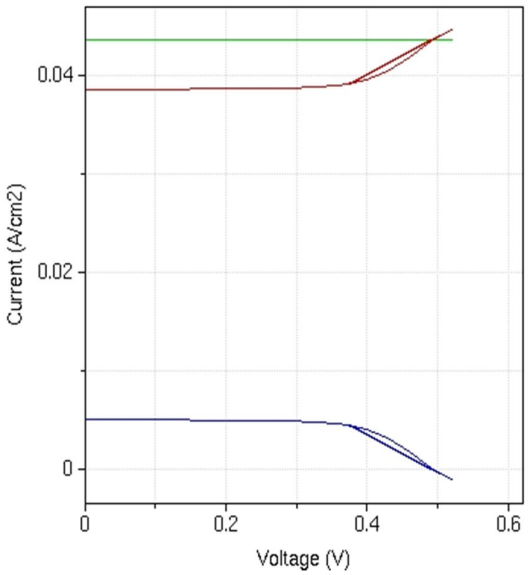

Fig. 3.43 Light J-V curve for x=0.42

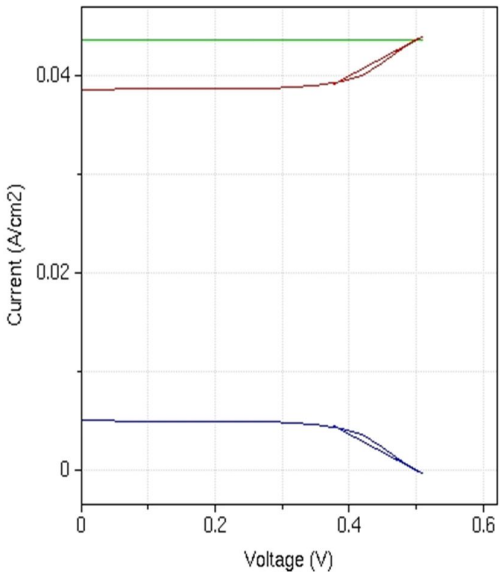

Fig. 3.44 Light J-V curve for x=0.43

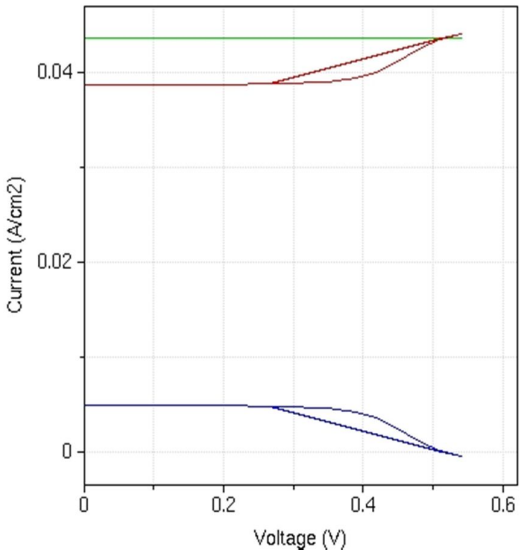

Fig. 3.45 Light J-V curve for x=0.44

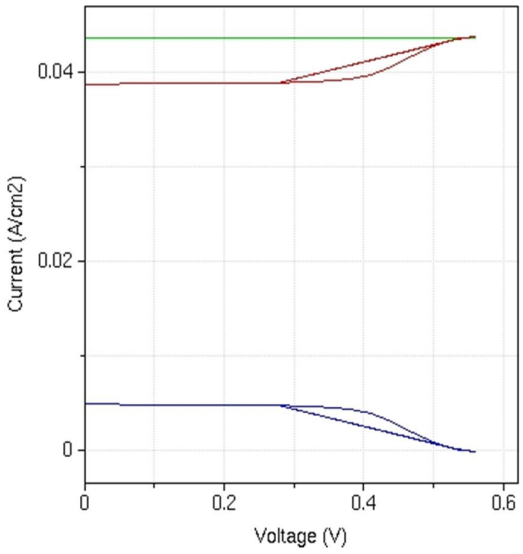

Fig. 3.46 Light J-V curve for x=0.45

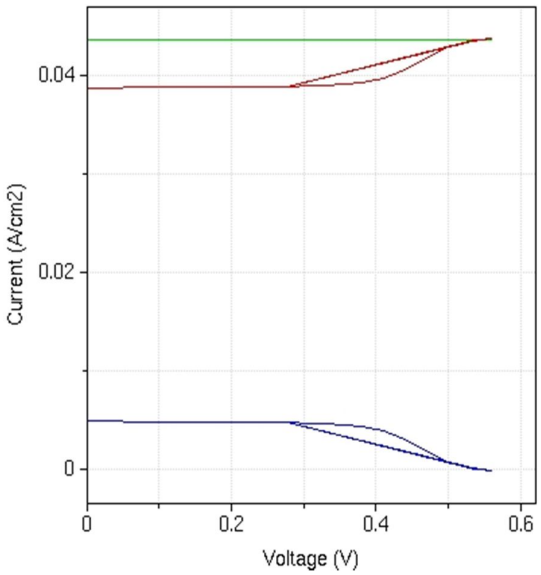

Fig. 3.47 Light J-V curve for x=0.46

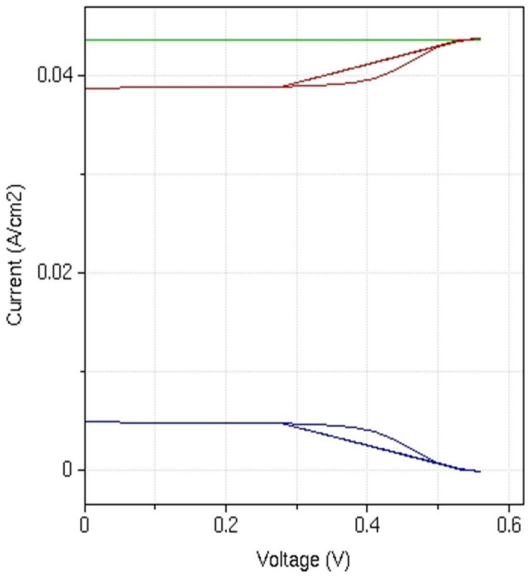

Fig. 3.48 Light J-V curve for x=0.47

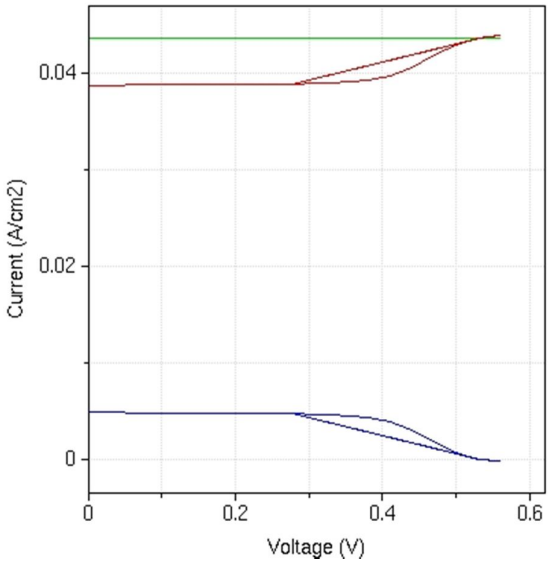

Fig. 3.49 Light J-V curve for x=0.48

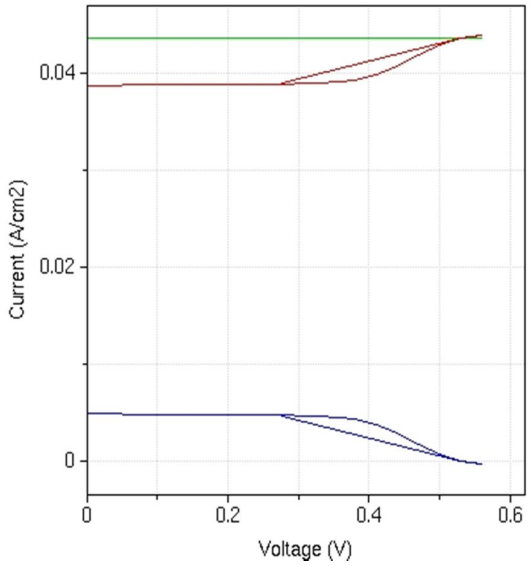

Fig. 3.50 Light J-V curve for x=0.49

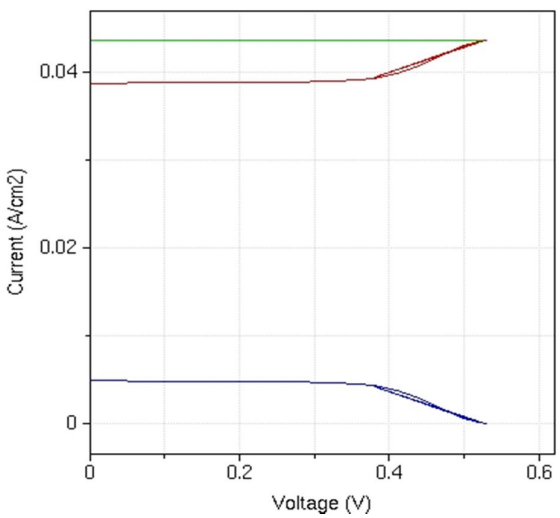

Fig. 3.51 Light J-V curve for x=0.50

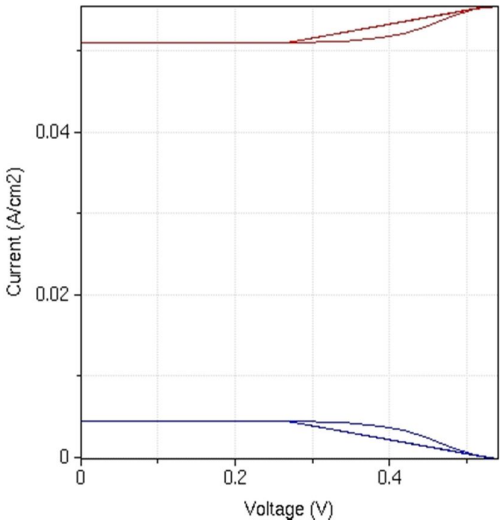

Fig. 3.52 Light J-V curve for x=0.51

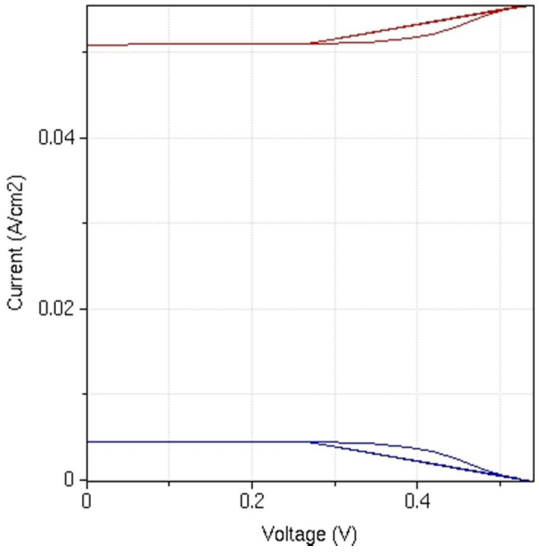

Fig. 3.53 Light J-V curve for x=0.52

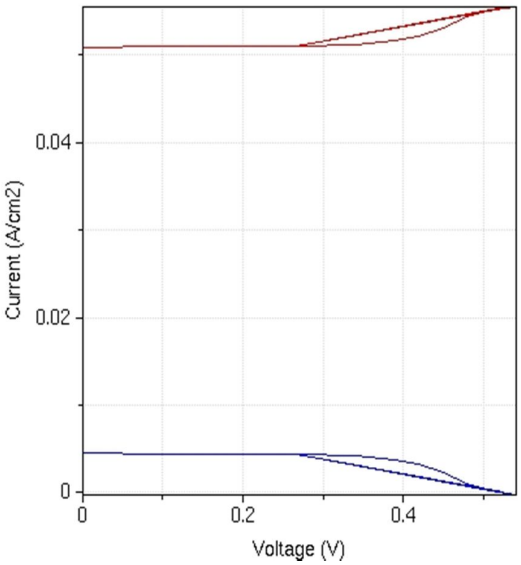

Fig. 3.54 Light J-V curve for x=0.53

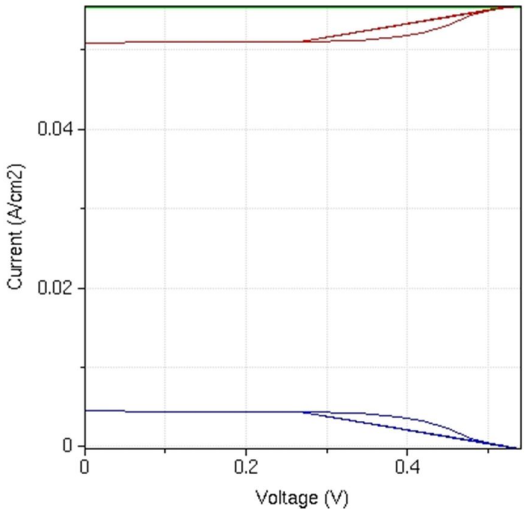

Fig. 3.55 Light J-V curve for x=0.54

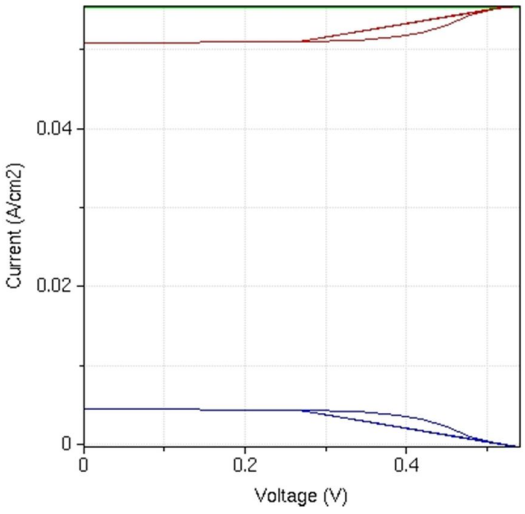

Fig. 3.56 Light J-V curve for x=0.55

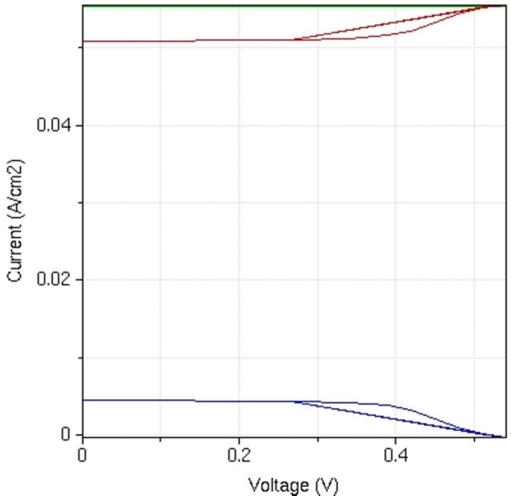

Fig. 3.57 Light J-V curve for x=0.56

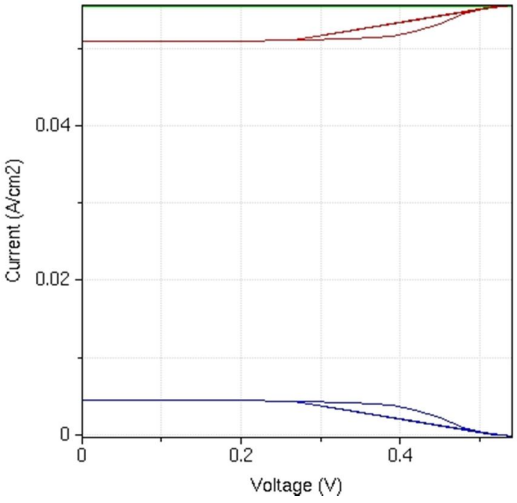

Fig. 3.58 Light J-V curve for x=0.57

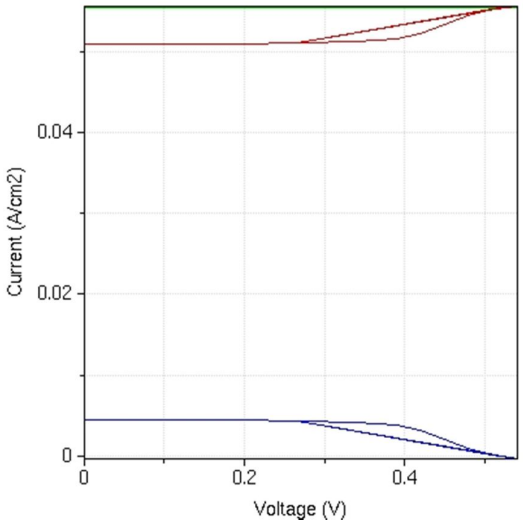

Fig. 3.59 Light J-V curve for x=0.58

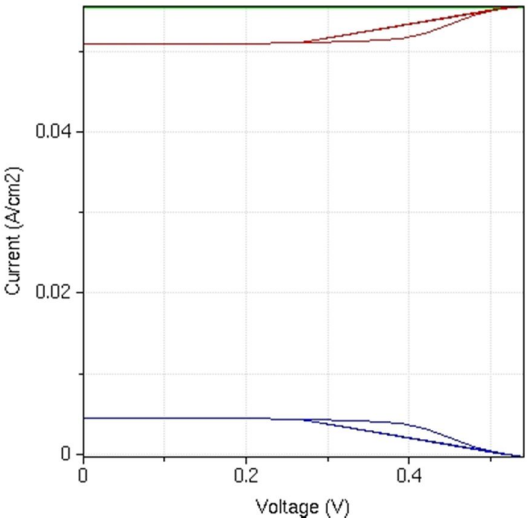

Fig. 3.60 Light J-V curve for x=0.59

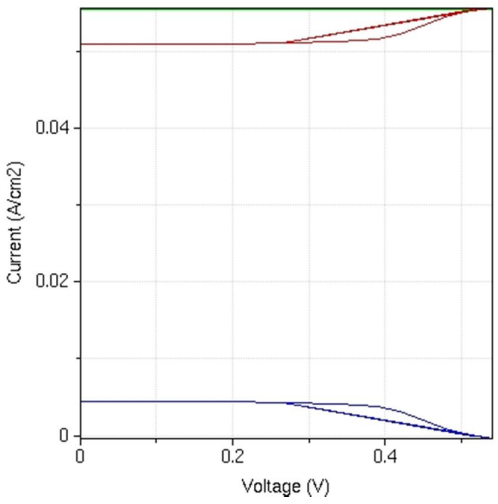

Fig. 3.61 Light J-V curve for x=0.60

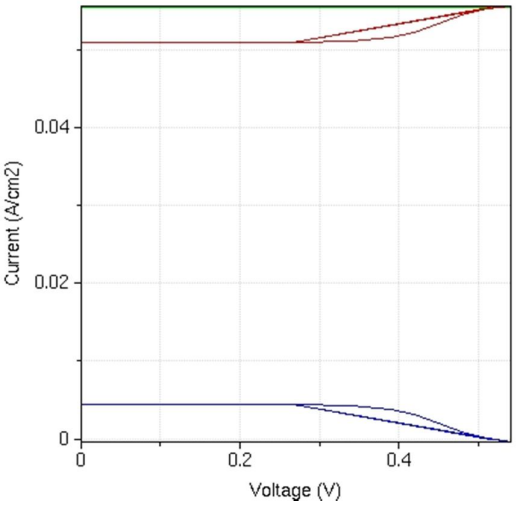

Fig. 3.62 Light J-V curve for x=0.61

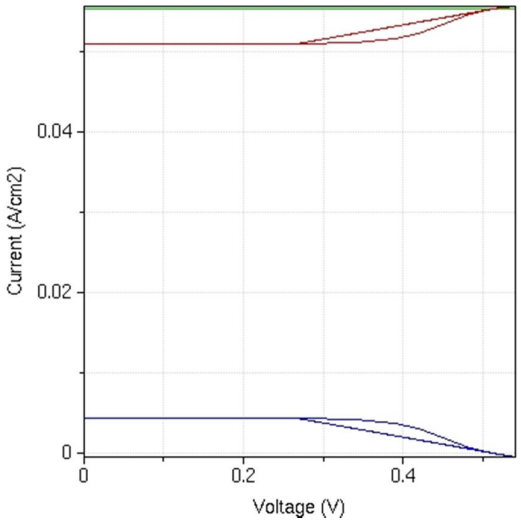

Fig. 3.63 Light J-V curve for x=0.62

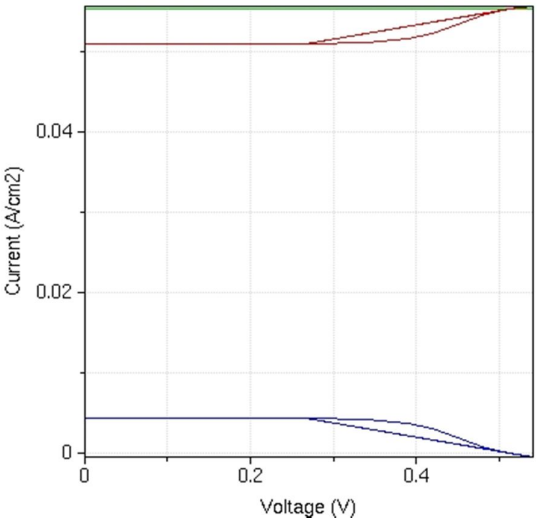

Fig. 3.49 Light J-V curve for x=0.63

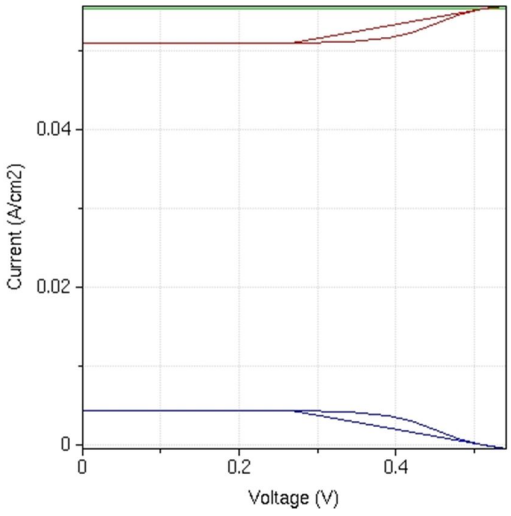

Fig. 3.65 Light J-V curve for x=0.64

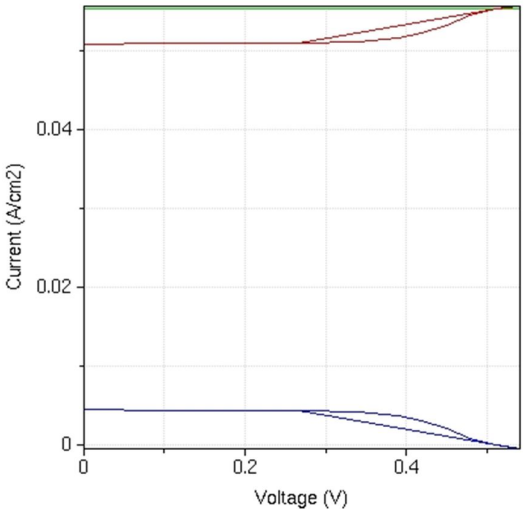

Fig. 3.66 Light J-V curve for x=0.65

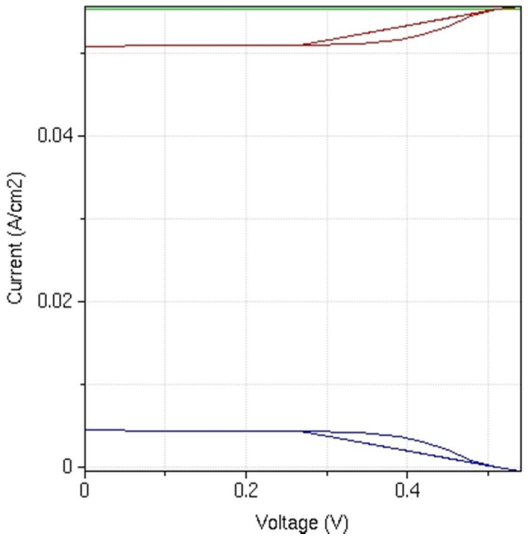

Fig. 3.67 Light J-V curve for x=0.66

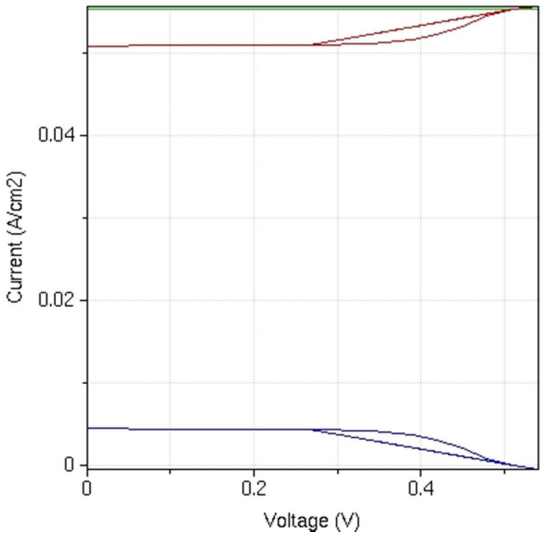

Fig. 3.68 Light J-V curve for x=0.67

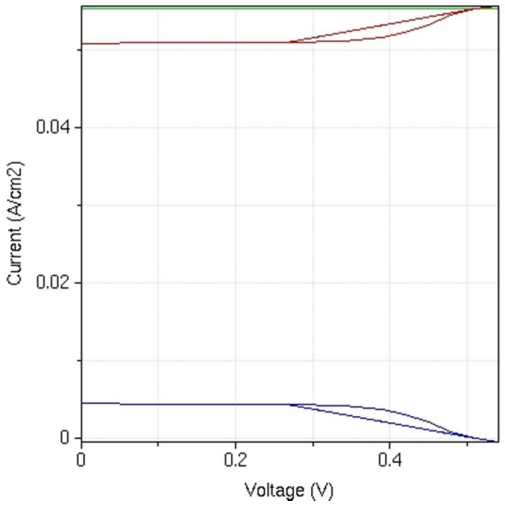

Fig. 3.69 Light J-V curve for x=0.68

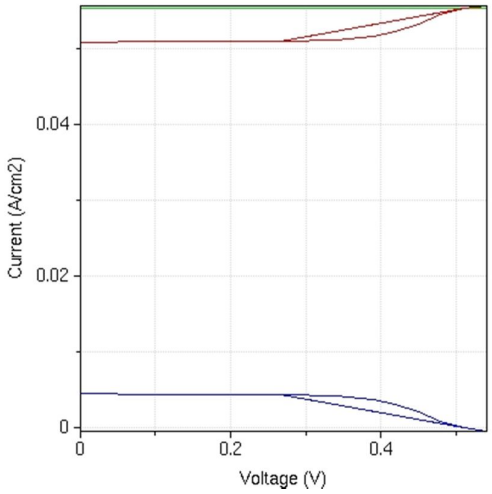

Fig. 3.70 Light J-V curve for x=0.69

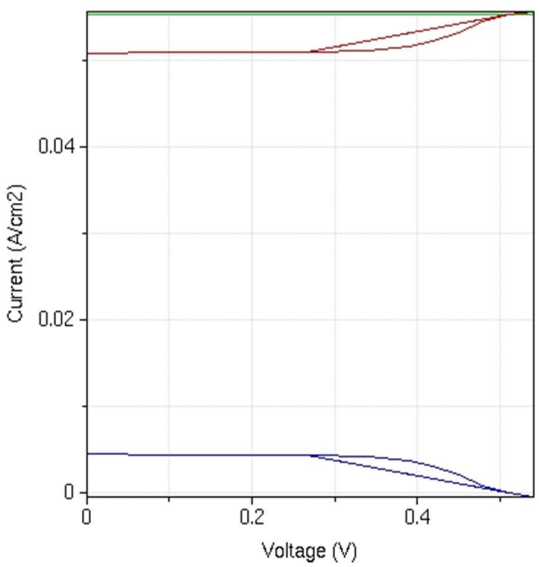

Fig. 3.71 Light J-V curve for x=0.70

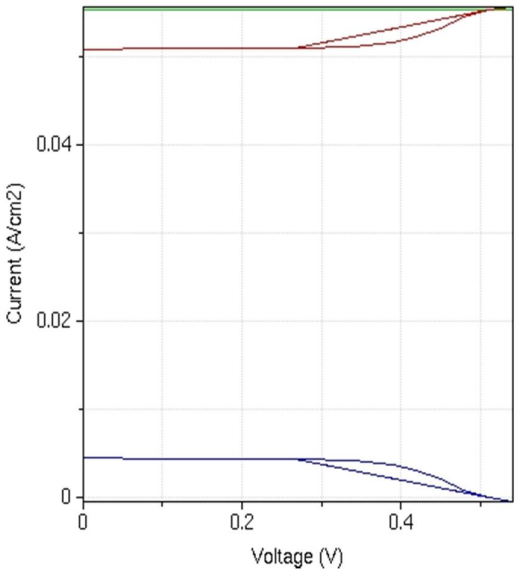

Fig. 3.72 Light J-V curve for x=0.71

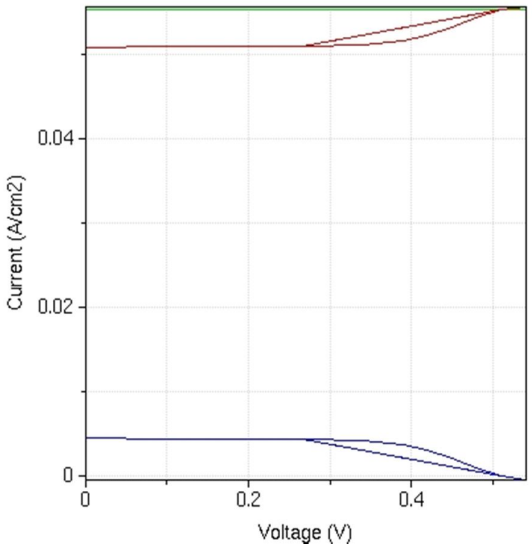

Fig. 3.73 Light J-V curve for x=0.72

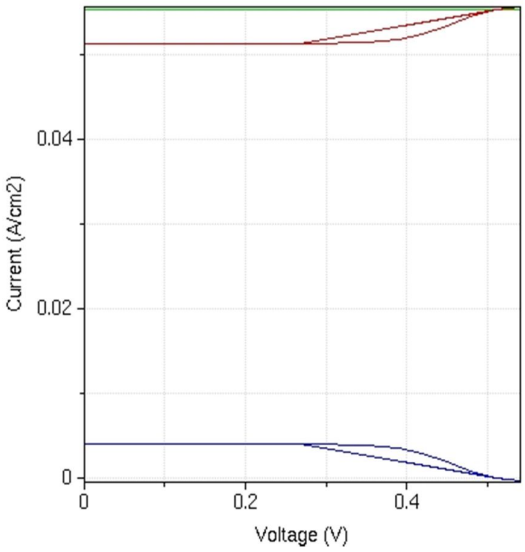

Fig. 3.74 Light J-V curve for x=0.73

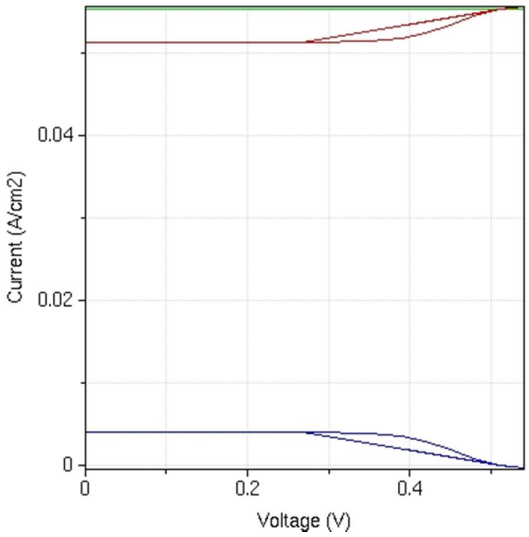

Fig. 3.75 Light J-V curve for x=0.74

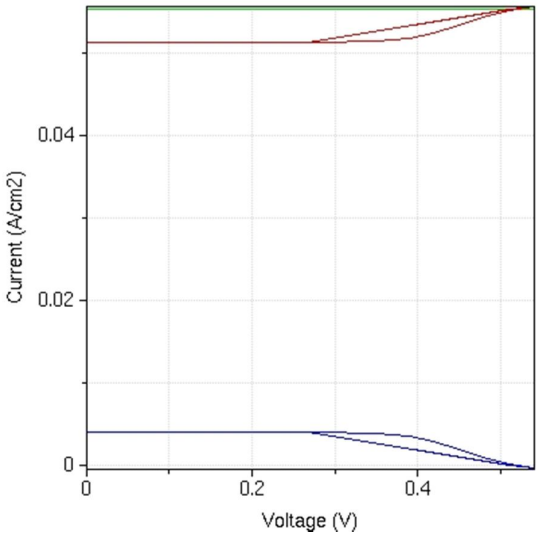

Fig. 3.76 Light J-V curve for x=0.75

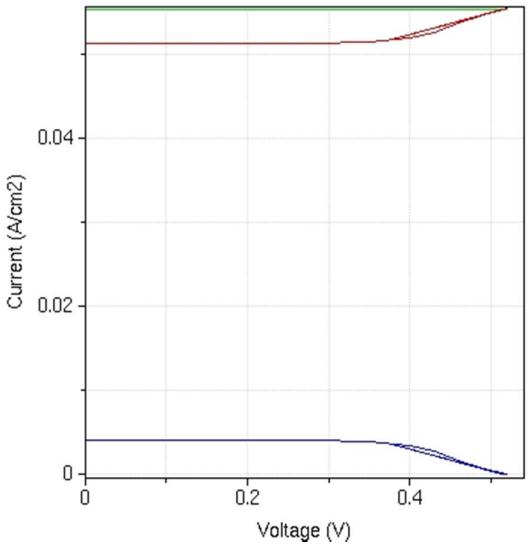

Fig. 3.77 Light J-V curve for x=0.76

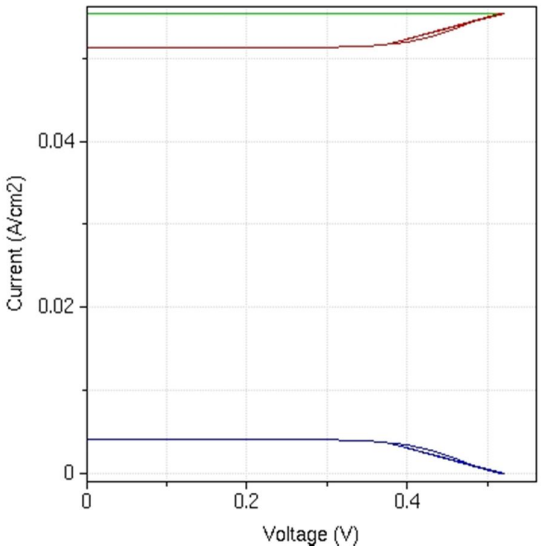

Fig. 3.76 Light J-V curve for x=0.77

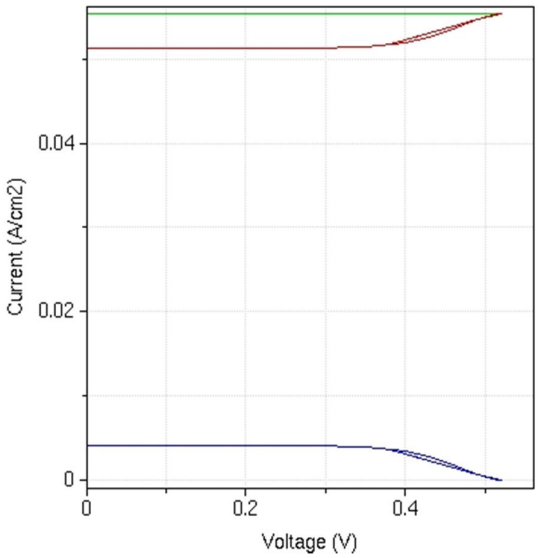

Fig. 3.79 Light J-V curve for x=0.78

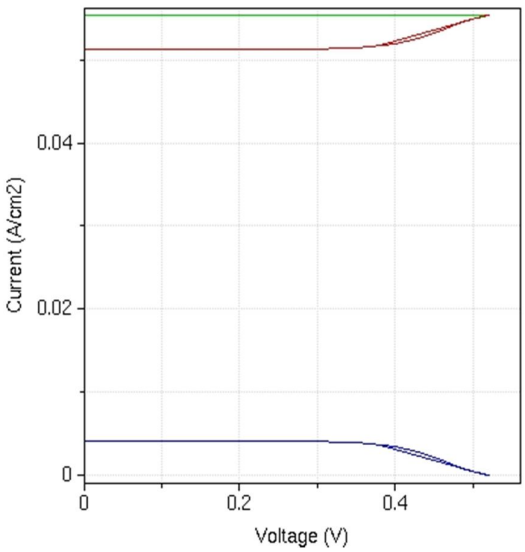

Fig. 3.80 Light J-V curve for x=0.79

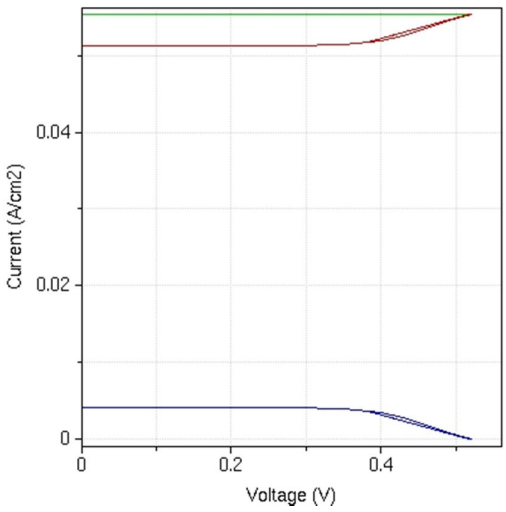

Fig. 3.81 Light J-V curve for x=0.80

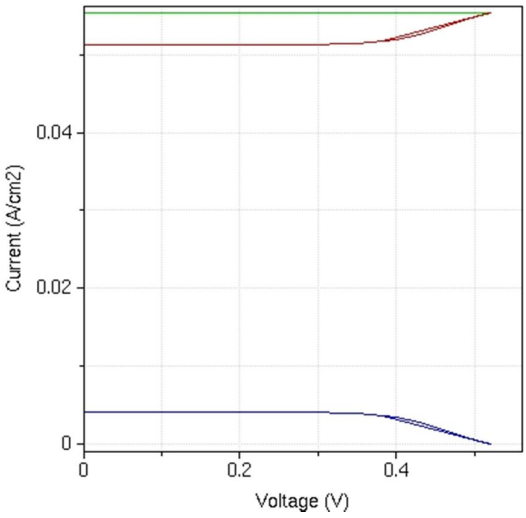

Fig. 3.82 Light J-V curve for x=0.81

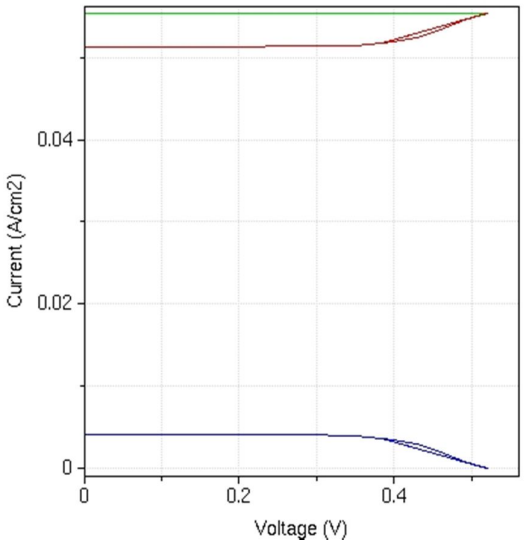

Fig. 3.83 Light J-V curve for x=0.82

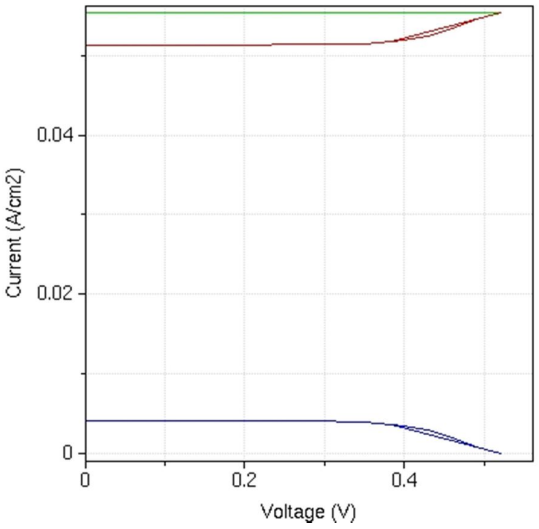

Fig. 3.84 Light J-V curve for x=0.83

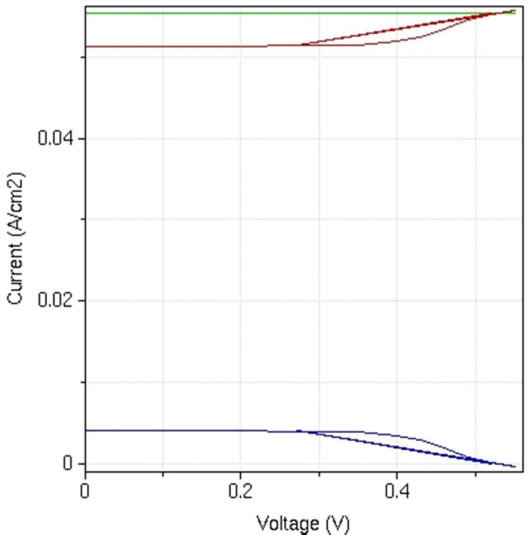

Fig. 3.85 Light J-V curve for x=0.84

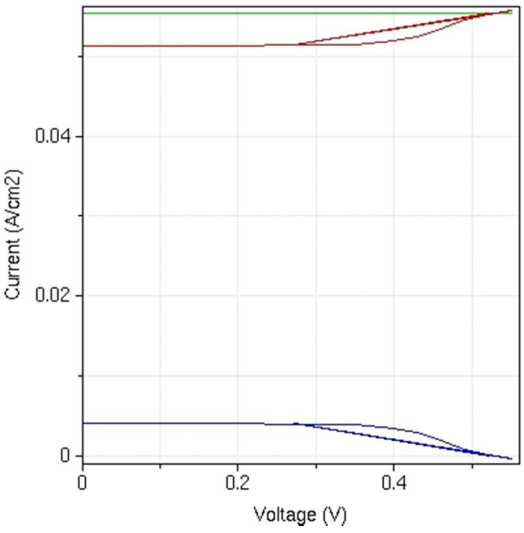

Fig. 3.86 Light J-V curve for x=0.85

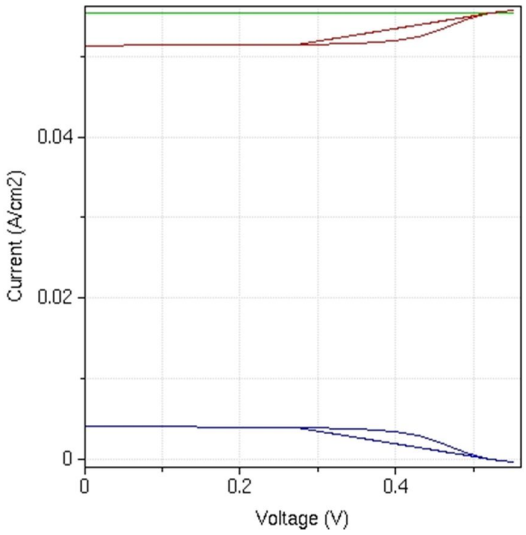

Fig. 3.87 Light J-V curve for x=0.86

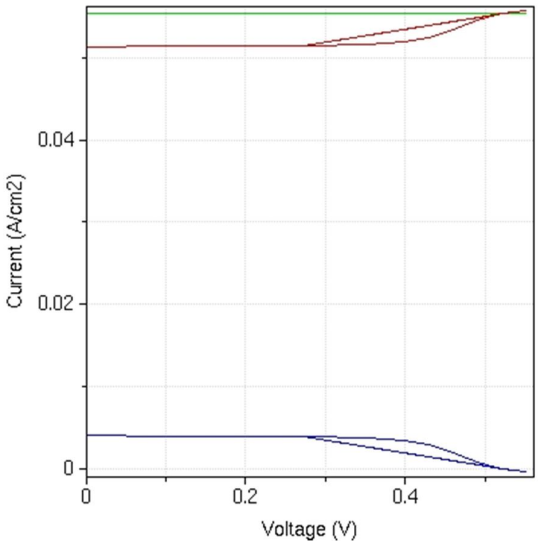

Fig. 3.88 Light J-V curve for x=0.87

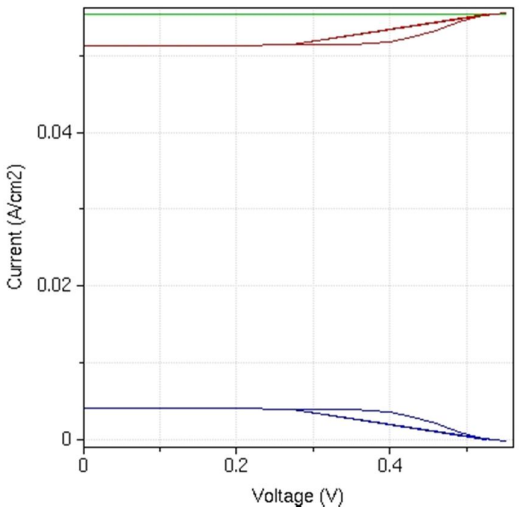

Fig. 3.89 Light J-V curve for x=0.88

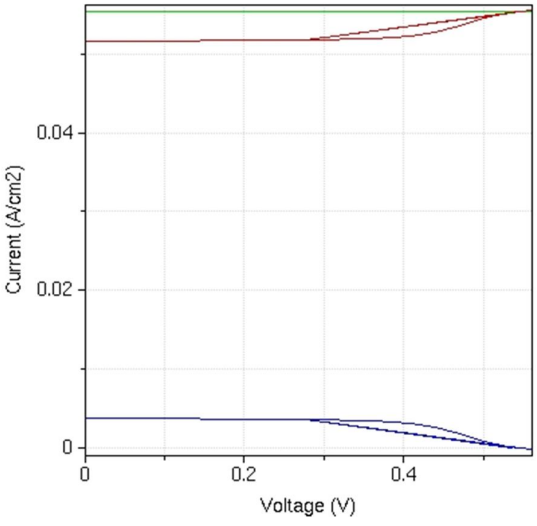

Fig. 3.90 Light J-V curve for x=0.89

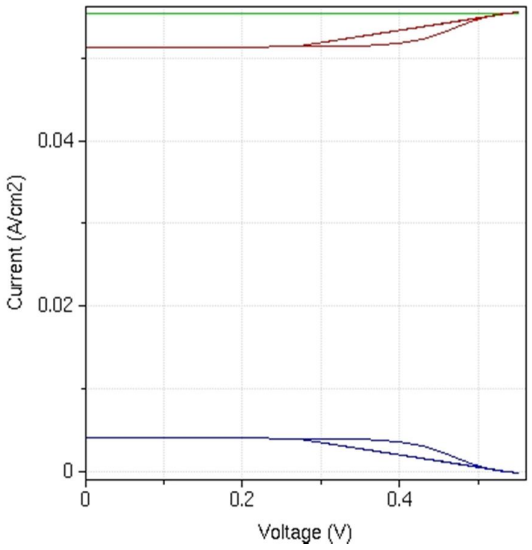

Fig. 3.91 Light J-V curve for x=0.90

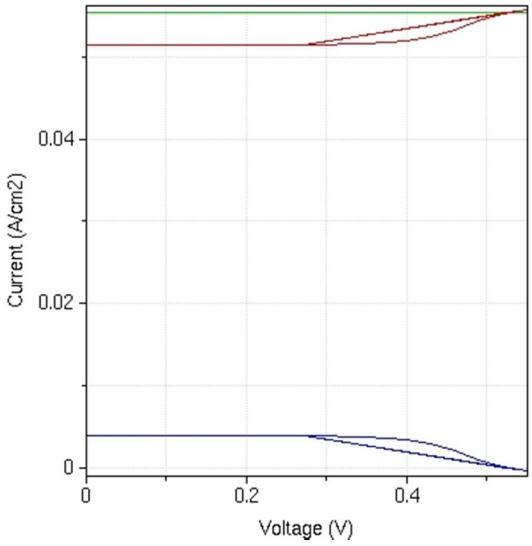

Fig. 3.91 Light J-V curve for x=0.91

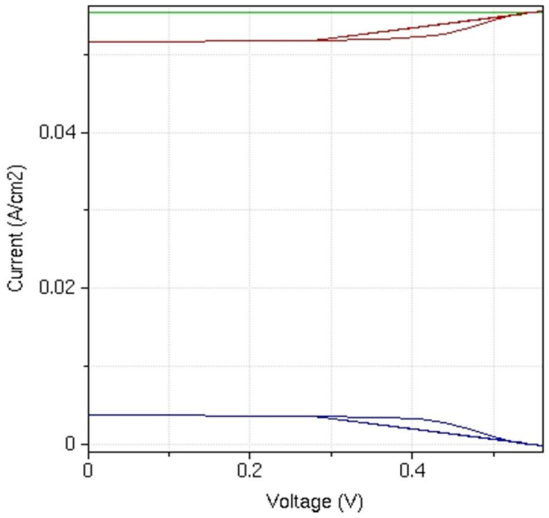

Fig. 3.93 Light J-V curve for x=0.92

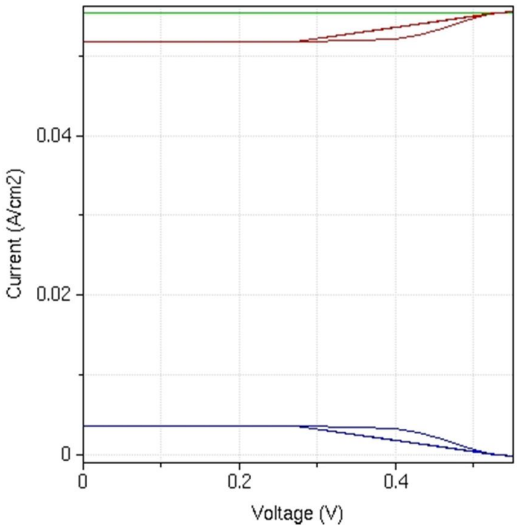

Fig. 3.94 Light J-V curve for x=0.93

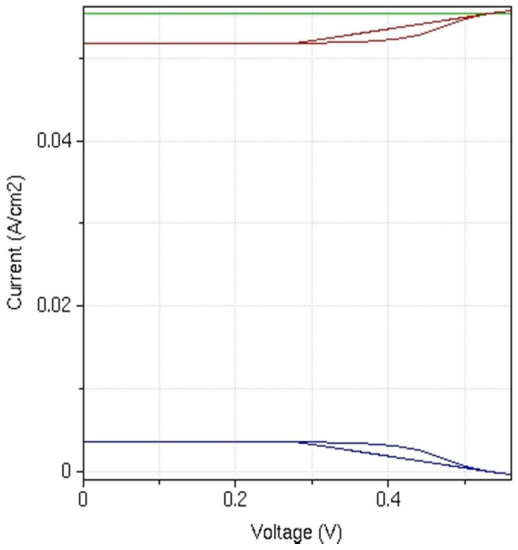

Fig. 3.95 Light J-V curve for x=0.94

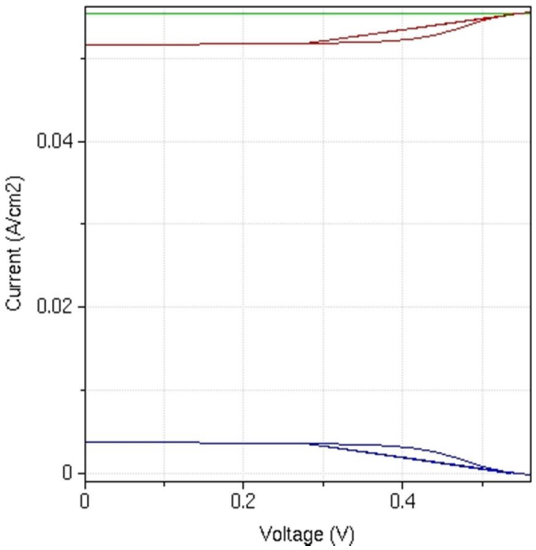

Fig. 3.96 Light J-V curve for x=0.95

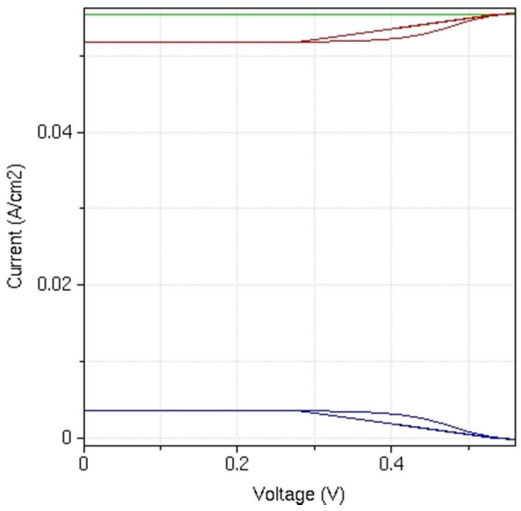

Fig. 3.97 Light J-V curve for x=0.96

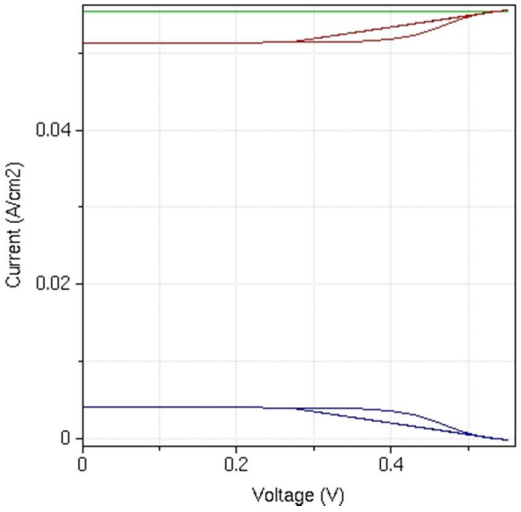

Fig. 3.98 Light J-V curve for x=0.97

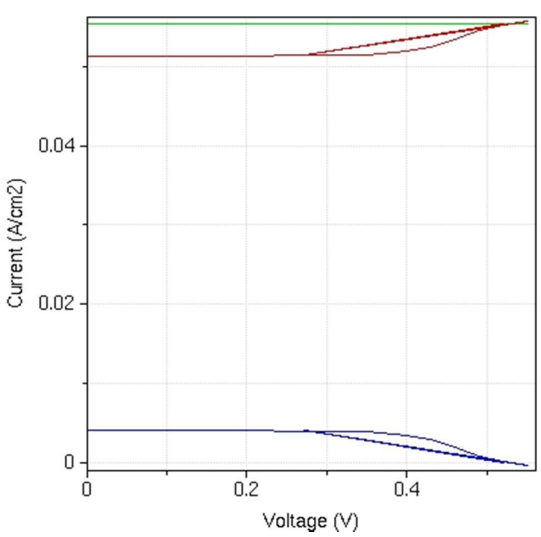

Fig. 3.99 Light J-V curve for x=0.98

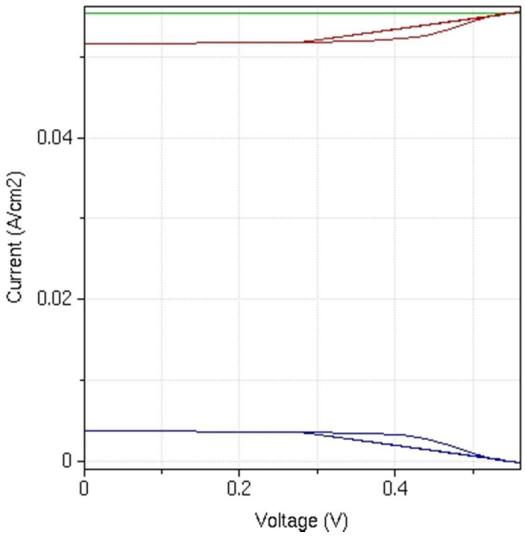

Fig. 3.100 Light J-V curve for x=0.9

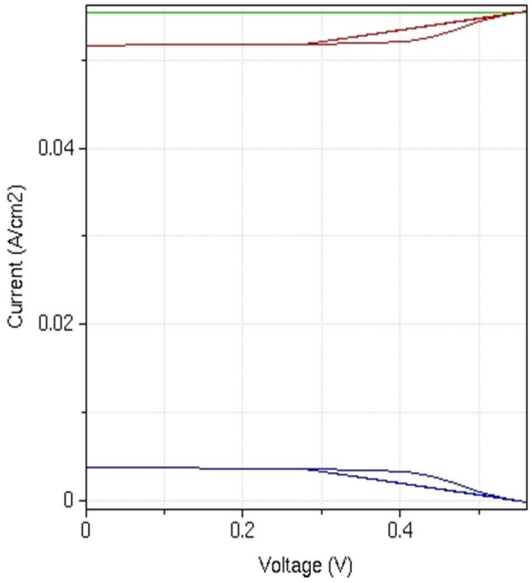

Fig. 3.101 Light J-V curve for x=1.00

Chapter 3.3 Result

3.3.1 Short-Circuit Current Density (J_{SC})

From the J-V curve two quantities are found. One of them is Short-Circuit Current Density (J_{SC}).The short-circuit condition occurs when the resistive load is zero, so that V= 0. In this case, I_F is zero, and the short-circuit current density, J_{sc} is given by equation

$$J_{sc} = J_L$$

When comparing solar cells of the same material type, the most critical material parameter is the diffusion length and surface passivation. In a cell with perfectly passivated surface and uniform generation, the equation for the short-circuit current can be approximated as:

$$J_{sc}=q*G*W \qquad [31]$$

Here, W = Thickness of absorber(AlGaAs layer).
q = Charge of an electron.
G = Generation rate of electron hole pair.

3.3.2 Open-Circuit Voltage (V_{OC})

Open-circuit condition occurs when the load resistance is infinity. The net current is zero in this case, which finally gives the expression of the open-circuit voltage, V_{oc}, as shown in equation .

$$V_{oc} = (nkT / q) \ln (1 + (J_L/ J_S))$$

3.3.3 Fill Factor (FF)

Fill Factor is used to measure the squareness of the I-V curve of a solar cell. This is the ratio of the maximum output power, Pm, to the product of short-circuit current (I_{sc}) and the open-circuit voltage (V_{oc}). Fill factor is commonly abbreviated as FF. A higher FF is desirable, since it increases the maximum output power.

$$FF = \frac{V_{OC} - \ln(V_{OC} + 0.72)}{V_{OC} + 1} \qquad [32]$$

where v_{oc} is defined as a "normalized V_{oc}":

$$V_{oc} = \frac{q}{nkT} V_{oc} \quad [32]$$

Here,

n= Ideality factor

q= Charge of an electron = 1.6 × 10-19 Coulomb

k= Boltzmann constant

T= Temperature in K

3.3.4 Efficiency (η)

The efficiency is the most commonly used parameter to compare the performance of one solar cell to another. Efficiency is defined as the ratio of energy output from the solar cell to input energy from the sun. In addition to reflecting the performance of the solar cell itself, the efficiency depends on the spectrum and intensity of the incident sunlight and the temperature of the solar cell.

$$\eta = ((V_{OC} * I_{SC} * FF)/E)/100\%$$

Here,

E = Solar irradiance (in W/cm^2)

The use of the solar cell for terrestrial applications is considered. So, to account for the incident sunlight, AM1.5G illumination was considered in the simulation code, as this is the standard terrestrial illumination. According to this, the solar irradiance, E, is taken to be 1000 W/m^2 or 0.1 W/cm^2. It was also considered that the device is working under 1 sun i.e. no concentrator is used.

3.4 J_{SC}, V_{OC}, FF and Efficiency For Different Values of Mole Fraction(x)

Table 3.1 Values J_{SC}, V_{OC}, FF and Efficiency from Mole Fraction 0.00 to 1.00

x	I_{SC} (A/cm2)	V_{OC}(V)	Fill Factor	Efficiency
0.00	0.0196	0.5483	0.8158	8.695
0.01	0.01915	0.548	0.8157	8.56
0.02	0.01901	0.5475	0.8156	8.49
0.03	0.01843	0.5472	0.8156	8.225
0.04	0.01812	0.5467	0.8154	8.078
0.05	0.01749	0.5456	0.8152	7.78
0.06	0.01672	0.5453	0.8151	7.43
0.07	0.01577	0.545	0.815	7.0046
0.08	0.014162	0.5447	0.8149	6.2862
0.09	0.01459	0.5443	0.8149	6.4714
0.10	0.01201	0.54	0.8138	5.2778
0.11	0.0116	0.5446	0.8149	5.148
0.12	0.009872	0.5443	0.8149	4.3487
0.13	0.009284	0.5441	0.8148	4.1159
0.14	0.008905	0.5438	0.8147	3.9452
0.15	0.008368	0.5437	08147	3.7066
0.16	0.008117	0.5434	0.8146	3.593

x	I_{SC} (A/cm2)	V_{OC}(V)	Fill Factor	Efficiency
0.17	0.007922	0.54	0.8138	3.4813
0.18	0.007747	0.5427	0.8145	3.4244
0.19	0.007683	0.5424	0.8144	3.3938
0.20	0.007411	0.5427	0.8145	3.2759
0.21	0.007382	0.5425	0.8145	3.2615
0.22	0.007081	0.5427	0.8145	3.13
0.23	0.007064	0.5426	0.8145	3.1217
0.24	0.006953	0.5427	0.8145	3.0734
0.25	0.006934	0.5429	0.8145	3.0662
0.26	0.006777	0.54	0.8145	2.9782
0.27	0.006303	0.5458	0.8152	2.8044
0.28	0.0066534	0.5438	0.8147	2.9477
0.29	0.006776	0.5434	0.8146	2.999
0.30	0.006374	0.5441	0.8148	2.8258
0.31	0.006362	0.544	0.8148	2.8199
0.32	0.006353	0.5448	0.815	2.8208
0.33	0.006334	0.5452	0.8151	2.8148
0.34	0.005924	0.543	0.8145	2.62
0.35	0.005898	0.549	0.816	2.6422
0.36	0.005878	0.5504	0.8163	2.6409
0.37	0.00546	0.5529	0.8169	2.4661
0.38	0.005453	0.5551	0.8174	2.4742
0.39	0.005439	0.5596	0.8185	2.4912
0.40	0.00542	0.5631	0.8193	2.5005
0.41	0.005376	0.6015	0.8277	2.6765

x	I_{SC} (A/cm2)	V_{OC}(V)	Fill Factor	Efficiency
0.42	0.005009	0.4913	0.8008	1.9707
0.43	0.004985	0.4999	0.8033	2.0018
0.44	0.004945	0.5129	0.8068	2.0463
0.45	0.004852	0.5397	0.8137	2.1308
0.46	0.004848	0.5374	0.8132	2.1186
0.47	0.004846	0.53	0.8113	2.0837
0.48	0.004842	0.5328	0.812	2.0948
0.49	0.004836	0.5303	0.8114	2.0809
0.50	0.004839	0.5182	0.8082	2.0266
0.51	0.004492	0.527	0.8015	1.8974
0.52	0.00449	0.5213	0.809	1.8936
0.53	0.004492	0.5254	0.8101	1.9119
0.54	0.004492	0.524	0.8097	1.9059
0.55	0.004491	0.5227	0.8094	1.9
0.56	0.00449	0.5199	0.8087	1.8878
0.57	0.004488	0.5189	0.8084	1.8826
0.58	0.004487	0.5175	0.808	1.8762
0.59	0.004486	0.5165	0.8078	1.8717
0.60	0.004484	0.5154	0.8075	1.8662
0.61	0.004482	0.5144	0.8072	1.861
0.62	0.00448	0.5134	0.807	1.8561
0.63	0.004475	0.5123	0.8067	1.8494
0.64	0.004478	0.513	0.8068	1.8534
0.65	0.004473	0.5119	0.8065	1.8467
0.66	0.00447	0.5114	0.8064	1.8434
0.67	0.004466	0.5111	0.8063	1.8404
0.68	0.004463	0.5108	0.8063	1.8381

X	I_{SC} (A/cm2)	V_{OC}(V)	Fill Factor	Efficiency
0.69	0.004458	0.5107	0.8062	1.8355
0.70	0.004453	0.5106	0.8062	1.8331
0.71	0.004447	0.5105	0.8062	1.8302
0.72	0.004438	0.5107	0.8062	1.8272
0.73	0.004092	0.513	0.8068	1.6936
0.74	0.00409	0.5134	0.807	1.6945
0.75	0.004088	0.5138	0.8071	1.6952
0.76	0.004086	0.5144	0.8072	1.6966
0.77	0.004084	0.5148	0.8073	1.6973
0.78	0.004081	0.5157	0.8076	1.6997
0.79	0.004079	0.5163	0.8077	1.701
0.80	0.004076	0.5172	0.808	1.7034
0.81	0.004075	0.5182	0.8082	1.7066
0.82	0.00407	0.519	0.8084	1.7076
0.83	0.004066	0.52	0.8087	1.7099
0.84	0.004062	0.5209	0.8089	1.7115
0.85	0.004059	0.522	0.8092	1.7145
0.86	0.003681	0.5321	0.8118	1.59
0.87	0.00424	0.5281	0.8108	1.8155
0.88	0.004049	0.525	0.81	1.7218
0.89	0.004029	0.5261	0.8103	1.7176
0.90	0.004032	0.5269	0.8105	1.7219
0.91	0.004049	0.5242	0.8098	1.7188
0.92	0.004047	0.5284	0.8109	1.7341
0.93	0.004054	0.5231	0.8095	1.7167
0.94	0.00367	0.5366	0.813	1.6011
0.95	0.003674	0.5353	0.8126	1.5981
0.96	0.003677	0.5343	0.8124	1.5961
0.97	0.004093	0.5204	0.8088	1.7227
0.98	0.004088	0.5184	0.8083	1.713
0.99	0.004079	0.5163	0.8077	1.701
1.00	0.004084	0.5148	0.8073	1.6973

3.5 Mole Fraction Vs. Efficenency Graph (Simulation Based)

The following graph was drawn using the MATLAB

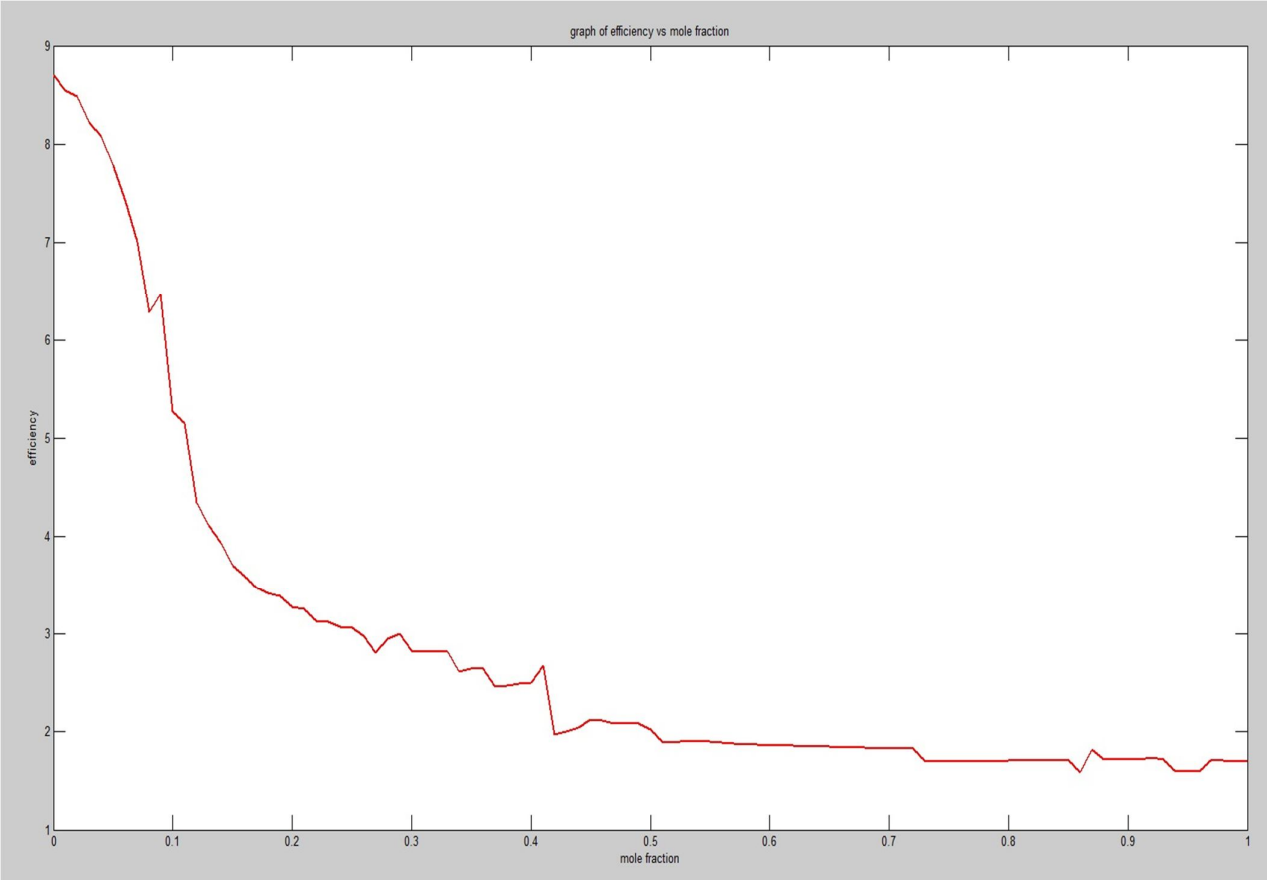

Fig 3.102: Simulation Based Efficiency vs mole fraction plot using MATLAB

Remarks:

In this chapter it is discussed about the calculation of efficiency of the solar cell theoretically, the coding that is used for simulation and the plotting of the the graph of mole fraction vs efficiency.

Chapter 4 Solar Radiation Measurements

4.1 Solar Radiation Components at the Ground Level

In a point at the top of Earth's atmosphere, the beam of nearly parallel incident sunrays is referred to as extraterrestrial radiation (ETR). ETR fluctuates about 6.9 % during a year (from 1412.0 Wm-2 in January to 1321.0Wm-2 in July) due to the Earth's varying distance from the Sun. Figure 4.1 shows the spectral distribution of ETR at the mean Sun–Earth distance. The graph is plotted at low resolution with data from Gueymard and Myers (2008), which is detailed enough for many engineering applications, like forecasting of PV plants output. The extraterrestrial spectrum is also available online (NREL 2012), along with other reference radiation spectra. The integration of the extraterrestrial spectrum over all wavelengths defines the solar constant G_{sc}. Thus, G_{sc} represents the flux density of incoming solar radiation on a unitary surface perpendicular to the rays at the mean Sun–Earth distance. Since the Sun radiance varies to some extent over short and long periods (Fröhlich 1991), the solar constant does not remain steady over time. There is a variation of about ± 1 Wm-2 around the mean solar constant during a typical Sun cycle of 11 years (Gueymard and Myers 2008). Based on data collected over 25 years from terrestrial to space observations, the actual best estimate of the average solar constant is G_{sc} = 1366.1 Wm-2 (Gueymard 2004). When the solar radiation flux passes through the Earth's atmosphere, its spectral distribution is modified by absorption and scattering processes. The complex effect experienced by solar radiation flux spectral distribution when transiting the Earth's atmosphere is also illustrated in Fig. 4.1, which displays the AM1.5G global spectrum defined by the Commision Internationale de l'Eclairage (CIE) and the American Society for Testing and Materials (ASTM) for testing the terrestrial solar cells. The standard assumes the following: the receiving surface is tilted 37_toward the equator, the solar zenith angle is 48_19', the total ozone column content is 0.34 cm atm, the Ångstrom turbidity coefficient at wavelength 0.5 lm is 0.084and the water vapor column content is 1.42 g cm-2. The Air Mass (AM)

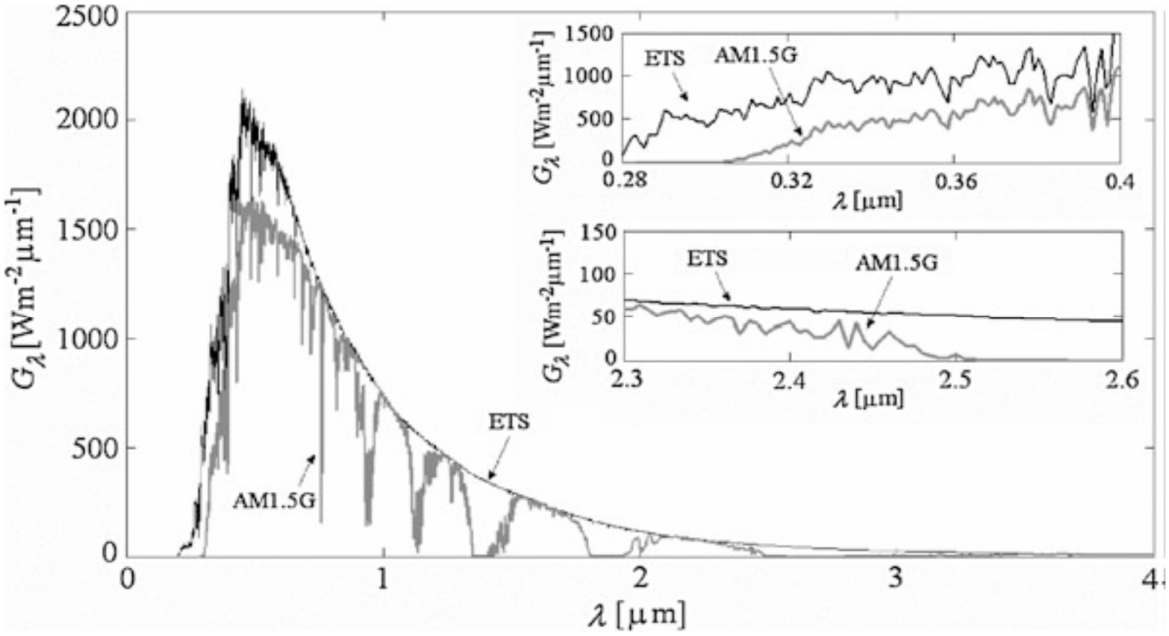

Fig. 4.1 Extraterrestrial solar spectrum (ETS) and terrestrial standard solar spectrum AM1.5G.

Details of ultraviolet and infrared spectral domains are presented inset. Gk is the extraterrestrial spectral flux density and k is the photon wavelength if approximated by the inverse of the cosine of the zenith angle, is 1/cos (48^o 19') = 1.5

As a result of its passage through the atmosphere, the ETR is separated into different components. The beam component of solar radiation is that part of ETR which directly reaches Earth's surface. Scattering of the ETR in the atmosphere generates the diffuse component. A part of the solar radiation that is reflected by the ground may also be present in the total solar radiation. More precisely, the following quantities associated to solar radiation are commonly measured:

Direct beam irradiance (G_n) is the energy flux density (units: W/m^2) of the solar radiation incoming from the solid angle subtended by the Sun's disk on a unitary surface perpendicular to the rays.

Direct horizontal irradiance (G_b) differs from the direct beam irradiance in that it is measured on a flat horizontal plane. Lambert's cosine law states that the energy flux density on a plane surface is directly proportional to the cosine of the

incidence angle. Since the incidence angle of the solar beam striking the horizontal ground is equal to sun the zenith angle θz (Fig. 4.2), then:

$$G_b = G_n \cos \theta z$$

Diffuse irradiance (G_d) represents the energy flux density of the solar radiation incoming from the entire sky dome on a horizontal surface, excluding the direct beam coming from the Sun's disk.

Global irradiance (G) is the sum of the direct horizontal and diffuse components, given as:

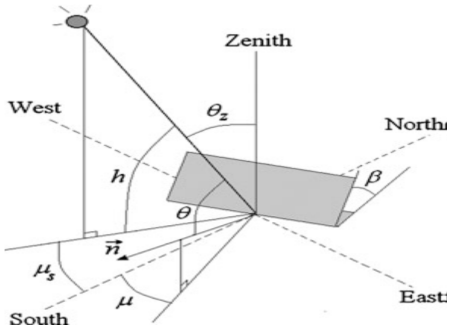

Fig. 4.2 Angles describing the position of the sun: θz—zenith angle; h—elevation angle, μ_s—azimuth angle. Angles describing the position of the surface: β—slope angle, μ—surface azimuth angle. The incidence angle θ is the angle between the sun direction and the surface's normal n.

$$G = G_b + G_d = G_n \cos \theta_z + G_d$$

The term ''global'' is associated to the fact that the solar radiation is received from the entire 2π solid angles of the sky vault.

The total irradiance (G_t) received by a surface tilted with an angle β in respect to the horizontal plane (Fig. 4.2) is the sum of beam flux density, diffuse flux density, and the additional flux density G_r of the solar radiation reflected from the ground, respectively. Hence we get:

$$G_t = G_n \cos\theta + R_d G_d + Gr$$

where θ is the incidence angle (i.e., the angle between the sun direction and the normal to the surface (Fig. 4.2), R_d is the conversion coefficient taking into account the sky view factor and G_r is the energy flux density of radiation reflected by the ground that is intercepted by the tilted surface. Models for

estimating global solar irradiance on tilted surfaces differ generally in their treatment of R_d which is considered the main potential source of errors.
By summing up over a finite time period $\Delta t = t_2 - t_1$ one obtains the solar irradiation components:

$$H=\int_{t1}^{t2} G(t)dt$$

usually measured in J/m^2 or Wh/m^2. G(t) stands for any of the above solar irradiance components, and consequently H refers to the corresponding solar irradiation component.
For proper characterization of the radiative regime the state of the sky should also be assessed. Two quantities are commonly used to describe the state of the sky. The most usual indicator is the total cloud cover amount C which represents the fraction of the celestial vault covered by clouds (estimated in tenths or oktas).
The second quantity describing indirectly the state of the sky is the relative sunshine σ (also called sunshine fraction). It is defined as σ =s/S, where S is the length of a given time interval and s is the bright sunshine duration during that interval.

4.2 Energy Of Photon

A photon is characterized by either a wavelength, denoted by λ or equivalently an energy, denoted by E. There is an inverse relationship between the energy of a photon (E) and the wavelength of the light (λ) given by the equation:

$$E=hc/\lambda$$

Where h is Planck's constant and c is the speed of light.
$h = 6.626 \times 10^{-34}$ joule·s
$c = 2.998 \times 10^8$ m/s
By multiplying to get a single expression, $hc = 1.99 \times 10^{-25}$ joules-m

The above inverse relationship means that light consisting of high energy photons (such as "blue" light) has a short wavelength. Light consisting of low energy photons (such as "red" light) has a long wavelength.

When dealing with "particles" such as photons or electrons, a commonly used unit of energy is the electron-volt (eV) rather than the joule (J). An electron volt is the energy required to raise an electron through 1 volt, thus a photon with an energy of 1 eV = 1.602×10^{-19} J.

Therefore, we can rewrite the above constant for hc in terms of eV:

$hc = (1.99 \times 10^{-25}$ joules-m) × (1ev/1.602×10^{-19} joules) = 1.24×10^{-6} eV-m

Further, we need to have the units be in μm (the units for λ):

$$hc = (1.24 \times 10^{-6} \text{ eV-m}) \times (10^{6} \text{ μm/ m}) = \underline{1.24 \text{ eV-μm}}$$

By expressing the equation for photon energy in terms of eV and μm we arrive at a commonly used expression which relates the energy and wavelength of a photon, as shown in the following equation:

$$E(eV)=1.24/\lambda(\mu m)$$

The exact value of 1×10^{6}(hc/q) is 1.2398 but the approximation 1.24 is sufficient for most purposes.

To find the energy of a photon at a particular wavelength, click on the map above.

4.3 Photon Flux

The photon flux is defined as the number of photons per second per unit area:

$$\Phi = \frac{\#\ of\ photons}{\sec m^2}$$

The photon flux is important in determining the number of electrons which are generated, and hence the current produced from a solar cell. As the photon flux does not give information about the energy (or wavelength) of the photons, the energy or wavelength of the photons in the light source must also be specified. At a given wavelength, the combination of the photon wavelength or energy and the photon flux at that wavelength can be used to calculate the power density for photons at the particular wavelength. The power density is calculated by multiplying the photon flux by the energy of a single photon. Since the photon flux gives the number of photons striking a surface in a given time, multiplying

by the energy of the photons comprising the photon flux gives the energy striking a surface per unit time, which is equivalent to a power density. To determine the power density in units of W/m², the energy of the photons must be in Joules.

The equation is:

$$H(W/m2)=\Phi \times hc/\lambda \text{ using SI units}$$

$$H(W/m2)=\Phi \times q1.24\lambda(\mu m) \text{ for wavelength in } \mu m$$

$$H(W/m2)=\Phi \times qE(eV) \text{ for energy in eV}$$

where Φ is the photon flux and q is the value of the electronic charge $1.6 \cdot 10^{-19}$

Table 4.1 Percentage Of Solar Radiation and Photon Chart according to different Wavelengths (nm)

Range	Percentage (%) of solar radiation in that range	Average Wave Length (nm)	Energy Of that Wavelength	Total Photons	Percentage (%) Of Photons
0-280 (UVC)	0	140	$1.42X10^{-18}$	$7.042X10^{20}$	0
280-320 (UVB)	0.1	300	$6.63X10^{-19}$	$1.508X10^{21}$	$1.508X10^{18}$
320-400 (UVB)	4.5	360	$5.525X10^{-19}$	$1.809X10^{21}$	$8.141X10^{19}$
400-450	7.3	425	$4.68X10^{-19}$	$2.137X10^{21}$	$1.56X10^{20}$
450-500	10.5	475	$4.187X10^{-19}$	$2.388X10^{21}$	$2.507X10^{20}$
500-550	9.8	525	$3.789X10^{-19}$	$2.639X10^{21}$	$2.586X10^{20}$
550-600	10	575	$3.46X10^{-19}$	$2.89X10^{21}$	$2.89X10^{20}$
600-650	9	625	$3.182X10^{-19}$	$3.143X10^{21}$	$2.829X10^{20}$
650-700	8.1	675	$2.947X10^{-19}$	$3.393X10^{21}$	$2.748X10^{20}$
700-800	11.3	750	$2.652X10^{-19}$	$3.771X10^{21}$	$4.261X10^{20}$
800-900	7.3	850	$2.34X10^{-19}$	$4.274X10^{21}$	$3.12X10^{20}$
900-10000	4.7	950	$2.093X10^{-19}$	$4.778X10^{21}$	$2.246X10^{20}$

4.4 Absorption Co-efficient, α

The absorption coefficient determines how far into a material light of a particular wavelength can penetrate before it is absorbed. In a material with a low absorption coefficient, light is only poorly absorbed, and if the material is thin enough, it will appear transparent to that wavelength. The absorption coefficient depends on the material and also on the wavelength of light which is being absorbed. Semiconductor materials have a sharp edge in their absorption coefficient, since light which has energy below the band gap does not have sufficient energy to excite an electron into the conduction band from the valence band. Consequently this light is not absorbed. The absorption coefficient for several semiconductor materials is shown below.

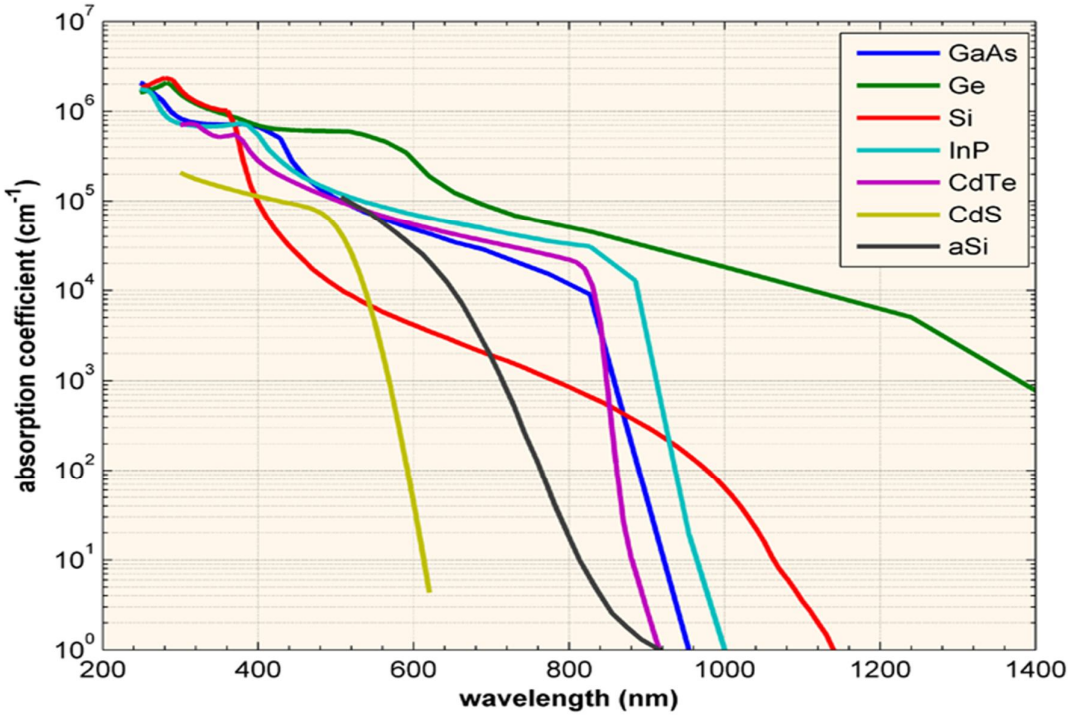

Fig 4.3: The absorption coefficient, α, in a variety of semiconductor materials at 300K as a function of the vacuum wavelength of light.

The above graph shows that even for those photons which have an energy above the band gap, the absorption coefficient is not constant, but still depends strongly on wavelength. The probability of absorbing a photon depends on the likelihood of having a photon and an electron interact in such a way as to move

from one energy band to another. For photons which have an energy very close to that of the band gap, the absorption is relatively low since only those electrons directly at the valence band edge can interact with the photon to cause absorption. As the photon energy increases, not just the electrons already having energy close to that of the band gap can interact with the photon. Therefore, a larger number of electrons can interact with the photon and result in the photon being absorbed.

The absorption coefficient, α, is related to the extinction coefficient, k, by the following formula:

$$\alpha = \frac{4\pi k}{\lambda}$$

where λ is the wavlength. If λ is in nm, multiply by 10^7 to get the absorption coefficient in the the units of cm^{-1}.

A graph can represent the variation of absorption co-efficients for different values of energy which is given below:

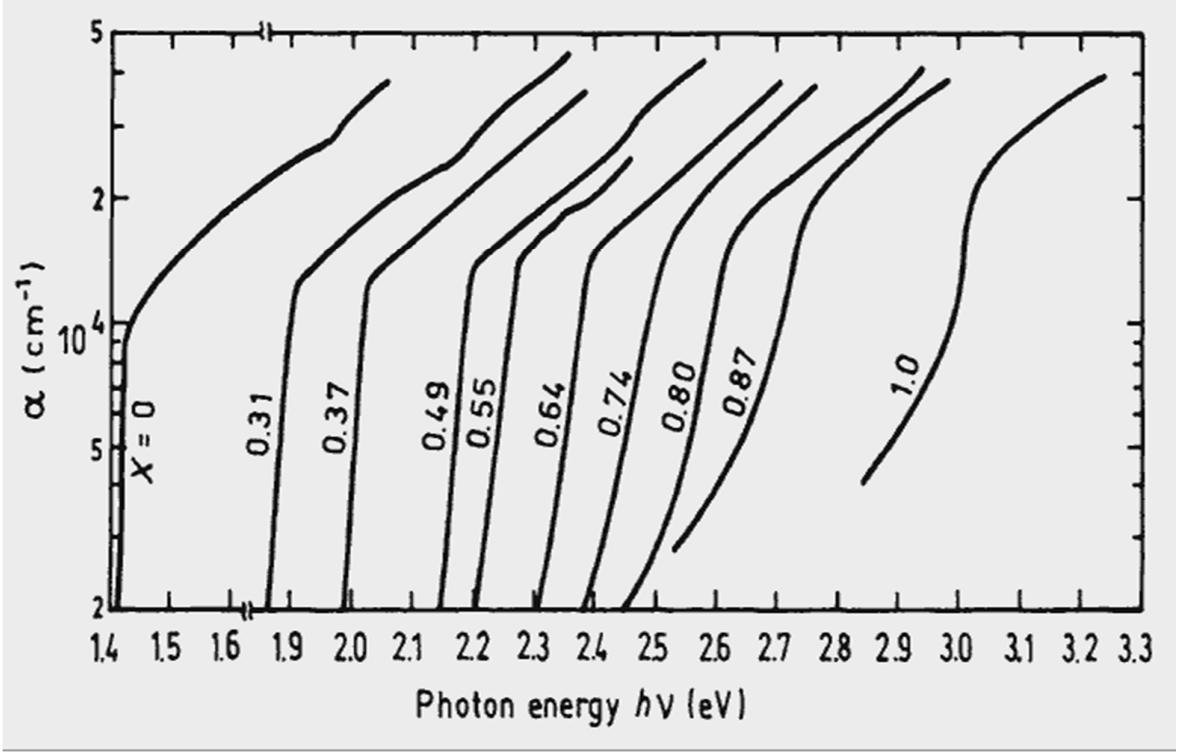

Fig 4.4 : Absorption Co-efficient vs Photon Energy graph[64]

4.5 Remarks:

In this chapter, it is discussed about the different parameters of the solar radiation spectrum which are essential for the calculation of our desired efficiency and modelling the characteristics of our solar cell.

Chapter 5: Efficiency Calculation and Theoretical Modelling

5.1 Generation Rate

The generation rate gives the number of electrons generated at each point in the device due to the absorption of photons. Generation is an important parameter in solar cell operation.[59]

Neglecting reflection, the amount of light which is absorbed by a material depends on the absorption coefficient (α in cm^{-1}) and the thickness of the absorbing material. The intensity of light at any point in the device can be calculated according to the equation:

$$I = I_0 e^{-\alpha x}$$

where α is the absorption coefficient typically in cm^{-1};
x is the distance into the material at which the light intensity is being calculated; and
I_0 is the light intensity at the top surface.
The above equation can be used to calculate the number of electron-hole pairs being generated in a solar cell. Assuming that the loss in light intensity (i.e., the absorption of photons) directly causes the generation of an electron-hole pair, then the generation G in a thin slice of material is determined by finding the change in light intensity across this slice. Consequently, differentiating the above equation will give the generation at any point in the device. Hence:

$$G = \alpha N_0 e^{-\alpha x}$$ [59]

where N_0=photon flux at the surface (photons/unit-area/sec.);
α=*absorption coefficient*
x = distance into the material.
If we assume that each photon absorbed creates an electron hole pair,then the generation rate of electron-hole pairs as a function of distance x can be written as:

$$G_{L=}\,\alpha\,(\lambda)N_0\,(\lambda)[1\text{-}R(\lambda)]e^{-\alpha(\lambda)x}$$ [59]

The above equations show that the light intensity exponentially decreases throughout the material and further that the generation is highest at the surface of the material.

5.2 Calculation Of G_L :

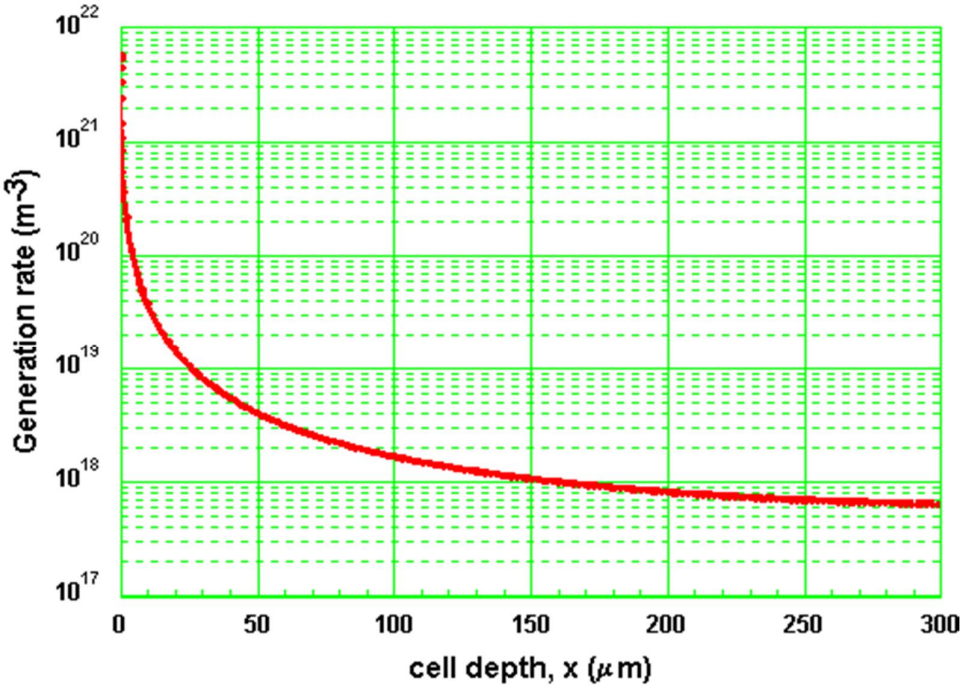

Fig 5.1: Normalised Generation rate (m-3) vs cell depth (μm) curve

The figure above shows our cell depth vs generation rate curve. Here cell depth x is the width of our AlGaAs layer which is 2μm. Here GL is the area under the curve, which is an exponential curve. In order to calculate area under this curve we have to integrate the function e-α(λ)x which yields a result -α e-α(λ)x. Here α is our absorption co-efficient and it is a function of the wavelength λ. This quantity is unknown. So GL was calculated in the following procedure:

1. For every mole fraction (0.1 to 1), the interval x=2μm was divided into 10 intervals (x=0,0.2,0.4,…2)
2. For every value of x, GL was calculated using the formula

$$GL= \alpha(\lambda)N0(\lambda)[1-R(\lambda)]e^{-\alpha(\lambda)x}$$

Here, R(λ)=0.35 and it is fixed;

3. The values of GL for each value of x were added and the average was taken by dividing the result by 11. This was done for linear approximation of the area. The area was calculated by approximating it as a rectangular surface rather than an exponential curve.
4. The result we got was multiplied by 2μm, the length of the rectangle, GL being the width.

5.3 Calculation of short circuit Current Density J_{sc} and open circuit Voltage Density V_{OC}:

To calculate J_{SC} the value of G_L was multiplied by the charge of an electron $1.6*10^{-19}$:

$$J_{sc}=q*G*W$$

The value of V_{OC} was calculated by the following equations:

$V_{oc}= V_t*\ln(1+J_{SC}/J_s)$
Where, J_s=Reverse saturation current density = 10^{-14} A/cm^2
and V_t=Thermal voltage = 0.0259 V

5.4 Fill Factor

The short-circuit current and the open-circuit voltage are the maximum current and voltage respectively from a solar cell. However, at both of these operating points, the power from the solar cell is zero. The "fill factor", more commonly known by its abbreviation "FF", is a parameter which, in conjunction with V_{oc} and I_{sc}, determines the maximum power from a solar cell. The FF is defined as the ratio of the maximum power from the solar cell to the product of V_{oc} and I_{sc}. Graphically, the FF is a measure of the "squareness" of the solar cell and is also the area of the largest rectangle which will fit in the IV curve.[32] The FF is illustrated below.

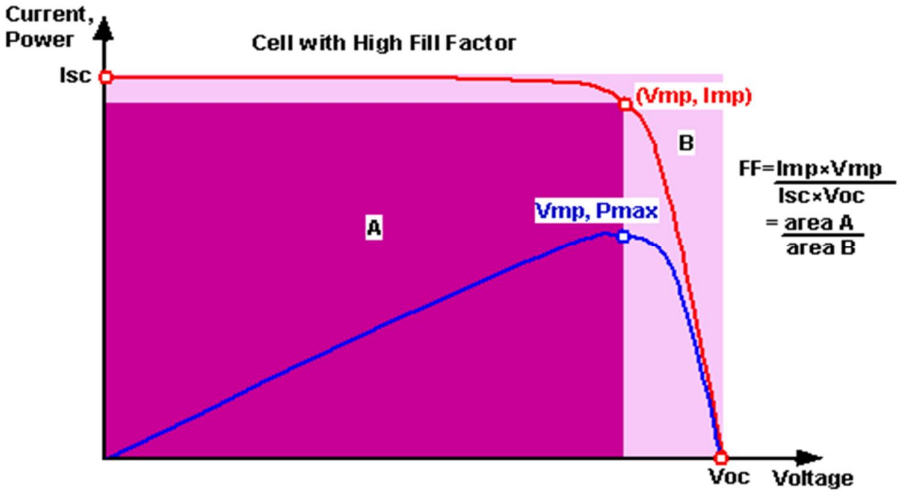

Fig 5.2: Graph of cell output current (red line) and power (blue line) as function of voltage. [32]

As FF is a measure of the "squareness" of the IV curve, a solar cell with a higher voltage has a larger possible FF since the "rounded" portion of the IV curve takes up less area. The maximum theoretical FF from a solar cell can be determined by differentiating the power from a solar cell with respect to voltage and finding where this is equal to zero. Hence:

$$\frac{d(IV)}{dV} = 0$$

giving:

$$V_{MP} = V_{OC} - \frac{nkT}{q}\ln\left(\frac{V_{mp}}{nkT/q} + 1\right) \quad [32]$$

However, the above technique does not yield a simple or closed form equation. The equation above only relates V_{oc} to V_{mp}, and extra equations are needed to find I_{mp} and FF. A more commonly used expression for the FF can be determined empirically as:

$$FF = \frac{V_{OC} - \ln(V_{OC} + 0.72)}{V_{OC} + 1}$$

where V_{OC} is defined as a "normalized V_{OC}":

$$V_{OC} = \frac{q}{nkT} V_{OC} \quad [32]$$

5.5 Efficiency

The efficiency is the most commonly used parameter to compare the performance of one solar cell to another. Efficiency is defined as the ratio of energy output from the solar cell to input energy from the sun. In addition to reflecting the performance of the solar cell itself, the efficiency depends on the spectrum and intensity of the incident sunlight and the temperature of the solar cell. Therefore, conditions under which efficiency is measured must be carefully controlled in order to compare the performance of one device to another. Terrestrial solar cells are measured under AM1.5 conditions and at a temperature of 25°C. Solar cells intended for space use are measured under AM0 conditions.

The efficiency of a solar cell is determined as the fraction of incident power which is converted to electricity and is defined as:

$$P_{max} = V_{OC} I_{SC} FF$$

$$\eta = \frac{V_{OC} I_{SC} FF}{P_{in}}$$

The theoretical results are given in the table below:

Table 5.1: Theoretical Date Table

Mole fraction (x)	**Short Circuit Current Density, Jsc (A/cm^2)**	**Open Circuit Voltage, Voc (V)**	**Fill Factor, FF**	**Efficiency, n**
0.00	0.01669	0.9208	0.8745	13.57
0.01	0.01829	0.9273	0.8742	14.84
0.02	0.01759	0.9279	0.8744	14.28
0.03	0.01761	0.9279	0.8744	14.30
0.04	0.01573	0.9297	0.8746	12.80
0.05	0.01569	0.9298	0.8746	12.77
0.06	0.01569	0.9298	0.8746	12.77
0.07	0.01554	0.9299	0.8746	12.65
0.08	0.013	0.9251	0.8749	10.62

Mole fraction (x)	**Short Circuit Current Density, Jsc (A/cm^2)**	**Open Circuit Voltage, Voc (V)**	**Fill Factor, FF**	**Efficiency, n**
0.09	0.01542	0.93	0.8755	12.55
0.10	0.01536	0.9301	0.876	12.51
0.11	0.01514	0.9303	0.8755	12.33
0.12	0.01532	0.9309	0.8754	12.47
0.13	0.0152	0.9303	0.8755	12.38
0.14	0.01488	0.9306	0.8755	12.12
0.15	0.01496	0.9305	0.8755	12.19
0.16	0.01488	0.9306	0.8747	12.12
0.17	0.01484	0.9306	0.8747	12.09
0.18	0.01466	0.9308	0.8747	11.95
0.19	0.01452	0.9309	0.8747	11.83
0.20	0.01232	0.9333	0.8750	10.07
0.21	0.01224	0.9334	0.8751	10.01
0.22	0.01222	0.9335	0.8751	9.99
0.23	0.01216	0.9336	0.8751	9.94
0.24	0.0123	0.9334	0.8751	10.06
0.25	0.0102	0.9337	0.8752	9.83
0.26	0.01202	0.9337	0.8752	9.83
0.27	0.01184	0.9336	0.8752	9.68
0.28	0.01158	0.9343	0.8753	9.48
0.29	0.01164	0.9342	0.8753	9.52
0.30	0.01152	0.9343	0.8753	9.43
0.31	0.0114	0.9345	0.8759	9.33
0.32	0.0116	0.9342	0.8759	9.49
0.33	0.0112	0.9347	0.8759	9.17
0.34	0.0107	0.9353	0.876	8.767
0.35	0.0102	0.9359	0.876	8.36
0.36	0.0093	0.9474	0.8772	7.72
0.37	0.0073	0.9590	0.8783	6.65
0.38	0.0075	0.9584	0.8783	6.31
0.39	0.0098	0.9390	0.8763	8.06
0.40	0.0075	0.9584	0.8783	6.31
0.41	0.0063	0.9623	0.8786	5.32
0.42	0.0072	0.9593	0.8783	6.07
0.43	0.0071	0.9596	0.8784	5.985
0.44	0.0069	0.9603	0.8784	5.82
0.45	0.0067	0.9609	0.8785	5.65
0.46	0.0064	0.9620	0.8786	5.41
0.47	0.0061	0.9631	0.8787	5.16

Mole fraction (x)	**Short Circuit Current Density, Jsc (A/cm^2)**	**Open Circuit Voltage, Voc (V)**	**Fill Factor, FF**	**Efficiency, n**
0.48	0.0058	0.9641	0.8788	4.91
0.49	0.0049	0.9679	0.8792	4.17
0.50	0.0045	0.9697	0.8793	3.83
0.51	0.0044	0.9701	0.8794	3.75
0.52	0.0042	0.9711	0.8795	3.59
0.53	0.0043	0.9706	0.8794	3.67
0.54	0.0041	0.9716	0.8795	3.503
0.55	0.0040	0.9721	0.8796	3.42
0.56	0.0039	0.9727	0.8796	3.34
0.57	0.0040	0.9721	0.8796	3.42
0.58	0.0040	0.9721	0.8796	3.42
0.59	0.0041	0.9716	0.8795	3.50
0.60	0.0041	0.9716	0.8795	3.50
0.61	0.0042	0.9711	0.8795	3.59
0.62	0.0043	0.9706	0.8794	3.67
0.63	0.0043	0.9706	0.8794	3.67
0.64	0.0044	0.9701	0.8794	3.75
0.65	0.0043	0.9706	0.8794	3.67
0.66	0.0041	0.9716	0.8795	3.505
0.67	0.00403	0.972	0.8796	3.446
0.68	0.0046	0.9694	0.8793	3.885
0.69	0.0039	0.9727	0.8796	3.327
0.70	0.00382	0.9731	0.8797	3.2677
0.71	0.00374	0.9735	0.8797	3.2077
0.72	0.00367	0.9739	0.8797	3.1476
0.73	0.0036	0.9743	0.8798	3.088
0.74	0.0035	0.9734	0.8797	2.9612
0.75	0.0034	0.9756	0.8799	2.8988
0.76	0.0033	0.976	0.8799	2.8305
0.77	0.0032	0.9766	0.88	2.7617
0.78	0.0031	0.977	0.88	2.692
0.79	0.003	0.9776	0.8801	2.622
0.80	0.0033	0.9761	0.8799	2.8238
0.81	0.0028	0.9796	0.8803	2.3742
0.82	0.0026	0.9803	0.8803	2.2847
0.83	0.0025	0.9811	0.8804	2.186
0.84	0.0024	0.982	0.8805	2.087
0.85	0.0023	0.9829	0.8806	1.9886
0.86	0.0022	0.9839	0.8807	1.889

Mole fraction (x)	**Short Circuit Current Density, Jsc (A/cm^2)**	**Open Circuit Voltage, Voc (V)**	**Fill Factor, FF**	**Efficiency, n**
0.87	0.0019	0.9858	0.8808	1.688
0.88	0.0030	0.9778	0.8801	2.5913
0.89	0.0028	0.9798	0.8803	2.4534
0.90	0.0027	0.98	0.8803	2.3142
0.91	0.0025	0.98125	0.8804	2.1744
0.92	0.0024	0.9825	0.8805	2.034
0.93	0.0022	0.9838	0.8807	1.8925
0.94	0.002	0.9852	0.8808	1.75
0.95	0.0018	0.9867	0.8809	1.6067
0.96	0.0022	0.9835	0.8806	1.9294
0.97	0.0015	0.9899	0.8812	1.3174
0.98	0.0013	0.9942	0.8816	1.174
0.99	0.0012	0.9937	0.8816	1.024
1.00	0.0008	1.0158	0.8835	0.7409

The MATLAB plot of theoretical efficiency vs mole fraction is given below:

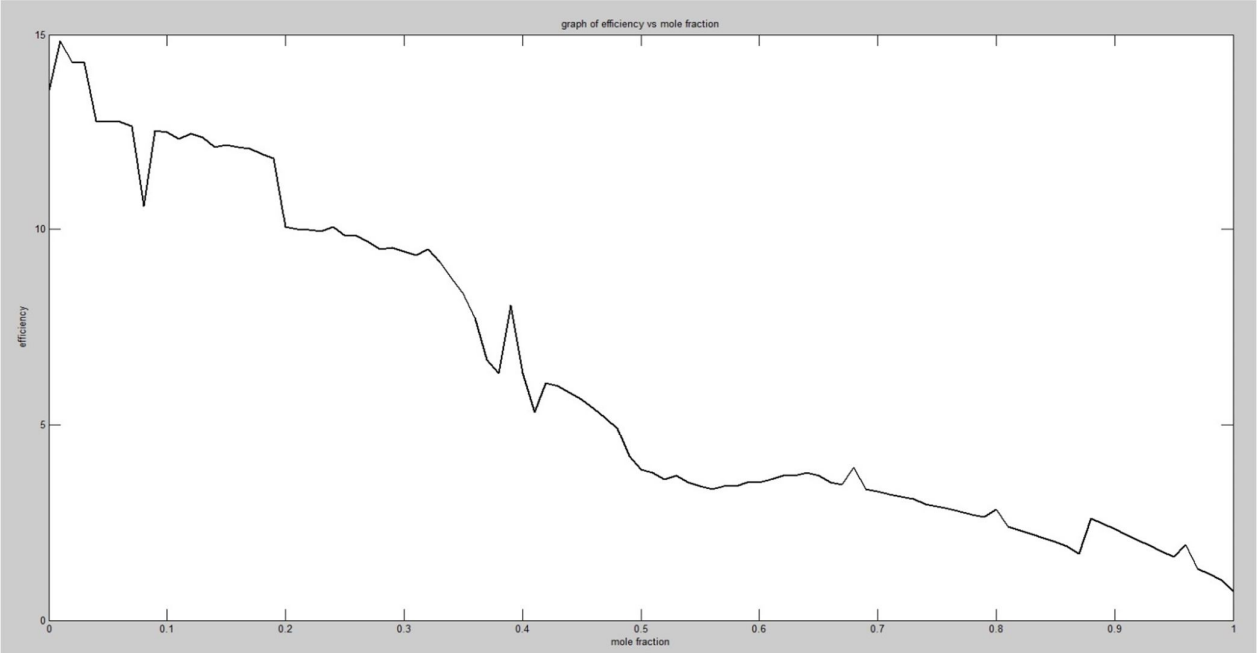

Fig 5.3: Theoretical Efficiency vs mole fraction plot using MATLAB

5.6: Efficiency Loss

The value of simulation based efficiency and theoretical efficiency are not the same. There is significant difference between these two values for each value of the mole fraction. Apart from some calculation errors defects in hetero-junction structure is primarily responsible for the loss of efficiency. The simulation based results are taken considering the losses into account, while the theoretical values overlook these issues. So in the later case, the efficiency values are comparatively high. These gap of efficiency values in two cases is termed as efficiency loss, and these happens mainly due to defects.

5.6.1 Losses in Hetero-junction

From the structure of $Al_xGa_{1-x}As$, for the value of x=0, we know AlGaAs remains as a direct bandgap material upto 45% of Al in the material(Starting from x=0). As the percentage of Al exceeds 45%, the material turns into an indirect bandgap semiconductor. The bandgap energies for GaAs and AlAs are 1.46 eV and 2.13 eV respectively.

Due to this change in the lattice constant, a mismatch occurs in the lattice structure.These mismatch is termed as lattice defect.Lattice defects are plane defects, line defects, point defects, volume defects, etc.

The efficiency loss vs mole fraction MATLAB plot is given below:

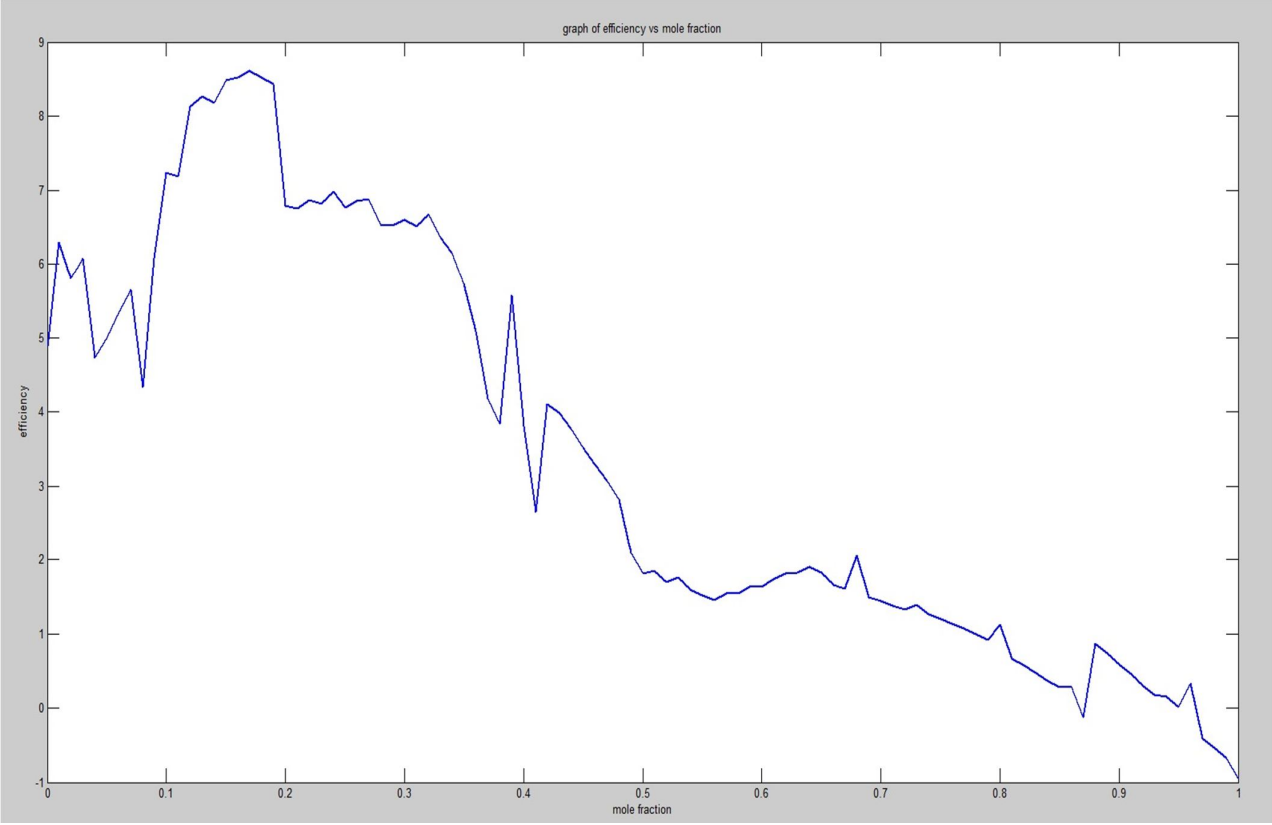

Fig 5.4: Efficiency Loss vs mole fraction MATLAB plot

5.7 Comparison Between Theoretical, Simulation Based and Efficiency Loss graphs:

As was stated earlier, the theoretical results are calculated ignoring the losses and so they are greater than simulation based results for each mole fraction value, which are calculated considering loss. The difference between these two graphs is the efficiency loss graph.

A comparative MATLAB plot of theoretical, simulation based results and their difference is shown below:

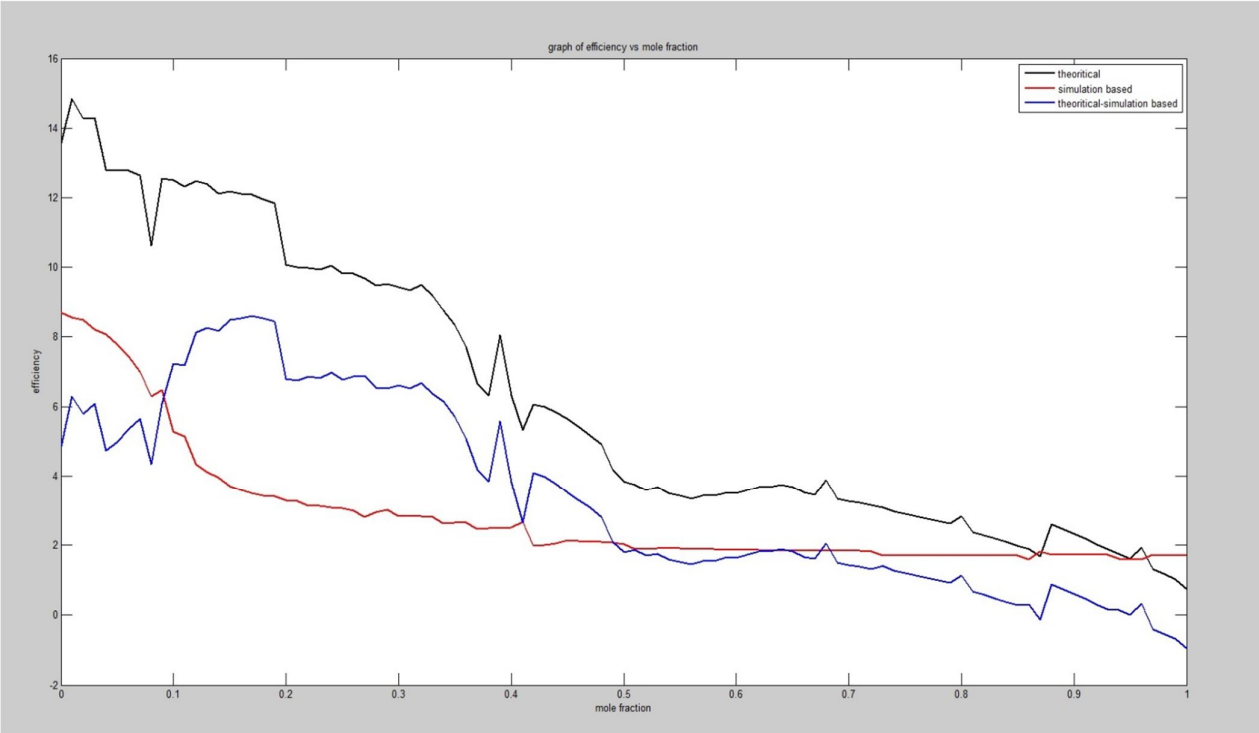

Fig 5.5: Theoretical and simulation based efficiency plots vs mole fraction and their difference as Efficiency Loss vs mole fraction

Remarks:

In this chapter, it is discussed about the calculation of the efficiency of the solar cell by theoretical calculation methods and discussed the efficiency loss due to defects in hetero-junction solar cells. It is discussed about the plotting of the theoretical efficiencies and the efficiency losses with respect to mole fraction using MATLAB.

Chapter 6- Summary

6.1 Overview of the Work

In chapter 1, we discussed about the basic operational principles of solar cells, along with the basics of hetero-junction solar cells. we discussed the application of III-V compounds in solar cells, with defects in the hetero-junction materials which is the limiting factor for the efficiency of these solar cells. We have also given a brief outline of our research, and discussed the novelty in our work with appropriate references.

In chapter 2, we discussed about the software we used in the simulation and different parameters that are used in simulation. In chapter the different values of these parameters for different mole fraction are also given.

In chapter 3, we discussed about the J-V curve which is result of the simulation. Also the short circuit current and open circuit voltage which is obtained from the J-V curve and the efficiency calculation is discussed.

In chapter 4, the solar spectrum and absorption coefficient calculation is discussed. From the solar spectrum, calculation of photon flux is discussed.

In chapter 5, the generation rate of electron-hole pair as a function of distance is discussed. The approach that is used in calculation of generation rate of electron hole pair (using average method) is discussed. Also, the calculation of therotical efficiency and calculation of efficiency loss due to defects are also discussed.

6.2 Future Work

There are many factors that are responsible for efficiency loss in the solar cells. Like Spectral mismatch, Solar cell optical properties, Solar cell collection losses, Additional Defects. Further work can be done to minimize the efficiency loss in the solar cell. That method used for calculation of generation rate of electron-hole pair can have some errors in calculation. As a result there is some negative efficiency loss. So this method can be studied for further improvement.

The solar cell introduced in this work does not have an anti-reflective (AR) coating to reduce photon loss due to reflection, or a bragg reflector that would increase the quantum efficiency of the cell. Including such layers in the solar cell would give higher efficiency.

References

1. B. Jensen and A. Torabi "Dispersion of the refractive index of GaAs and AlxGa1â ”xAs", IEEE J. Quantum Electron., vol. JQE-19, pp.877 - 882 1983
2. Peter Gevorkian, Sustainable energy systems engineering: the complete green building design resource, p. 498, McGraw-Hill Professional, New York, USA, 2007, ISBN: 978-0071473590.
3. Marius Grundmann, The Physics of Semiconductors: An Introduction Including Nanophysics and Applications, 2nd ed., p. 3, Springer-Verlag, Berlin, Germany, 2010, ISBN: 978-3642138843.
4. K. A. Tsokos, Physics for the IB Diploma, 5th ed., Cambridge University Press, Cambridge, UK, 2008, ISBN: 978-0521708203.
   Available:http: //www. ioffe.ru/SVA/NSM/Semicond/
5. Harish Palaniappan. (2012) Solar Cells. [Online]. Available: http://solar_cells.tripod.com/notes_sel_1.html
6. T.V. Torchynska, and G.P. Polupan, “III-V material solar cells for space application”, Semiconductor Physics, Quantum Electronics & Optoelectronics, vol. 5, no. 1, pp. 63-70, 2002.
7. Ioffe Physical Technical Institute. (2005) NSM Archive - Physical Properties of Semiconductors. Available: http://www.ioffe.ru/SVA/NSM/Semicond/GaAs/index.html
8. Ioffe Physical Technical Institute. (2005) NSM Archive - Physical Properties of Semiconductors. Available: http://www.ioffe.ru/SVA/NSM/Semicond/AlGaAs/index.html
9. Ioffe Physical Technical Institute. (2005) NSM Archive - Physical Properties of Semiconductors. Available: http://www.ioffe.ru/SVA/NSM/Semicond/Ge/index.html
10. Casey and Panish, 1978; Sharma and Purohit, 1974; Milnes and Feucht, 1972
11. Chang and Esaki, 1980
12. Sakaki et al., 1977.
13. Ioffe Physical Technical Institute. (2005) NSM Archive - Physical Properties of Semiconductors.
14. Stuart Bowden. (2010) Energy of a Photon | pveducation.org. [Online]. Available: http://pveducation.org/pvcdrom/solar-cell-operation/solar-cell-structure

15. Available: http://whatis.techtarget.com/definition/dielectric-constant
16. Streetman, Ben G.; Sanjay Banerjee (2000). Solid State electronic Devices(5th ed.). New Jersey: Prentice Hall. p. 524. ISBN 0-13-025538-6.
17. Hecht, Eugene (2002). Optics. Addison-Wesley. ISBN 0-321-18878-0.
18. Zh.I.Alferov,"Heterostructures and their applications in optoelectronics", Akademiia Nauk SSSR, vol. 7, pp.28-40, 1976.
19. Stephen J. Fonash, Solar Cell Device Physics, 2nd Ed., Academic Press, Elsevier, Massachusetts, USA, 2010,ISBN: 978-0123747747.
20. U. S. Department of Energy. (2011) Energy Basics. [Online]. Available:http://www.eere.energy.gov/basics/renewable_energy/pv_cell_structures.html
21. Peter Wurfel, Physics of Solar Cells: From Principles to New Concepts, Wiley-VCH Verlag GmbH & Co. KGaA, Weinheim, Germany, 2005, ISBN: 3-527-40428-7
22. Walter Ashley Harrison (1989). Electronic Structure and the Properties of Solids. Dover Publications. ISBN 0-486-66021-4.
23. G. D. Boyd and G. Livescu "Electro-absorption and refraction in Fabry-Perot quantum well modulators: A general discussion", Opt. Quantum Electron., vol. 24, pp.S147 -S165 1992
24. L. J. A. Koster, E. C. P. Smits, V. D. Mihailetchi, and P. W. M. Blom, "Device model for the operation of polymer/fullerene bulk heterojunction solar cells", Physical Review B, vol. 72, pp. 085205-1 - 085205-9, 2005,DOI: 10.1103/PhysRevB.72.085205
25. T. Tiedje, E. Yablonovitch, G. D. Cody, and B. G. Brooks, "Limiting efficiency of Silicon solar cells", IEEE Transactions on Electron Devices, vol. ED-31, pp. 711-716, 1984.
26. L.W. James, "III-V Compound heterojunction solar cells", in Proceedings of IEEE International Electron Devices Meeting, vol. 21, pp. 87-90, Washington, USA, 1975.
27. J.E. Sutherland, and J.R. Hauser, "Optimum bandgap of several III–V heterojunction solar cells", Solid-State Electronics, vol. 22, no.1, pp.3-5, 1979.
28. B. L. Anderson and R. L. Anderson, "Fundamentals of Semiconductor Devices, " Mc Graw Hill, 2005.
29. European Transactions on Telecommunications Volume 1, Issue 4, pages 433–437, July/August 1990.

30. Chapter 2: Semiconductor Fundamentals. Online textbook by B. Van Zeghbroeck].
31. Stuart Bowden. (2010) Energy of a Photon | pveducation.org. [Online]. Available: http://pveducation.org/pvcdrom/solar-cell-operation/short-circuit-current.
32. Stuart Bowden. (2010) Energy of a Photon | pveducation.org. [Online]. Available: http://pveducation.org/pvcdrom/solar-cell-operation/fill-factor.
33. M. A. Green, K. Emery, Y. Hishikawa, W. Warta, and E. D. Dunlop, "Solar cell efficiency tables (version 39)",Progress in Photovoltaics: Research and Applications, vol. 20, pp. 12-20, 2012.
34. B. Garcia, Jr., "Indium Gallium Nitride Multijunction Solar Cell Simulation Using Silvaco Atlas", M. Sc. Thesis, Naval Postgraduate School, Monterey, California, June 2007.
35. F. Dimroth, "High-efficiency solar cells from III-V compound semiconductors", Physica Status Solidi (c), vol.3, no. 3, pp. 373-379, 2006.
36. M. Meyer, and R.A. Metzger, "Flying high: The Commercial Satellite Industry Convert to Compound Semiconductor Solar Cells", Compound Semiconductor, vol. 2, no. 6, pp. 22-24, 1996.
37. A. Goetzberger, C. Heblinga, and H. Schockb, "Photovoltaic materials, history, status and outlook", Materials Science and Engineering: R: Reports, vol. 40, no. 1, pp. 1-46, 2003.
38. J.J. Schermer, G.J. Bauhuis, P. Mulder, E.J. Haverkamp, J. van Deelen, A.T.J. van Niftrik, and P.K. Larsen, "Photon confinement in high-efficiency, thin-film III–V solar cells obtained by epitaxial lift-off", Thin Solid Films, vol. 511, pp. 645 – 653, 2006.
39. Solar Cell Conversion Efficiency Limits, vol. 5,pp.5.1-5.12.
40. J. L. Gray and Michael McLennan. (2008) Adept. [Online]. Available: http://nanohub.org/resources/adept/
41. A. S. Brown, U. K. Mishra, J. A. Henige, and M. J. Delaney, Journal of Vacuum Science & Technology B, vol.6, no. 2, pp. 678-681, 1988.
42. ECEn IMMERSE Web Team, Brigham Young University. (2009) Energy Gap in III-V Ternary Semiconductors. [Online]. Available: http://www.cleanroom.byu.edu/EW_ternary.phtml

43. J. G. Fossum, “Physical operation of back-surface-field silicon solar cells,” IEEE Transactions on Electron Devices, vol. 24, no. 4, pp. 322-325, Apr. 1977.
44. Md. Sharafat Hossain, Nowshad Amin, M. A. Matin, M. Mannir Aliyu, Takhir Razykov, and Kamaruzzaman Sopian, “A numerical study on the prospects of high efficiency ultra thin ZnxCd1-xS/ CdTe solar cell,”Chalcogenide Letters, vol. 8, no. 3, pp. 263-272, Mar. 2011.
45. Lin Aiguo, Ding Jianning, Yuan Ningyi, Wang Shubo, Cheng Guanggui, and Lu Chao, “Analysis of the p+/p window layer of thin film solar cells by simulation,” Journal of Semiconductors, vol. 33, no. 2, pp. 023002-1 -023002-6 , 2012. DOI:10.1088/1674-4926/33/2/023002
46. C. Lee, H. Efstathiadis, J. E. Raynolds, and P. Haldar, “Two-dimensional Computer Modeling of Single Junction a-Si:H Solar Cells”, in IEEE Proceedings of 34th Photovoltaic Specialists Conference, pp. 1118-1122, Philadelphia, USA, 2009.
47. S. Bothra, and J.M. Borrego, “Design of GaAs solar cells with low doped base,” Solar Cells, vol. 28, no. 1, pp.95-102, Jan. 1990.
48. N. Bouarissa, and M. Boucenna, “Band parameters for AlAs, InAs and their ternary mixed crystals”, Physica Scripta, vol. 79, pp. 015701-1 - 015701-7 , 2009, DOI: 10.1088/0031-8949/79/01/015701
49. J.W. Matthews, and A.E. Blakeslee, “Defects in epitaxial multilayers: I. Misfit dislocations”, Journal of Crystal Growth, vol. 27, pp. 118- 125, 1974.
50. P. K. Nayak, G. G. Belmonte, A. Kahn, J. Bisquert, and D. Cahen, “Photovoltaic efficiency limits and material disorder”, Energy and Environmental Science, 2012, vol. 5, pp. 6022-6039, DOI: 10.1039/c2ee03178g
51. P. P. Boix, M.M.Wienk, R. A. J. Janssen, and G.Garcia-Belmonte, “Open-Circuit Voltage Limitation in LowBandgap Diketopyrrolopyrrole-Based Polymer Solar Cells Processed from Different Solvents”, Journal of Physical Chemistry C, vol. 115, pp. 15075–15080, 2011.
52. T. H. Glisson, J. R. Hauser, M. A. Littlejohn, and C. K. Williams, “Energy bandgap and lattice constant contours of III-V quaternary alloys”, Journal of Electronic Materials, vol. 7, no. 1, pp. 1-16, 1978.
53. A.W. Bett , F. Dimroth , G. Stollwerck, and O.V. Sulima, “III-V compounds for solar cell applications”, Applied Physics A, vol. 69, pp. 119–129, 1999, DOI: 10.1007/s003399900062

54. Sadao Adachi: "GaAs and Related Materials", World Scientific Publishing Co. 1994
55. G. D. Boyd and G. Livescu "Electro-absorption and refraction in Fabry-Perot quantum well modulators: A general discussion", Opt. Quantum Electron., vol. 24, pp.S147 -S165 1992
56. C.-H. Lin , J. M. Meese and Y.-C. Chang "Optical properties of GaAs/AlxGax-1 As multiple quantum wells versus electric field including exciton transition broadening effects in optical modulators", J. Appl. Phys., vol. 75, no. 5, pp.2618 -2627 1994
57. C.-H. Lin and J. M. Meese "Optical properties of bulk AlxGax-1 As", J. Appl. Phys., vol. 74, no. 10, pp.6341 -6348 1993
58. Îš. Î'. Kahen and J. P. Leburton "Structure variation of the index of refraction of GaAs-AlAs superlattices and multiple quantum wells", Appl. Phys. Lett., vol. 47, pp.508 -510 1985
59. Donald A. Neamen, Semiconductor Physics And Devices, 3rd Ed.,Tata Mcgraw Hill Education Private Limited,2007, pp.596-618
60. K. H. Goetz, D. Bimberg, H. Jurgensen, J. Selders, A.V.Solomonov, G.F.Glinskii, and M. Razeghi, "Optical and crystallographic properties and impurity incorporation of GaxIn1−xAs ($0.44<x<0.49$) grown by liquid phase epitaxy, vapor phase epitaxy, and metal organic chemical vapor deposition", Journal of Applied Physics, vol. 54, no.8, pp.4543-4552, 1983.
61. Lindholm FA, Fossum JG, Burgess EL. Application of the superposition principle to solar-cell analysis IEEE Transactions on Electron Devices. 1979 ;26:165–171
62. Baruch P, De Vos A, Landsberg PT, Parrott JE. On some thermodynamic aspects of photovoltaic solar energy conversion. Solar Energy Materials and Solar Cells. 1995 ;36:201-222.
63. Levy MY, Honsberg CB. Rapid and precise calculations of energy and particle flux for detailed-balance photovoltaic applications. Solid-State .
64. B.Monemar, K.K. Shih, and G.D.Pettit, *J. Appl. Phys.*, **47**, no.6, pp.2604-2613 (1976).